Some topics in spatial probability and statistics

Murphy, Sean

Award date:
1989

Awarding institution:
University of Bath

Some Topics in Spatial Probability and Statistics

submitted by Sean Murphy
for the degree of Ph.D.
of the University of Bath
1989

COPYRIGHT

S. Murphy Sean Murphy.

ProQuest LLC
789 East Eisenhower Parkway
P.O. Box 1346
Ann Arbor, MI 48106-1346

Abstract of Thesis.

Some Topics in Spatial Probability and Statistics.

by

Sean Murphy,

University of Bath.

In this thesis we shall be investigating three different problems in spatial probability and statistics : random mosaics ; the relationship between plant spacing and yield ; and Gaussian random fields.

A mosaic is a tessellation in which each cell of the tessellation is assigned to one of a number of different phases or "colours". A random mosaic is simply a mosaic which is obtained from a random tessellation and a random assignment of phases. The proportion in one phase over a given region is known as the volume/area/line fraction in stereology and is a random variable. We shall be deriving moments and, where possible, the distribution of this random variable over a sphere for a general stationary random mosaic and for the specific random mosaics arising from the Poisson plane/line process and the Dirichlet tessellation.

Given data about the positions of plants in a seed tray from two different species together with a yield (seed number) for each plant of one of the species, there are a number of aspects concerning plant position and yield which we shall investigate. These include the evidence of a trend in the positions of plants of a particular species, whether there is any attraction or inhibition between species, and whether there is any correlation between plant position and yield. An interesting question is whether there is any correlation between a plant's yield and its Dirichlet tile, since its Dirichlet tile will contain all the soil nutrients nearer to that plant than any other.

A real-valued random field is a suitably well-defined random function from $\mathbf{R}^N$ to $\mathbf{R}$, and a Gaussian random field is a random field whose joint distribution at any finite collection of points is multivariate Gaussian. If we needed to simulate a Gaussian random field at a given set of points, we could just simulate a multivariate normal random variable, but we may however need to simulate a Gaussian random field that can be evaluated anywhere. The existing methods approximate an isotropic Gaussian random field with a given covariance function by taking the average of a number of isotropic non-Gaussian random fields with the same covariance function. The method we shall give simulates a homogeneous, but not necessarily isotropic, Gaussian random field with a given covariance function by defining it in terms of a complex-valued stochastic integral, and then estimating the value of this integral.

Acknowledgements

I would like to thank all the staff and graduate students of the School of Mathematics at Bath University for their help with this thesis, especially Dr. Pam Davy. In particular, I would like to thank my supervisor, Professor Robin Sibson, and Dr. Henry Ford, who collected the plant data.

I also wish to thank the Science and Engineering Research Council for their financial support.

Contents

Introduction

Spatial patterns or spatially arranged sets of measurements occur widely. However, it is only in recent years that such spatial data has been analysed with regard to the spatial structure. Early attempts to analyse spatial data were usually centred on non-robust techniques, such as quadrat measures, for example Greig-Smith (1952). The quadrats could be randomly or systematically positioned. In the latter case the results of any statistical tests are heavily dependent on the origin and orientation of the quadrats, but the regular structure of the data allowed statistics to be easily calculated. Some more recent techniques were based on the spatial generalisations of well-known one dimensional techniques, for example regression or autocorrelation, Cliff and Ord (1973). It is only with the advent of modern computers that some spatial data sets can be adequately analysed, many by techniques that are qualitatively different from the usual one dimensional techniques. For example statistical tests involving Dirichlet tessellations have only been practical since the advent of the TILE4 computer package, see Green and Sibson (1978). In addition some of the basic machines of spatial data collection, like image analysers, are only feasible with a large amount of computing power. Naturally there has been much theoretical study of spatial probability as interest in random spatial problems has grown. Among the first modern studies of the subject were Bartlett's work on point and line processes, for example Bartlett (1964), and Miles' work on random polygons, Miles (1964). The subject of stochastic geometry was given a firm theoretical basis by the random set theory of Kendall and Matheron, Kendall (1974b) and Matheron (1975), which has led to much further work, particularly in stereology.

This thesis is concerned with various theoretical and practical problems in the field of spatial probability and statistics. The work studied falls naturally into three disjoint sections : random mosaics, the relationship between plant spacing and yield, and Gaussian random fields.

In the first section, we consider random mosaics. A mosaic is a tessellation in which each cell of the tessellation is assigned to one of a number of different phases, that is to say "coloured" one of a number of different colours. A random mosaic is a mosaic arising from a random tessellation and a random assignment of phases. Naturally, a random mosaic may be used to model physical situations, and we shall mainly be studying the two phase mosaic, which can be used to model data given in the form of the presence or absence of something in various different regions. The proportion in one phase over a region is known as the

volume/area/line fraction in stereology and is a random variable. Various analytical and asymptotic properties of this random variable for stationary mosaics, that is those random mosaics whose distributions are invariant under translations, will be derived, and we shall then proceed to study the proportion random variable of specific mosaics, the Poisson mosaic, determined by random lines in the plane, random planes in space etc., and the Dirichlet mosaic, determined by the Dirichlet tessellation of a set of points, and giving results for the proportion random variable for these mosaics. We shall conclude this section with a simulation study of the distribution of the proportion random variable of the Poisson mosaic.

In the second section, we are given data concerning the positions of plants in a seed tray from two different species of plants, and a yield, seed number, for one of the species. Using this data we shall be considering three statistical problems concerning the relationship between plant positions, and between plant positions and yield. The first statistical problem is whether there is any evidence of a trend in the positions of plants of either species. We shall be using a number of statistical tests to test for this, and to try to work out the underlying mechanism behind any trend. The second question is whether there is any attraction or repulsion between the plants of different species, and to try to calculate the distances between plants up to which attraction or repulsion occurs. The third question is whether there is any correlation between a plant's position and its yield. It is plausible that a plant will obtain its soil nutrients from any piece of soil nearer it than any other plant, that is to say a plant's Dirichlet tile in a Dirichlet tessellation constructed from the positions of all the plants. We shall be investigating the relationship between a plant's Dirichlet tile and its yield.

In the final section, we shall be considering Gaussian random fields. A real-valued random field is a suitably well-defined random function from $\mathbf{R}^N$ to $\mathbf{R}$. A Gaussian random field is a random field whose joint distribution at any finite collection of points is multivariate Gaussian. If we need to simulate a Gaussian random field at a given set of points, we can just simulate a multivariate normal random variable. We may however need an algorithm that returns a function that can be evaluated anywhere, rather than at a discrete set of values. Most of the existing methods approximate an isotropic Gaussian random field with a given covariance function by averaging a number of isotropic non-Gaussian random fields with the same covariance function. By considering the covariance function of a stationary Gaussian random field to be the characteristic function of some symmetric N-dimensional random variable, it is possible to define a complex stochastic integral function such that the real and imaginary parts of this integral function are independent anisotropic Gaussian random fields. We can then

evaluate the Gaussian random field at any point by evaluating a realisation of the stochastic integral function at that point. We can do this in one of two ways. Firstly, we can approximate the integral by its Riemann sum and then evaluate this sum, and secondly, we can use a Monte-Carlo simulation approach to simulate the random integral.

Stationary Mosaic Processes

1. Introduction

One of the least studied classes of spatial patterns are those in which two or more phases form a mosaic. Mosaics can occur in a number of different ways ; examples in two dimensions include patterns of vegetation and geological maps and in three dimensions rock grains and pores. In addition, it is also possible that a point process may be clustered in such a manner so the empty and full regions of space give the appearance of a mosaic. Since there is no obvious candidate for modelling random mosaics, in the sense that the Poisson point process is used for modelling random point processes, there is a far wider class of models available for modelling the clustered point pattern as a mosaic rather than as a point pattern. We shall be considering two-phase mosaics, probably the most useful as they can be used either for the point pattern described above or for data given in the form of presence or absence from a collection of regions, and in particular the proportion in one phase in a sphere.

In order to describe a random mosaic, we need to be able to describe the process of the division of space into regions and the assignment of phases. We shall be assuming that the division of space is performed by polyhedral segments, and it may be possible to approximate other divisions of space by curved surfaces by such a division process. We shall also be making the assumption that the phase of any region is independent of the phase of any other region. Under this assumption, by combining phases, it is possible to derive results for n-phase mosaics from the results for two-phase mosaics. Mosaic processes may be susceptible to analysis using random set theory, as developed by Kendall and Matheron, Kendall (1974b) and Matheron (1975), but it is almost certainly easier to use the conditions imposed by the model directly. In the next section we shall formalise the idea of a mosaic and give some of the basic properties of the proportion random variable, and in Section 3 the asymptotic distribution of the proportion random variable as the sphere size increases. The later sections will be concerned with the properties of particular kinds of mosaic, as determined by their division of space. These are described below.

Lower dimensional cross-sections of mosaics give rise to mosaics, and the theory of reconstructing some mosaics from their cross-sections has been studied in Stereology, for example in the well-known Wicksell problem, Wicksell (1925). In the later sections, we shall be considering two types of mosaics which arise

from divisions of space with good sectioning properties. There are naturally many models for the random division of space, for example Miles (1972),(1973) and (1974), but the two divisions we shall be considering are the higher dimensional extension of the division of the plane by Poisson lines, (lines that are uniformly distributed in the plane), which gives the Poisson mosaic, and the Dirichlet tessellation of a Poisson point process, where a region consists of all points nearer to one Poisson point than any other, giving the Dirichlet mosaic. These two division processes are the most tractable mathematically and have useful sectioning properties. The cross-section of a Poisson hyperplane process is a lower dimensional Poisson hyperplane process, and the cross-section of a Dirichlet tessellation is a generalised Dirichlet tessellation.

Both these mosaic processes can be used for modelling physical situations. The Poisson line process could be used to model ditches, which could be assumed to be straight lines over small distances, and hence the Poisson mosaic could be used as a model for presence or absence of a particular species of plant in the regions defined by the ditches. It has been studied extensively by Pielou, Pielou (1964),(1965) and (1977), in this context. The Dirichlet mosaic can be used to model the area of nutrients available to one species of plant rather than another, under the assumption that a plant uses only those nutrients nearer to it than to any other plant.

We shall be considering the Poisson mosaic in Sections 4 and 5, and the Dirichlet mosaic in Section 6. We shall be concluding in Section 7 with a simulation study of the Poisson mosaic.

2. The Mosaic Process

Let $(r,\varphi_1,\ldots,\varphi_{N-1})$ be spherical polar coordinates in $\mathbf{R}^N$, where $r\geq 0$, $0\leq\varphi_1<2\pi$ and $0\leq\varphi_i<\pi$ for $i=2,\ldots,(N-1)$. For $N>1$, there exists a function J_N, defined recursively by

$$J_2(\varphi_1) = 1$$

$$J_N(\varphi_1,\ldots,\varphi_{N-1}) = \sin^{N-2}\varphi_{N-1}\, J_{N-1}(\varphi_1,\ldots,\varphi_{N-2}) , \qquad (2.1)$$

such that the uniform distribution of points in $\mathbf{R}^N$ is given by

$$r^{N-1}J_N(\varphi)\, dr d\varphi ,$$

and, of course,

$$r^{N-1}J_N(\varphi)$$

is just the Jacobian of the transformation from Cartesian coordinates to spherical

polars in $\mathbf{R}^N$. Then, the unit ball Q_N has surface $(N-1)$-content

$$S_N = \int_{\partial Q_N} J_N(\varphi)\, d\varphi = \frac{N\pi^{\frac{1}{2}N}}{\Gamma(\frac{1}{2}N+1)}\ , \tag{2.2}$$

and N-content

$$\alpha_N = \int_{\partial Q_N}\int_0^1 r^{N-1}\, J_N(\varphi)\, dr d\varphi = \frac{S_N}{N} = \frac{\pi^{\frac{1}{2}N}}{\Gamma(\frac{1}{2}N+1)}\ . \tag{2.3}$$

Suppose we let P_N denote the set of all bounded open convex polyhedra in $\mathbf{R}^N$, then following Stoyan et al. (1985), we can define a tessellation of $\mathbf{R}^N$ to be a subset of P_N, whose polyhedral members are pairwise disjoint, the union of whose closures fill the N-dimensional space, and which are locally finite. More formally, if B is any bounded subset of $\mathbf{R}^N$, then $\theta \subset P_N$ is a tessellation of $\mathbf{R}^N$ if the following three conditions are satisfied :

(i) $p_1, p_2 \in \theta$ and $p_1 \neq p_2 \ \Rightarrow\ p_1 \cap p_2 = \varnothing$;

(ii) $\bigcup_{p\in\theta} \bar{p} = \mathbf{R}^N$;

(iii) if $B \subset \mathbf{R}^N$ is bounded, then $\#\{\, p\in\theta \mid p \cap B \neq \varnothing \,\}$ is finite.

Thus a tessellation of $\mathbf{R}^N$ is a partition of $\mathbf{R}^N$ by hyperplane sections into countably many regions (connected non-empty subsets of $\mathbf{R}^N$). If each region is assigned to one of n phases we obtain an n-phase *mosaic*. For two phase mosaics we can call these phases phase 0 and phase 1.

We can now define an *independent* mosaic to be one whose regions exhibit pairwise independence. To obtain an independent mosaic of two phases, we can allocate a region to phase 1 with probability p, and phase 0 with probability $q=1-p$, independently of any other region. Let

$$Z(\mathbf{x}) = \begin{cases} 0 & \text{if } \mathbf{x} \text{ in phase 0} \\ 1 & \text{if } \mathbf{x} \text{ in phase 1} \end{cases} \tag{2.4}$$

so Z is an indicator variable, with

$$\mathbf{P}\{Z(\mathbf{x})=0\}=q \quad \text{and} \quad \mathbf{P}\{Z(\mathbf{x})=1\}=p\ .$$

Then we can define V_λ, the proportion in phase 1 over a sphere of radius λ, by

$$V_\lambda = \frac{1}{\alpha_N}\lambda^N \int_{\lambda Q_N} Z(\mathbf{x})\, d\mathbf{x}\ . \tag{2.5}$$

The mean of V_λ can then be evaluated using Fubini's Theorem,

$$\mathrm{E}(V_\lambda) = \frac{1}{\alpha_N}\mathrm{E}\left\{\int_{Q_N} Z\right\} = \frac{1}{\alpha_N}\int_{Q_N}\mathrm{E}\{Z\} = p \ . \qquad (2.6)$$

Generally, we shall be interested in the proportion over a unit sphere, $V=V_1$.

Clearly V_λ is a random variable taking values in the range [0,1] and having discrete masses at 0 and 1.

If the boundary between two phases is assigned to phase 1 we obtain a random closed set, as first defined by Kendall (1974b), and Matheron (1975). These are formally defined in the following manner.

Suppose $\mathbf{F}$ is the family of closed subsets of $\mathbf{R}^N$, then for any compact subset of $\mathbf{R}^N$, K, we can define $\mathbf{F}_K$ by

$$\mathbf{F}_K = \{\ F\in\mathbf{F} \mid F\cap K\neq\varphi\ \} \ ,$$

that is to say $\mathbf{F}_K$ contains precisely the members of $\mathbf{F}$ that "hit" K. If we let $\mathcal{F}$ denote the smallest σ-algebra of subsets of $\mathbf{F}$ that contains all the $\mathbf{F}_K$, then $\mathcal{F}$ is the Borel σ-algebra on $\mathbf{F}$ with respect to a suitable topology. A *random closed set* is a random variable taking values in $(\mathbf{F},\mathcal{F})$ and hence generates a distribution on $(\mathbf{F},\mathcal{F})$ which is called the distribution of the random closed set. This definition naturally gives rise to two classes of random closed sets, the stationary random closed sets, whose distributions are invariant under translations, and the isotropic random closed sets, whose distributions are invariant under translations and rotations.

We are interested in those mosaics which are invariant under these transformations, in particular those invariant under translation, the stationary mosaics, and those invariant under translation and rotation, and the isotropic mosaics. We can define these formally as follows.

A mosaic is *stationary* if the underlying division process is stationary, and the probability of a region being in phase 1 is constant.

A mosaic is *isotropic* if it is a stationary mosaic and the division process is isotropic.

Note that these definitions are consistent with random set theory in the sense that a stationary mosaic is a stationary random closed set and an isotropic mosaic is an isotropic random closed set.

Of course V_λ is of interest in stereological problems and is generally known as the volume, area or line fraction. In many problems parallel slices through the medium will be taken perpendicular to some arbitrarily-oriented axis. For each

slice the line or area fraction will be measured and these will then be analysed to estimate the area or volume fraction respectively. We shall show in the following lemma that, for a stationary mosaic, subject to a technical condition on the orientation of the region boundaries (or facets), the line or area fractions vary continuously along this axis.

The orientation of a facet, that is to say the angles the normal from the origin to the facet makes with $(N-1)$ of the co-ordinate axes, is an $(N-1)$-dimensional random variable, and can obviously be represented as a point on the surface of Q_N, the unit N-sphere. We shall call a mosaic *non-atomic* if joint distribution of the orientations of any finite collection of facets is continuous or non-atomic on the surface of Q_N.

If we define $W_{N-1}(z)$ to be the proportion in phase 1 over a unit $(N-1)$-sphere in the $x_N=z$ plane centred on the point $(0,\ldots,0,z)$ with respect to some arbitrary orientation of the co-ordinate axes, then we can show that W_{N-1} varies continuously as a sample function.

Lemma.

For a stationary non-atomic mosaic,

$$\mathbf{P}\ \{\ W_{N-1} \text{ is continuous everwhere }\}\ =\ 1.$$

Proof.

Suppose $\mathbf{P}_{i_F}$ denotes the orthogonal projection of $\mathbf{R}^N$ onto a facet F, then $\mathbf{P}_{i_F}x_N$ is a line in F. We can define the angle between the facet F and the x_N axis to be the angle between $\mathbf{P}_{i_F}x_N$ and x_N. For a non-atomic mosaic, this angle is a continuous random variable.

Consider the open bounded cylinder defined by

$$C\ =\ \{\ (x_1,\ldots,x_N)\in\mathbf{R}^N\ \mid\ \sum_1^{N-1} x_i^2<1\ ,\ |x_N|<1\ \}\ ,$$

then, because a mosaic is locally finite, there are only finitely many regions in C, and hence only finitely many facets in C. For k facets in N-dimensional space to intersect in a point we require that $k\geq N$, and hence there will only be finitely many intersections of N or more facets at a point inside C. Suppose there are n such points inside C, having x_N co-ordinates

$$-1 < z_1 < \ldots < z_n < 1\ ,$$

say.

On (z_i,z_{i+1}) $[i=1,\ldots,n-1]$, the cross-sectional slices change shape but not structure, whereas at z_i the structure of the cross-section changes. Suppose we have L facets in the cylinder

$$\{ (x_1,\ldots,x_N) \mid \sum_{1}^{N-1} x_i^2 < 1 \ , \ z_{i-1} < x_N < z_i \} \ ,$$

making angles $\theta_1,\ldots,\theta_L$ with the x_N axis respectively. If $z \in (z_i,z_{i+1})$ and $h>0$ such that $(z-h,z+h) \subset (z_i,z_{i+1})$, then

$$| W_{N-1}(z \pm h) - W_{N-1}(z) | \ \leq \ h\alpha_{N-1} \sum_{j=1}^{L} \tan\theta_j \ , \qquad (2.7)$$

where $\alpha_0=1$. However, for a non-atomic mosaic the joint distribution of $\{\theta_j\}$ $(j=1,\ldots,L)$ is continuous, so in particular, $\theta_j \neq \pi/2$ almost surely. Hence the sum in (2.7) is almost surely finite and so

$$| W_{N-1}(z \pm h) - W_{N-1}(z) | \ = \ O(h) \quad \text{almost surely.}$$

Thus W_{N-1} is uniformly continuous on each (z_i,z_{i+1}) almost surely, and similarly on $(-1,z_1)$ and $(z_n,1)$.

We can write down a similar expression to (2.7) for z_i. Suppose $h<z_{i+1}-z_i$, then

$$| W_{N-1}(z_i+h) - W_{N-1}(z_i) | \ \leq \ h\alpha_{N-1} \sum_{j=1}^{L} \tan\theta_j \ ,$$

and so

$$| W_{N-1}(z_i+h) - W_{N-1}(z_i) | \ = \ O(h) \quad \text{almost surely.}$$

Thus, W_{N-1} is right continuous at z_i almost surely. Almost sure left continuity at z_i follows similarly, so W_{N-1} is continuous at z_i almost surely. It follows that W_{N-1} is almost surely continuous on some open neighbourhood of z_i, and so W_{N-1} is almost surely continuous on a finite number of open sub-intervals of $(-1,1)$ which cover $(-1,1)$. W_{N-1} is therefore almost surely continuous on $(-1,1)$ and hence on $\mathbf{R}$. Note that the proof of this lemma applies to non-convex mosaics as well. □

Because $\mathrm{E}(V_\lambda)=p$, (see (2.6)), the first order properties do not yield any information about the structure of a mosaic, so the second moment properties of mosaics will obviously be of interest to us. These are best summarised by means of the *covariance function*. In general this is a function $C:\mathbf{R}^{2N} \to \mathbf{R}$, which is defined by

$$C(\mathbf{x},\mathbf{y}) = \mathrm{Cov} \ (\ Z(\mathbf{x}),Z(\mathbf{y}) \ ) = \mathrm{E} \ [\ Z(\mathbf{x})Z(\mathbf{y}) \ ] - p^2 \ ,$$

but, for a stationary mosaic, we can rewrite the covariance function as $C:\mathbf{R}^N \to \mathbf{R}$,

where

$$C(\mathbf{x}-\mathbf{y}) = \mathrm{Cov}\ (\ Z(\mathbf{x}),Z(\mathbf{y})\ ) = \mathbf{E}\ [\ Z(\mathbf{x})Z(\mathbf{y})\ ] - p^2\ .$$

If we let $A(\mathbf{z}_1,\ldots,\mathbf{z}_k)$ denote the event that $\mathbf{z}_1,\ldots,\mathbf{z}_k$ are all in the same region, with respect to the underlying division process, then we can define a function $Q:\mathbf{R}^N \rightarrow [0,1]$ as

$$Q(\mathbf{x}) = \mathbf{P}\ [\ A(\mathbf{0},\mathbf{x})\ ]\ .$$

So for a stationary mosaic $Q(\mathbf{x})$ is just the probability that two points separated by $\mathbf{x}$ are in the same region. The functions Q and C are simply related since

$$\begin{aligned} C(\mathbf{x}) &= \mathbf{E}\ [\ Z(\mathbf{x})Z(\mathbf{0})\ ] - p^2 = p\ \mathbf{E}\ [\ Z(\mathbf{x})\ |\ Z(\mathbf{0}=1)\ ] - p^2 \\ &= p\ [\ Q(\mathbf{x}) + p(1-Q(\mathbf{x}))\ ] - p^2 = p^2 + pqQ(\mathbf{x}) - p^2 \\ &= pqQ(\mathbf{x}) \quad (\text{where } q=1-p)\ . \end{aligned}$$

The following lemma gives one of the simplest and most useful properties of the function C for a stationary mosaic.

Lemma.

For a stationary mosaic, Q, and hence C, are continuous functions.

Proof.

Let $L(\mathbf{x})$ be the event that the intersection of the division process and the line segment $[\mathbf{0},\mathbf{x}]$ is non-empty, ie. a region boundary crosses the line segment $[\mathbf{0},\mathbf{x}]$. Then, if $\mathbf{x}_0 \in \partial Q_N$ and $h>k>0$, then

$$L(k\mathbf{x}_0) \subseteq L(h\mathbf{x}_0)\ ,$$

and so

$$0 \leq \mathbf{P}[L(k\mathbf{x}_0)] \leq \mathbf{P}[L(h\mathbf{x}_0)]\ .$$

Thus,

$$\mathbf{P}\ [\ L(h\mathbf{x}_0)\ ] \rightarrow 0 \quad \text{as} \quad h \rightarrow 0\ ,$$

for if not, then the origin is part of the division process with a non-zero probability and the mosaic will be non-stationary. If ^{c} denotes complementation then, conditioning on the event $L(h\mathbf{x}_0)$,

$$\begin{aligned} \mathbf{P}\ [\ A(\mathbf{0},h\mathbf{x}_0)^c\ ] &= \mathbf{P}\ \{\ A(\mathbf{0},h\mathbf{x}_0)^c\ |\ L(h\mathbf{x}_0)^c\ \}\ \mathbf{P}\ [\ L(h\mathbf{x}_0)^c\ ] \\ &\quad + \mathbf{P}\ \{\ A(\mathbf{0},h\mathbf{x}_0)^c\ |\ L(h\mathbf{x}_0)\ \}\ \mathbf{P}\ [\ L(h\mathbf{x}_0)\ ] \\ &\leq \mathbf{P}\ \{\ A(\mathbf{0},h\mathbf{x}_0)^c\ |\ L(h\mathbf{x}_0)\ \}\ \mathbf{P}\ [\ L(h\mathbf{x}_0)\ ] \end{aligned}$$

$$\leq \mathbf{P}\,[L(hx_0)] \to 0 \quad \text{as} \quad h \to 0 \ .$$

Thus

$$Q(hx_0) = \mathbf{P}\,[\,A(\mathbf{0},hx_0)\,]$$

$$= 1 - \mathbf{P}\,[\,A(\mathbf{0},hx_0)^c\,] \to 1 \quad \text{as} \quad h \to 0 \ ,$$

and hence

$$Q(\mathbf{x}) \to 1 \quad \text{as} \quad |\mathbf{x}| \to 0 \ ,$$

since $\mathbf{x}_0 \in \partial Q_N$ was arbitrary.

However

$$Q(\mathbf{x}) = \mathbf{P}\,[\,A(\mathbf{0},\mathbf{x})\,]$$

$$= \mathbf{P}\,[\,A(\mathbf{0},\mathbf{x}) \cap A(\mathbf{x},\mathbf{y})\,] + \mathbf{P}\,[\,A(\mathbf{0},\mathbf{x}) \cap A(\mathbf{x},\mathbf{y})^c\,]$$

$$= \mathbf{P}\,[\,A(\mathbf{0},\mathbf{x}) \cap A(\mathbf{x},\mathbf{y})\,] + \mathbf{P}\,[\,A(\mathbf{0},\mathbf{x}) \mid A(\mathbf{x},\mathbf{y})^c\,]\,\{\,1 - Q(\mathbf{x}-\mathbf{y})\,\}$$

$$= \mathbf{P}\,[\,A(\mathbf{0},\mathbf{x},\mathbf{y})\,] + \mathbf{P}\,[\,A(\mathbf{0},\mathbf{x}) \mid A(\mathbf{x},\mathbf{y})^c\,]\,\{\,1 - Q(\mathbf{x}-\mathbf{y})\,\} \ ,$$

and similarly,

$$Q(\mathbf{y}) = \mathbf{P}\,[\,A(\mathbf{0},\mathbf{x},\mathbf{y})\,] + \mathbf{P}\,[\,A(\mathbf{0},\mathbf{y}) \mid A(\mathbf{x},\mathbf{y})^c\,]\,\{\,1 - Q(\mathbf{x}-\mathbf{y})\,\} \ .$$

Hence

$$|\,Q(\mathbf{x}) - Q(\mathbf{y})\,| = \{\,1 - Q(\mathbf{x}-\mathbf{y})\,\}\,|\,\mathbf{P}\,[\,A(\mathbf{0},\mathbf{x}) \,|\, A(\mathbf{x},\mathbf{y})^c\,] - \mathbf{P}\,[\,A(\mathbf{0},\mathbf{y}) \,|\, A(\mathbf{x},\mathbf{y})^c\,]\,|$$

$$\leq 2\,\{\,1 - Q(\mathbf{x}-\mathbf{y})\,\} \to 0 \quad \text{as} \quad \mathbf{y} \to \mathbf{x} \ .$$

Thus Q, and hence C, are continuous functions. □

3. Asymptotic Distribution

The asymptotic distribution of a process which has a circle radius tending to infinity will be of interest to us. For a stationary mosaic, this is the same as re-scaling the intensity, not necessarily linearly, and considering the asymptotic distribution as the intensity increases. We showed in (2.6) that the mean of V_λ is p for all λ, ~~so~~ again we are interested in the second order properties.

If we let R be the content of a region and R_0 the content of a region containing a specified point, say the origin, then as Gilbert (1962) argued

$$E[R_0] = \frac{E[R^2]}{E[R]} \ , \tag{3.1}$$

essentially because a larger region has a proportionately larger chance of

containing the origin. However

$$E[R_0] = E\int_{R_0} d\mathbf{x} = \int_{R^N} Q(\mathbf{x})d\mathbf{x} \quad ,$$

and therefore

$$\int_{R^N} C(\mathbf{x})d\mathbf{x} = \frac{pqE[R^2]}{E[R]} \quad . \tag{3.2}$$

Hence Q and the covariance function, C, are integrable if and only if the second moment of region content exists.

We can derive an expression for the variance by noting that

$$E[(\lambda^N\alpha_N)V_\lambda^2] = \frac{1}{\lambda^N\alpha_N}\int_{\lambda Q_N}\int_{\lambda Q_N} E[Z(\mathbf{x})Z(\mathbf{y})]\, d\mathbf{x}d\mathbf{y} \quad ,$$

and so

$$Var[(\lambda^N\alpha_N)^{\frac{1}{2}}V_\lambda] = \frac{1}{\lambda^N\alpha_N}\int_{\lambda Q_N}\int_{\lambda Q_N} C(\mathbf{x}-\mathbf{y})\, d\mathbf{x}d\mathbf{y} \quad .$$

To simplify this, we can first define the region formed by the intersection of two N-spheres of radius r whose centres are a distance $2|\mathbf{z}|$ apart,

$$R_N(\mathbf{z},r) = \{\mathbf{v}:|\mathbf{v}+\mathbf{z}|<r\}\cap\{\mathbf{v}:|\mathbf{v}-\mathbf{z}|<r\} \qquad [|\mathbf{z}|<r] \ ,$$

having N-content $A_N(|\mathbf{z}|,r)$ say. It is now a matter of making the substitutions $\mathbf{z}=(\mathbf{x}-\mathbf{y})$ and $\mathbf{v}=(\mathbf{x}+\mathbf{y})$ to obtain

$$Var[(\lambda^N\alpha_N)^{\frac{1}{2}}V_\lambda] = \frac{1}{(2\lambda)^N\alpha_N}\int_{2\lambda Q_N}\int_{R_N(|\mathbf{u}|,2\lambda)} C(\mathbf{v})\, d\mathbf{u}d\mathbf{v}$$

$$= \int_{2\lambda Q_N} \frac{A_N(|\mathbf{v}|,2\lambda)}{(2\lambda)^N\alpha_N} C(\mathbf{v})\, d\mathbf{v} \quad . \tag{3.3}$$

Since $R_N(\mathbf{v},2\lambda)$ is contained in an N-sphere of radius 2λ, we have

$$A_N(|\mathbf{v}|,2\lambda) \le (2\lambda)^N\alpha_N \quad ,$$

so, from (3.3), we have

$$Var[(\lambda^N\alpha_N)^{\frac{1}{2}}V_\lambda] \le \int_{2\lambda Q_N} C(\mathbf{v})\, d\mathbf{v} \quad .$$

However $R_N(\mathbf{v},2\lambda)$ itself contains an N-sphere of radius $2\lambda-|\mathbf{v}|$, so

$$A_N(|\mathbf{v}|,2\lambda) \ge (2\lambda-|\mathbf{v}|)^N\alpha_N \quad ,$$

and hence

$$\int_{2\lambda Q_N}\left[1-\frac{|\mathbf{v}|}{2\lambda}\right]^N C(\mathbf{v})\, d\mathbf{v} \le Var[(\lambda^N\alpha_N)^{\frac{1}{2}}V_\lambda] \le \int_{2\lambda Q_N} C(\mathbf{v})\, d\mathbf{v} \quad .$$

Trivially, as $\lambda\to\infty$,

$$\int_{2\lambda Q_N} C(\mathbf{v})\, d\mathbf{v} \to \int_{\mathbf{R}^N} C(\mathbf{v})\, d\mathbf{v} \quad ,$$

and, with C as the dominating function, the dominated convergence theorem shows that the lower bound also has the same limit as $\lambda \to \infty$ Thus, as $\lambda \to \infty$,

$$Var[(\lambda^N \alpha_N)^{\frac{1}{2}} V_\lambda] = \int_{\mathbf{R}^N} C(\mathbf{x}) d\mathbf{x} = \frac{pqE[R^2]}{E[R]} \quad ,$$

and hence

$$Var[V_\lambda] \sim \frac{pqE[R^2]}{E[R]} \frac{1}{\lambda^N \alpha_N} \quad \text{as } \lambda \to \infty \, . \tag{3.4}$$

For some cases, it may be possible to show that V_λ is asymptotically normally distributed, by using a higher dimensional extension of Billingsley's one dimensional φ-mixing processes, Billingsley (1968), and then using a theorem of Baddeley's about the asymptotic distribution of higher dimensional φ-mixing random processes, Baddeley (1980).

We can define higher dimensional φ-mixing processes as follows. Let ξ be a real-valued random field, that is separable and measurable, on $\mathbf{R}^N$. Let $\mathbf{B}(S)$ denote the σ-algebra generated by $\{\xi(\mathbf{x}):\mathbf{x}\in S\}$ for each Borel set $S\subset\mathbf{R}^N$, and consider the half-space index sets with incomplete intervals in the i^{th} place, $1\le i\le k$.

$$L_i = \mathbf{R}\times\ldots\times\mathbf{R}\times(-\infty,0]\times\mathbf{R}\times\ldots\times\mathbf{R}$$

$$R_i(r) = \mathbf{R}\times\ldots\times\mathbf{R}\times[r,\infty)\times\mathbf{R}\times\ldots\times\mathbf{R} \quad .$$

Let $A\in\mathbf{B}(L_i)$ and $B\in\mathbf{B}(R_i(r))$, then, we shall say that ξ is φ-mixing if there exists a monotonically decreasing function $\varphi:\mathbf{R}^+\to[0,1]$ with asymptote zero such that

$$|\mathbf{P}(B \cap A) - \mathbf{P}(A)\mathbf{P}(B)| \le \varphi(r)\mathbf{P}(A) \tag{3.5}$$

In other words, a φ-mixing process is one in which "distant" events are virtually independent, and φ gives a rate of convergence to independence.

To show asymptotic normality, we can use Baddeley's Theorem 1 (corrected).

Theorem (Baddeley).

If ξ is a zero-mean stationary φ-mixing process on $\mathbf{R}^N$, and

$$\int_0^\infty \varphi(t)^{\frac{1}{2}} t^{N-1} dt < \infty \, , \text{ then}$$

$$\sigma^2 = \int_{\mathbf{R}^N} E\{\xi(\mathbf{x})\xi(0)\}\, d\mathbf{x} \text{ converges, and}$$

$$(\alpha_N \lambda^N)^{-\frac{1}{2}} \int_{\lambda Q_N} \xi(\mathbf{x}) d\mathbf{x} \xrightarrow{D} N\left[0,\sigma^2\right] \quad \text{as } \lambda \to \infty \, . \tag{3.6}$$

If we let $\xi(\mathbf{x})=Z(\mathbf{x})-p$, then clearly ξ has zero mean and is φ-mixing, so if

$$\int_0^\infty \varphi(t)^{\frac{1}{2}} t^{N-1} dt < \infty \ ,$$

then

$$(\alpha_N \lambda^N)^{-\frac{1}{2}} \int_{\lambda Q_N} \xi(\mathbf{x}) d\mathbf{x} \xrightarrow{D} N\left[0,\sigma^2\right] \text{ as } \lambda \to \infty \ ,$$

where, from (3.2),

$$\sigma^2 = \frac{pqE[R^2]}{E[R]} \ ,$$

and hence we have the following corollary.

Corollary.

Let Z be a stationary mosaic on $\mathbf{R}^N$, with region content R, taking the value 1 with probability p and 0 with probability $q=1-p$. If Z is φ-mixing, where φ satisfies

$$\int_0^\infty \varphi(t)^{\frac{1}{2}} t^{N-1} dt < \infty \ ,$$

then

$$V_\lambda = \frac{1}{\alpha_N \lambda^N} \int_{\lambda Q_N} Z(\mathbf{x}) d\mathbf{x}$$

has an asymptotic distribution as $\lambda \to \infty$ of

$$N\left[p, \frac{pqE[R^2]}{E[R]} \frac{1}{\lambda^N \alpha_N}\right] \ \square \qquad (3.7)$$

4. The Poisson Mosaic

The Poisson mosaic can be defined in the following way. We can identify the Poisson Hyperplane process, parameter λ, in $\mathbf{R}^N$ with a Poisson Point process on the surface of the unit half-cylinder

$$\{ (x_1,\ldots,x_{N+1}) \in \mathbf{R}^{N+1} \mid \sum_1^N x_i^2 = 1 \ , \ x_{N+1} > 0 \} \ ,$$

by identifying a hyperplane with the polar coordinates of its nearest point to the origin, as explained by Kendall (1974a). Then the Poisson hyperplane process in $\mathbf{R}^N$ has as an element of measure

$$\lambda J_N(\varphi) d\varphi dr \ ,$$

so the measure of hyperplanes intersecting Q_N is

$$\lambda \int_0^1 \int_{\partial Q_N} J_N(\varphi)\, d\varphi dr = \lambda S_N \ .$$

Of course, this is just the measure of hyperplanes from a process of unit parameter intersecting an N-sphere. Hence, V_λ is both the distribution of the proportion in phase 1 of either a process with unit parameter over λQ_N or of a process with parameter λ over Q_N.

The mean of V_λ is p, (see (2.6)), and we can calculate the variance from (3.3),

$$\begin{aligned} Var\ (V_\lambda) &= \frac{1}{\alpha_N} \int_{2Q_N} \frac{A_N(|\mathbf{v}|,2)}{2^N \alpha_N}\, C(\mathbf{v})\, d\mathbf{v} \\ &= \frac{1}{\alpha_N} \int_{2Q_N} \frac{A_N(|\mathbf{v}|,2)}{2^N \alpha_N}\, C(\mathbf{v})\, d\mathbf{v} \\ &= \frac{1}{\alpha_N^2} \int_{Q_N} A_N(|\mathbf{u}|,1) C(2\mathbf{u})\, d\mathbf{u} \\ &= \frac{pq}{\alpha_N^2} \int_{Q_N} A_N(|\mathbf{u}|,1) Q(2\mathbf{u})\, d\mathbf{u} \ . \end{aligned}$$

The intersection of a Poisson hyperplane process with a line gives a Poisson point process, and in order to give an explicit form for Q we need to evaluate the parameter of this process. We can do this using Minkowski's functionals or quermassintegrales (mean cross-sectional measures). These are defined for a convex body K as follows. Suppose μ_r denotes r-dimensional measure and S is a uniformly distributed r-dimensional direction. If $\mathbf{P}_{i_S}$ denotes a projection onto the $(N-r)$-dimensional subspace determined by S, then we can define

$$\Psi_r(K) = \mathbf{E}\ [\ \mu_{N-r}(\mathbf{P}_{i_S} K)\ ] \quad \text{for } 0<r<N \ ,$$

$$\text{with} \quad \Psi_0(K) = \mu_N(K) \ .$$

The r^{th} Minkowski functional is then defined to be

$$W_r(K) = \frac{\alpha_N}{\alpha_{N-r}}\, \Psi_r(K) \quad \text{for } 0 \le r < N \ ,$$

$$\text{and} \quad W_N(K) = \alpha_N \ .$$

The r^{th} Minkowski functional is an $(N-r)$-dimensional invariant measure under rigid motions of N-dimensional space. Thus,

$$W_{N-1}(Q_N) = \alpha_N \ ,$$

and if K is a line of unit length then

$$W_{N-1}(K) = \frac{\alpha_{N-1}}{N} \quad .$$

We are now in a position to evaluate the probability that a random $(N-1)$-plane in Q_N hits a line of unit length in Q_N by using Santalo's (14.11),

$$\mathbf{P}\ \{\ (N-1)\text{-plane hits unit line}\ |\ (N-1)\text{-plane hits } Q_N\ \} = \frac{W_{N-1}(K)}{W_{N-1}(Q_N)} = \frac{\alpha_{N-1}}{S_N} \quad .$$

Thus the Poisson point process along any unit line is of intensity $\frac{\alpha_{N-1}}{S_N}\lambda$, and hence

$$Q(\mathbf{x}) = \mathbf{P}\ [\ \text{No points in } (\mathbf{0},\mathbf{x})\ ] = e^{-\frac{\alpha_{N-1}}{S_N}\lambda|\mathbf{x}|} \quad . \tag{4.1}$$

So we have

$$Var\ [V] = \frac{pq}{\alpha_N^2} \int_{Q_N} A_N(|\mathbf{u}|,1) \exp\left[-2\lambda\frac{\alpha_{N-1}}{S_N}|\mathbf{u}|\right] d\mathbf{u}$$

$$= \frac{Npq}{\alpha_N} \int_0^1 A_N(r,1) \exp\left[-2\lambda\frac{\alpha_{N-1}}{S_N}r\right] dr \quad . \tag{4.2}$$

Now for $0 \le r \le 1$, we have

$$A_1(r,1) = 2\ (1-r) \tag{4.3}$$

$$A_2(r,1) = 2\ [\arccos r - r(1-r^2)^{\frac{1}{2}}] \tag{4.4}$$

$$A_3(r,1) = \frac{2\pi}{3}\ (2-3r+r^3) \ . \tag{4.5}$$

In particular, in one dimension, we have

$$\mathrm{Var}(V) = 2pq\int_0^1 (1-r)e^{-\lambda r}dr = \frac{2pq}{\lambda}\left\{1-\frac{1}{\lambda}\left[1-e^{-\lambda}\right]\right\}, \tag{4.6}$$

and in three dimensions,

$$\mathrm{Var}(V) = 12pq\int_0^1 (2r^2-3r^3+r^5)e^{-\frac{1}{2}\lambda r}dr \tag{4.7}$$

$$= \frac{384pq}{\lambda^3}\left\{1-\frac{9}{\lambda}+\frac{240}{\lambda^3}\right\} + \frac{576pqe^{-\frac{1}{2}\lambda}}{\lambda^3}\left\{1+\frac{14}{\lambda}-\frac{80}{\lambda^2}-\frac{160}{\lambda^3}\right\}.$$

In two dimensions, we have

$$\mathrm{Var}(V) = \frac{16pq}{\pi}\int_0^1 [\arccos r - r(1-r^2)^{\frac{1}{2}}]re^{-\rho r}\,dr \ ,$$

where $\rho = \frac{2\lambda}{\pi}$. Now,

$$\int_0^1 re^{-\rho r}\arccos r\,dr = \frac{\pi}{2\rho^2} - \int_0^1 \left[\frac{r}{\rho}+\frac{1}{\rho^2}\right]e^{-\rho r}(1-r^2)^{-\frac{1}{2}}\,dr$$

$$= \frac{\pi}{2\rho^2} - \frac{1}{\rho}\int_0^{\pi/2}\sin\theta e^{-\rho\sin\theta}d\theta - \frac{1}{\rho^2}\int_0^{\pi/2}e^{-\rho\sin\theta}d\theta$$

$$= \frac{\pi}{2\rho^2} + \frac{1}{\rho}F'(\rho) - \frac{1}{\rho^2}F(\rho)\ ,$$

where

$$F(\rho) = \int_0^{\pi/2}e^{-\rho\sin\theta}d\theta\ . \tag{4.8}$$

Note that we can differentiate F under the integral sign as many times as we please since all the derivatives of $e^{-\rho\sin\theta}$ are bounded on $[0,\frac{1}{2}\pi]$. Similarly,

$$\int_0^1 r^2e^{-\rho r}(1-r^2)^{\frac{1}{2}}dr = \frac{2}{\rho^3} - \int_0^1 e^{-\rho r}\left[\frac{r^3}{\rho}+\frac{2\rho^2}{\rho^2}+\frac{2r}{\rho^3}\right](1-r^2)^{-\frac{1}{2}}dr$$

$$= \frac{2}{\rho^3} + \frac{1}{\rho}F'''(\rho) - \frac{2}{\rho^2}F''(\rho) + \frac{2}{\rho^3}F'(\rho)\ .$$

Thus, we have the following expression for the variance,

$$\mathrm{Var}(V) = \frac{16pq}{\pi}\left\{\frac{\pi}{2\rho^2}-\frac{2}{\rho^3}-\frac{1}{\rho^2}F(\rho)+\left[\frac{1}{\rho}-\frac{2}{\rho^3}\right]F'(\rho)+\frac{2}{\rho^2}F''(\rho)-\frac{1}{\rho}F'''(\rho)\right\}.$$

However, we can manipulate the integral form of F'' to obtain a differential equation for F.

$$F''(\rho) = \int_0^{\pi/2}\sin^2\theta e^{-\rho\sin\theta}d\theta$$

$$= F(\rho) - \int_0^{\pi/2}\cos^2\theta e^{-\rho\sin\theta}d\theta$$

$$= F(\rho) - \frac{1}{\rho} + \frac{1}{\rho}\int_0^{\pi/2}\sin\theta e^{-\rho\sin\theta}d\theta$$

$$= F(\rho) - \frac{1}{\rho} - \frac{1}{\rho}F'(\rho)\ .$$

Thus, we have

$$\rho F''(\rho) + F'(\rho) - \rho F(\rho) = -1\ , \tag{4.9}$$

and

$$\rho F'''(\rho)+2F''(\rho)-\rho F'(\rho)-F(\rho) = 0\ .$$

So, the variance is given by

$$\mathrm{Var}(V) = \frac{16pq}{\pi}\left\{\frac{\pi}{2\rho^2} - \frac{4}{\rho^3} - \frac{2}{\rho^2}F(\rho) - \frac{2}{\rho^3}F'(\rho) + \frac{4}{\rho^2}F''(\rho)\right\}$$

$$= \frac{16pq}{\pi}\left\{\frac{\pi}{2\rho^2} - \frac{6}{\rho^3} + \frac{2}{\rho^2}F(\rho) - \frac{6}{\rho^3}F'(\rho)\right\}. \qquad (4.10)$$

Now, by uniform convergence,

$$F(\rho) = \int_0^{\pi/2} \sum_{k=0}^{\infty} (-1)^k \frac{\rho^k}{k!} \sin^k\theta \, d\theta = \sum_{k=0}^{\infty} (-1)^k \frac{\rho^k}{k!} \int_0^{\pi/2} \sin^k\theta \, d\theta$$

$$= \sum_{k=0}^{\infty} I_{2k} \frac{\rho^{2k}}{(2k)!} - \sum_{k=0}^{\infty} I_{2k+1} \frac{\rho^{2k+1}}{(2k+1)!} ,$$

where

$$I_k = \int_0^{\pi/2} \sin^k\theta \, d\theta .$$

Integration by parts for $k \geq 2$ gives us

$$kI_k = (k-1)I_{k-2} \text{ , with } I_0 = \frac{\pi}{2} \text{ and } I_1 = 1 .$$

Thus

$$I_{2k} = \frac{\pi}{2} \prod_{j=1}^{k} \frac{2j-1}{2j} = \frac{\pi}{2} \frac{(2k)!}{(2^k k!)^2} ,$$

and

$$I_{2k+1} = \prod_{j=1}^{k} \frac{2j}{2j+1} = (2j+1)! \prod_{j=1}^{k} (2j+1)^{-2} .$$

Hence,

$$F(\rho) = \frac{\pi}{2} \sum_{k=0}^{\infty} \frac{1}{(2^k k!)^2} \rho^{2k} - \sum_{k=0}^{\infty} \left[\prod_{j=1}^{k} \frac{1}{(2j+1)^2}\right] \rho^{2k+1} . \qquad (4.11)$$

The sum of even powers in (4.11) is the first kind zero order Bessel function, which we might expect since the reduced equation of (4.9) is the zero order differential Bessel equation.

We now have an explicit formula for the variance given by (4.10) and (4.11), where $\rho = \frac{2\lambda}{\pi}$. In particular, we can derive the asymptotic variance as $\rho \to \infty$ by using Jordan's inequality,

$$\theta \frac{\sin\varphi}{\varphi} \leq \sin\theta \leq \theta \quad \text{for } 0 \leq \theta \leq \varphi \leq \frac{\pi}{2} .$$

Thus,

$$\int_0^{\pi/2} \rho e^{-\rho\sin\theta} d\theta \geq \int_0^{\pi/2} \rho e^{-\rho\theta} d\theta = 1-e^{-\rho\frac{\pi}{2}} ,$$

and for $0\leq\theta\leq\varphi\leq\frac{\pi}{2}$, we have

$$\int_0^{\varphi} \rho e^{-\rho\sin\theta} d\theta \leq \int_0^{\varphi} \rho e^{-\rho\frac{\sin\varphi}{\varphi}\theta} d\theta = \frac{\varphi}{\sin\varphi}(1-e^{-\rho\sin\varphi})$$

$$\leq \frac{\varphi}{\sin\varphi} < \frac{\varphi}{[\varphi-\varphi^3/6]} = \frac{1}{[1-\varphi^2/6]}$$

$$= 1+\frac{1}{6}\varphi^2+O(\varphi^4) \quad \text{as} \quad \varphi\to 0 ,$$

and

$$\int_{\varphi}^{\pi/2} \rho e^{-\rho\sin\theta} d\theta \leq \int_{\varphi}^{\pi/2} \rho e^{-\rho\sin\varphi} d\theta \leq \frac{\pi}{2}\rho e^{-\frac{2\rho\varphi}{\pi}} .$$

Hence, as $\varphi\to 0$,

$$\int_0^{\pi/2} \rho e^{-\rho\sin\theta} d\theta < 1+\frac{1}{6}\varphi^2+\frac{\pi}{2}e^{-\frac{2\rho\varphi}{\pi}}+O(\varphi^4)$$

$$= 1+\frac{1}{6\rho}+\frac{\pi}{2}e^{-\frac{2\sqrt{\rho}}{\pi}}+O(\rho^{-2})$$

$$= 1+O(\rho^{-1}) , \text{ where } \varphi=\rho^{-\frac{1}{2}} \text{ as } \rho\to\infty .$$

So we have,

$$1-e^{-\rho\frac{\pi}{2}} \leq \int_0^{\varphi} \rho e^{-\rho\sin\theta} d\theta \leq 1+O(\rho^{-1}) ,$$

and hence

$$F(\rho) = \frac{1}{\rho}+O(\rho^{-1}) \tag{4.12}$$

as $\rho\to\infty$. We also easily have

$$|F'(\rho)| \leq F(\rho) = O(\rho^{-1}) .$$

So, from (4.10) we obtain the asymptotic variance as $\rho\to\infty$,

$$\text{Var}(V) = \frac{16pq}{\pi}\left\{\frac{\pi}{2\rho^2}-\frac{6}{\rho^3}+\frac{2}{\rho^3}[1+O(\rho^{-1})]\right\}$$

$$= \frac{16pq}{\pi}\left\{\frac{\pi}{2\rho^2}-\frac{4}{\rho^3}+O(\rho^{-4})\right\}$$

Hence, as $\lambda \to \infty$,

$$\mathrm{Var}(V) \sim \frac{2\pi^2 pq}{\lambda^2} \ . \tag{4.13}$$

We know from above that

$$Q(\mathbf{x}) = e^{-\frac{\alpha_{N-1}}{S_N}\lambda|\mathbf{x}|} \ ,$$

so

$$\int_{\mathbf{R}^N} Q(\mathbf{x})\, d\mathbf{x} = S_N \int_0^\infty r^{N-1} e^{-\frac{\alpha_{N-1}}{S_N}\lambda r}\, dr = \alpha_N \left[\frac{S_N}{\alpha_{N-1}}\right]^N N! \ ,$$

hence from (3.4)

$$Var(V_\lambda) \sim \left[\frac{S_N}{\alpha_{N-1}}\right]^N N! pq \frac{1}{\lambda^N} \quad \text{as } \lambda \to \infty \ .$$

In particular V_λ has the following asymptotic variances, that are of course the asymptotic forms of (4.6), (4.13) and (4.7) respectively.

$$\text{1 dimension} \quad Var(V_\lambda) = \frac{2pq}{\lambda} \ , \tag{4.15}$$

$$\text{2 dimensions} \quad Var(V_\lambda) = \frac{2\pi^2 pq}{\lambda^2} \ , \tag{4.16}$$

$$\text{3 dimensions} \quad Var(V_\lambda) = \frac{384pq}{\lambda^3} \ . \tag{4.17}$$

We can also say something about the asymptotic distribution for small λ. If λ is small enough so that $O(\lambda^2)$ is negligible, ie. $\mathbf{P}\{$ 2 Planes cut $Q_N\}$ is negligible, then the distribution of V has masses at at 0 and 1, and has a density on $(0,1)$. This density is symmetric, since we have two regions, one of which is in phase 1, and the other in phase 0, and is proportional to the density of the conditional random variable W equal to V conditional on one cut and that $V \neq 0$ and $V \neq 1$, so we have two regions one in phase 1 and one in phase 0. In one dimension, the cut is uniformly distributed on $(-1,1)$, so the conditional density is uniform. In more than one dimension the argument that this density, f_W say, is U-shaped, is as follows.

We can define $g(R)$ for $R \in (-1,1)$ to be the volume to the 'right' of a plane perpendicular to the x_1 axis through $x_1 = R$. More formally,

$$g(R) = \frac{A_N(R,1)}{2\alpha_N} \quad 0 \le R < 1 \ , \quad 1 - \frac{A_N(R,1)}{2\alpha_N} \quad -1 < R < 0 \ , \tag{4.18}$$

where A_N is the volume function from earlier in this section. Clearly, $g:(-1,1)\to(0,1)$ is monotonic, and so has a monotonic inverse $h:(0,1)\to(-1,1)$, and, moreover, g' is symmetric, with a maximum at zero and

$$\lim_{R\to+1} g'(R) = \lim_{R\to-1} g'(R) = 0 \ .$$

Now, if $R\sim U(-1,1)$, then the random variable $Z=g(R)$ defined on (0,1) has the same density as W, namely,

$$f_W(z) = f_Z(z) = \frac{1}{2g'[h(z)]} \quad z\in(0,1) \ . \tag{4.19}$$

Hence f_W has a minimum at a $\frac{1}{2}$, and tends to infinity at 0 and 1, and so W, and hence V has a U-shaped symmetric density on (0,1).

5. One Dimensional Poisson Mosaic

In one dimension we can derive the density of V for the Poisson mosaic since we are essentially dealing with a Poisson point process on a bounded interval. We can assume without loss of generality that the interval we are considering is (0,1) rather than $Q_1=(-1,1)$, so the parameter of the Poisson point process is $\mu=\frac{1}{2}\lambda$.

Let L denote the number of points in (0,1), so $L\sim Poi(\mu)$, and $K(l)$ be the number of intervals in phase 1 given l points, so $K(l)\sim Bin(l+1,p)$. Then we have

$$\mathbf{P}(V=0) = \sum_{l=0}^{\infty} \mathbf{P}\{V=0\,|\,L=l\}\ \mathbf{P}[L=l] = \sum_{l=0}^{\infty} \frac{q^{l+1}e^{-\mu}\mu^l}{l!} = qe^{-\mu p} \ , \tag{5.1}$$

and similarly, $\mathbf{P}(V=1) = pe^{-\mu q}$.

To find the density of V on (0,1) we first define the conditional random variable V^* to be V given $V\neq 0$ and $V\neq 1$, then we can define T_l to be V^* given $L=l$, and $W_{l,k}$ to be T_l given that $K(l)=k$. Then

$$\mathbf{P}(V^*\le v) = \sum_{l=1}^{\infty} \mathbf{P}(T_l\le v)\mathbf{P}(L=l) \ ,$$

and so

$$\mathbf{P}(T_l\le v) = \sum_{k=1}^{l} \mathbf{P}(W_{l,k}\le v)\mathbf{P}(K(l)=k) \ .$$

However,

$$\mathbf{P}(W_{l,k}\le v) = \mathbf{P}\ \{\ k^{th} \text{ order statistic of } l\ U(0,1) \le v\ \}$$

$$= \sum_{j=k}^{l} \binom{l}{j} v^j (1-v)^{l-j} \quad , \tag{5.2}$$

which has derivative

$$k \binom{l}{k} v^{k-1} (1-v)^{l-k} \quad ,$$

the density function of a $\beta(k, l+1-k)$ distribution. Thus, the density of V^*, f_{V^*}, say, is zero outside $(0,1)$, and for $v \in (0,1)$ is given by

$$f_{V^*}(v) = \sum_{l=1}^{\infty} \frac{e^{-\mu} \mu^l}{l!} \sum_{k=1}^{l} \binom{l+1}{k} p^k q^{l+1-k} k \binom{l}{k} v^{k-1} (1-v)^{l-k} \quad . \tag{5.3}$$

6. The Dirichlet Mosaic

A realisation of a Poisson point process in $\mathbf{R}^N$, with parameter ρ, will give a set of "random" points $\{\mathbf{P}_i\}$, with each of which we can associate a cell,

$$C_i = \{ \mathbf{x} \in \mathbf{R}^N : |\mathbf{P}_i - \mathbf{x}| < |\mathbf{P}_j - \mathbf{x}| \ \forall j \neq i \} \quad , \tag{6.1}$$

that is the set of all points nearer to $\mathbf{P}_i$ than any other $\mathbf{P}_j$. Having obtained the cells, we can obviously define a mosaic in the usual manner. We shall call this the Dirichlet mosaic with parameters p and ρ. There are no mathematically tractable expressions for V for small ρ but we can derive an asymptotic expression for large ρ. Again we will do this by considering a process with unit parameter over a sphere of radius λ for large λ. Unlike the Poisson mosaic we cannot take the distributions of the two proportion random variables to be equal simply by equating λ with ρ. For a Dirichlet mosaic, the expected cell size, $E[R]$, is $1/\rho$, so we shall obtain equality of distributions by taking $\rho = \lambda^N$. As before, we can regard V_λ to be the proportion in phase 1 of either a process of parameter λ over a unit sphere or of a process of parameter 1 over a sphere of radius λ, so we will assume that we have a process of parameter 1 over a sphere of radius $\lambda = \rho^{1/N}$.

To evaluate a bound for the variance, we can use the results of Section 3. Our discussion will broadly follow that of Gilbert (1962). Suppose $|\mathbf{x}| = b$, and $K_\mathbf{0}$ and $K_\mathbf{x}$ are the two spheres centred on $\mathbf{0}$ and $\mathbf{x}$ respectively and having the random point $\mathbf{P}_i$ on their boundaries. Thus, given the location of $\mathbf{P}_i$, $\mathbf{0}$ and $\mathbf{x}$ are in the same cell, C_i, if and only if $K_\mathbf{0}$ and $K_\mathbf{x}$ contain no other $\mathbf{P}_j$. So,

$$\mathbf{P} \{ \mathbf{0}, \mathbf{x} \in C_i \mid \mathbf{P}_i \} = \exp [-\mathrm{Vol}(K_\mathbf{0} \cup K_\mathbf{x})] \quad , \tag{6.2}$$

and hence

$$Q(\mathbf{x}) = \mathbf{P} \{ \mathbf{0}, \mathbf{x} \in C_i \} = \int_{\mathbf{R}^N} \exp [-\mathrm{Vol}(K_\mathbf{0} \cup K_\mathbf{x})] \, d\mathbf{P}_i \tag{6.3}$$

In the one dimensional case we have for $x>0$, so

$$\mathrm{Vol}(K_0 \cup K_x) = \begin{cases} 2(x-P_i) & P_i<0 \\ 2x & 0\le P_i \le x \\ 2P_i & P_i>x \end{cases} \tag{6.4}$$

Thus,

$$Q(x) = \int_{-\infty}^{0} e^{-2(x-P_i)} dP_i + \int_0^x e^{-2x} dP_i + \int_x^{\infty} e^{-2P_i} dP_i = e^{-2x}(1+x) \ .$$

We know from Section 3 that in order to evaluate the asymptotic variance we have to evaluate

$$\int_R Q(x) dx = 2\int_0^{\infty} e^{-2x}(1+x)\, dx = 3/2 \ .$$

Thus the asymptotic variance is given by

$$Var(V_\lambda) \sim \frac{3pq}{4\lambda} = \frac{3pq}{4\rho} \qquad \lambda,\rho \to \infty \ .$$

In the N-dimensional case, we can obtain a bound for the asymptotic variance as follows. Suppose we let $|x|=b$ and $|P_i|=Rb$, so we can write

$$\mathrm{Vol}(K_0 \cup K_x) = V(R,\varphi) b^N \ , \tag{6.5}$$

for some function V. We can bound V as follows :

$$V(R,\varphi) > b^{-N} \mathrm{Max}\{\mathrm{Vol}(K_0), \mathrm{Vol}(K_x)\} > \alpha_N \mathrm{Max}\{R^N, (|1-R|)^N\} \ . \tag{6.6}$$

Thus, from (6.3)

$$\begin{aligned} Q(x) &= \int_{R^N} e^{-V(R,\varphi)b^N}\, dP_i \\ &= \int_0^{\infty} \int_{\partial Q_N} b^N\, e^{-V(R,\varphi)b^N}\, R^{N-1}\, J_N(\varphi)\, d\varphi\, dr \ , \end{aligned} \tag{6.7}$$

so

$$\begin{aligned} \int_{R^N} Q(x)\, dx &= S_N \int_{\partial Q_N} J_N(\varphi) \int_0^{\infty} R^{N-1} \int_0^{\infty} b^{2N-1}\, e^{-V(R,\varphi)b^N}\, db\, dR\, d\varphi \\ &= \frac{S_N}{N} \int_{\partial Q_N} J_N(\varphi) \int_0^{\infty} R^{N-1}\, V(R,\varphi)^{-2}\, dR\, d\varphi \\ &= \alpha_N \int_{\partial Q_N} J_N(\varphi) \int_0^{\infty} R^{N-1}\, V(R,\varphi)^{-2}\, dR\, d\varphi \ . \end{aligned}$$

But,

$$\int_{\frac{1}{2}}^{\infty} R^{N-1} V(R,\varphi)^{-2} dR < \alpha_N^{-2} \int_{\frac{1}{2}}^{\infty} R^{-(N+1)} dR = \frac{2^N}{N\alpha_N^2} \ ,$$

and

$$\int_{\frac{1}{2}}^{\infty} R^{N-1} V(R,\varphi)^{-2} dR < \alpha_N^{-2} \int_{\frac{1}{2}}^{\infty} R^{N-1} (1-R)^{-2N} dR < 2^{2N} \alpha_N^{-2} \int_{\frac{1}{2}}^{\infty} R^{N-1} dR = \frac{2^N}{N\alpha_N^2} \quad ,$$

so

$$\int_{\frac{1}{2}}^{\infty} R^{N-1} V(R,\varphi)^{-2} dR < \frac{2^{N+1}}{N\alpha_N^2} = \frac{2^{N+1}}{S_N \alpha_N} \quad ,$$

and

$$\int_{R^N} Q(\mathbf{x})\, d\mathbf{x} < \frac{2^{N+1}}{S_N \alpha_N} \int_{\partial Q_N} J_N(\varphi)\, d\varphi = \frac{2^{N+1}}{\alpha_N} \quad .$$

This gives us a bound on the asymptotic variance,

$$Var(V_\lambda) < \frac{2^{N+1} pq}{\alpha_N} \frac{1}{\lambda^N} = \frac{2^{N+1} pq}{\alpha_N} \frac{1}{\rho} \quad . \tag{6.8}$$

If we let C_N be the expected cell size in the N-dimensional case, then we can have the following expressions,

$$\text{1 dimension} \quad Var(V) = \frac{pq}{4\rho} = \frac{pq}{4} C_1 \quad , \tag{6.9}$$

$$\text{2 dimensions} \quad Var(V) < \frac{8pq}{\pi\rho} = \frac{8pq}{\pi} C_2 \quad , \tag{6.10}$$

$$\text{3 dimensions} \quad Var(V) < \frac{12pq}{\pi\rho} = \frac{12pq}{\pi} C_3 \quad . \tag{6.11}$$

The natural method to compare the Poisson and Dirichlet N-dimensional mosaics would be to compare their variances for mosaics with the same expected cell size. From Miles (1964) and (1973), we know that the expected cell sizes for the Poisson mosaic with parameter λ are given by

$$C_1 = \frac{1}{\lambda} \; , \; C_2 = \frac{4\pi}{\lambda^2} \; , \; C_3 = \frac{1024\pi^2}{9\lambda^3} \quad .$$

Hence the variances for the Poisson mosaics are given by

$$Var_P = 2pqC_1 \quad ,$$

$$Var_P = \tfrac{1}{2}\pi pqC_2 \quad ,$$

$$Var_P = \frac{27pq}{8} C_3 \quad .$$

Thus we have the following bounds for the ratio of the variances for small expected cell size, C_i.

$$\text{1 dimension} \quad \frac{Var_D}{Var_P} = \frac{3}{8} = 0.375 \ , \tag{6.12}$$

$$\text{2 dimensions} \quad \frac{Var_D}{Var_P} < \frac{16}{\pi^2} = 1.621 \ , \tag{6.13}$$

$$\text{3 dimensions} \quad \frac{Var_D}{Var_P} < \frac{32}{9\pi} = 1.131 \ . \tag{6.14}$$

The bound given by (6.8) for the variance of a Dirichlet mosaic is not very tight, and we can do better by evaluating (6.3) numerically by using Gilbert's results.

$$\text{In 2 dimensions} \quad Var(V_\lambda) = 0.407pq\frac{1}{\rho} = 0.407pqC_2 \ , \tag{6.15}$$

$$\text{and in 3 dimensions} \quad Var(V_\lambda) = 0.282pq\frac{1}{\rho} = 0.282pqC_3 \ . \tag{6.16}$$

Hence,

$$\text{in 2 dimensions} \quad \frac{Var_D}{Var_P} = 0.259 \ , \tag{6.17}$$

$$\text{and in 3 dimensions} \quad \frac{Var_D}{Var_P} = 0.084 \ . \tag{6.18}$$

7. The Simulation of V_λ

In the cases of some types of mosaics, where we cannot derive the distribution of V_λ analytically, it may be possible to simulate V_λ by simulating those mosaics and then calculating the proportion of the mosaic in phase 1. In this section, we consider such a simulation study for the planar Poisson mosaic.

The simulation of the planar Poisson line process in a unit disc is very easy. Firstly, we have to obtain a single realisation of a Poisson distribution in order to obtain the number of lines that cross the unit disc in a realisation of a Poisson line process. Then, to simulate one of the Poisson lines we need realisations of a uniform distribution on $[0,1]$ and a uniform distribution on $[0,2\pi]$, for the length of normal from the line to the origin and orientation of this normal respectively. Having simulated a Poisson line process, we can allocate regions to one phase or the other with the required probability by sampling from a uniform distribution on $[0,1]$. It thus only remains to find an efficient algorithm to find the areas of the regions and hence find the proportion in phase 1.

Suppose we have n lines in a realisation, $l_1,\ldots,l_n$, which divide the unit disc into r regions, $R_1,\ldots,R_r$. The two points where the line l_k meets the circle, $\mathbf{a}_k$ and $\mathbf{b}_k$, can be represented by a pair of angles, $0\leq\varphi_k<\theta_k<2\pi$, and we shall assume that φ_k represents the point **a**. Thus we can keep three lists for the circumference :

[C1] a list of these polar angles in increasing order ;

[C2] a list of the associated line numbers ;

[C3] a list of the regions bounded by the circle as we go round the circle.

Any point on line l_k inside the circle can be written as

$$(1-\mu)\,\mathbf{a} + \mu\mathbf{b} \quad \text{for some } 0<\mu<1 \ ,$$

which gives us an ordering for points on the line inside the disc. Hence we can order the intersections inside the disc of l_k with other lines. Accordingly we can keep four lists for each line :

[L1] a list of intersecting lines in order ;

[L2] a list of associated parameter values ;

[L3] a list of regions bounded by the line on the left in order ;

[L4] a list of regions bounded by the line on the right in order.

If we denote the circumference by line 0, then, starting at one vertex, we can keep two lists about each region, as we travel round the region boundary in an anti-clockwise sense :

[R1] a list of vertices ;

[R2] a list of bounding "lines".

Clearly, lists [R1] and [R2] are all that are needed to calculate the area of a region, since we calculate the area of the polygon defined by the vertices in [R1] and the area of any segments if part of the circle bounds the region. However, in order to make lists [R1] and [R2] efficiently we need to be able to make the other lists above. This will be done by sequentially adding the Poisson lines.

It is an easy enough matter to construct these lists for the first Poisson line, so assume that the lists are correct for $(k-1)$ lines, $l_1,\ldots,l_{k-1}$, then we can update the lists for the k^{th} line in the following way.

(i) By comparing polar angles, from lists [C1] and [C2], we can see with which other lines l_k intersects inside the unit disc. Considering both such lines as being sensed, the polar angles also tell us whether l_k hits the other line from its left or right hand side.

(ii) We can calculate parameter values for the point of intersection on both lines. Having done this for all lines intersecting l_k, we can order the intersections on l_k. Assuming at least one such point, this will divide l_k into a number of smaller line segments.

(iii) Taking each segment in turn, we know from the parameter value of the point of intersection on the other line, by consulting lists [L1] - [L4], and whether we are to the right or left of the other line, which region the segment cuts into two smaller regions.

(iv) We can number the region to the right of l_k by the next available region number, and construct lists [R1] and [R2] for this region from the lists [R1] and [R2] for the old region. We can number the region to the left of the line by the old region number and update lists [R1] and [R2].

(v) We can update lists [L1] - [L4] for the intersecting line, and list [L3] or [L4] for a line affected by the change of region number.

(vi) We can repeat the process for each segment in turn, updating [L1] - [L4] for l_k.

(vii) Finally, we can update [C1] - [C3].

(viii) If, however, there had been no point of intersection of line l_k with any of the other lines inside the disc, we would use [C3] to see which region l_k cuts into two parts, and rejoin the algorithm at step (iv). Having performed this algorithm for all the lines, as we noted above, it is a simple matter to calculate the area of a region from its lists [R1] and [R2], and hence to calculate the area in phase 1.

This algorithm was used to simulate 10,000 realisations of V_λ for $p=\frac{1}{2}$ and $\lambda=0.5,1,2,5,10$ respectively. The number of realisations for which $V_\lambda=0$ and $V_\lambda=1$ respectively are given below.

$$V_{0.5} = 3879 \quad 3814$$

$$V_{1.0} = 3057 \quad 2926$$

$$V_{2.0} = 1707 \quad 1699$$

$$V_{5.0} = 272 \quad 267$$

$$V_{10.0} = 7 \quad 6$$

Figures 1-5 show histograms for the realisations of V_λ, for λ=0.5,1,2,5,10 respectively, that lie in the open interval (0,1), that is to say realisations containing more than one phase. Note how the distribution of V_λ moves from a U-shaped distribution for λ=0.5 to a normal-shaped distribution for λ=10.

Figure 1

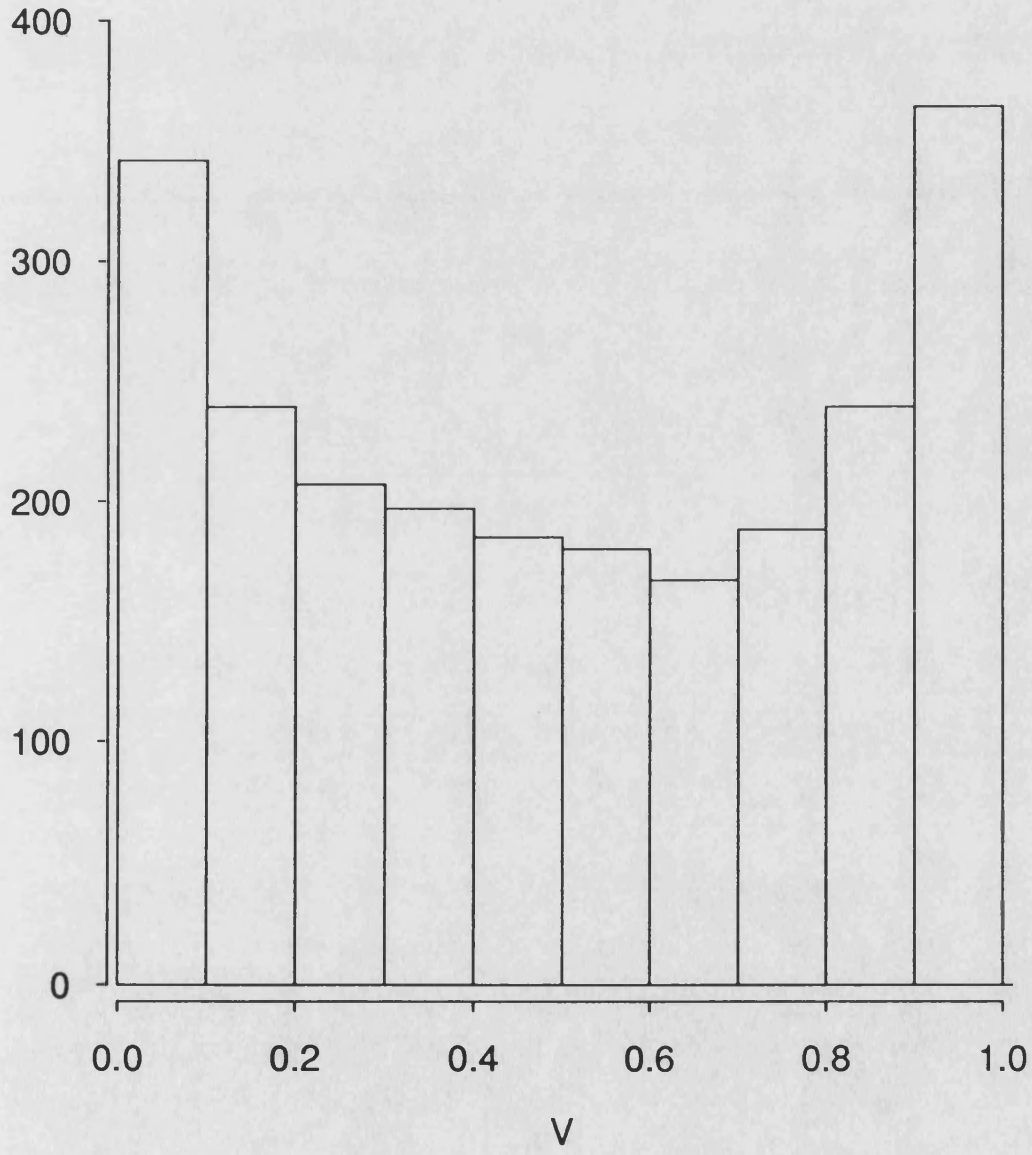

Figure 2

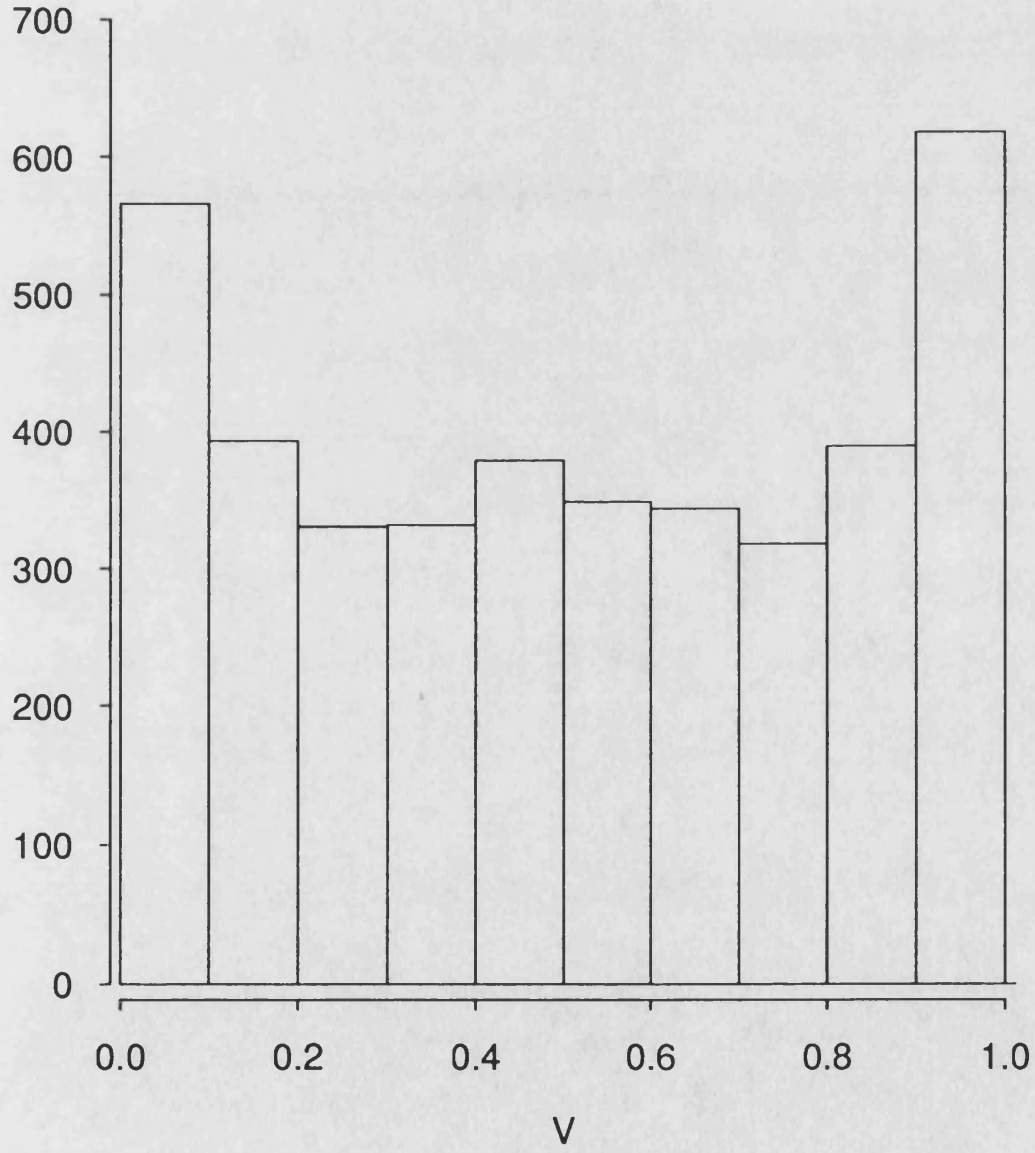

Figure 3

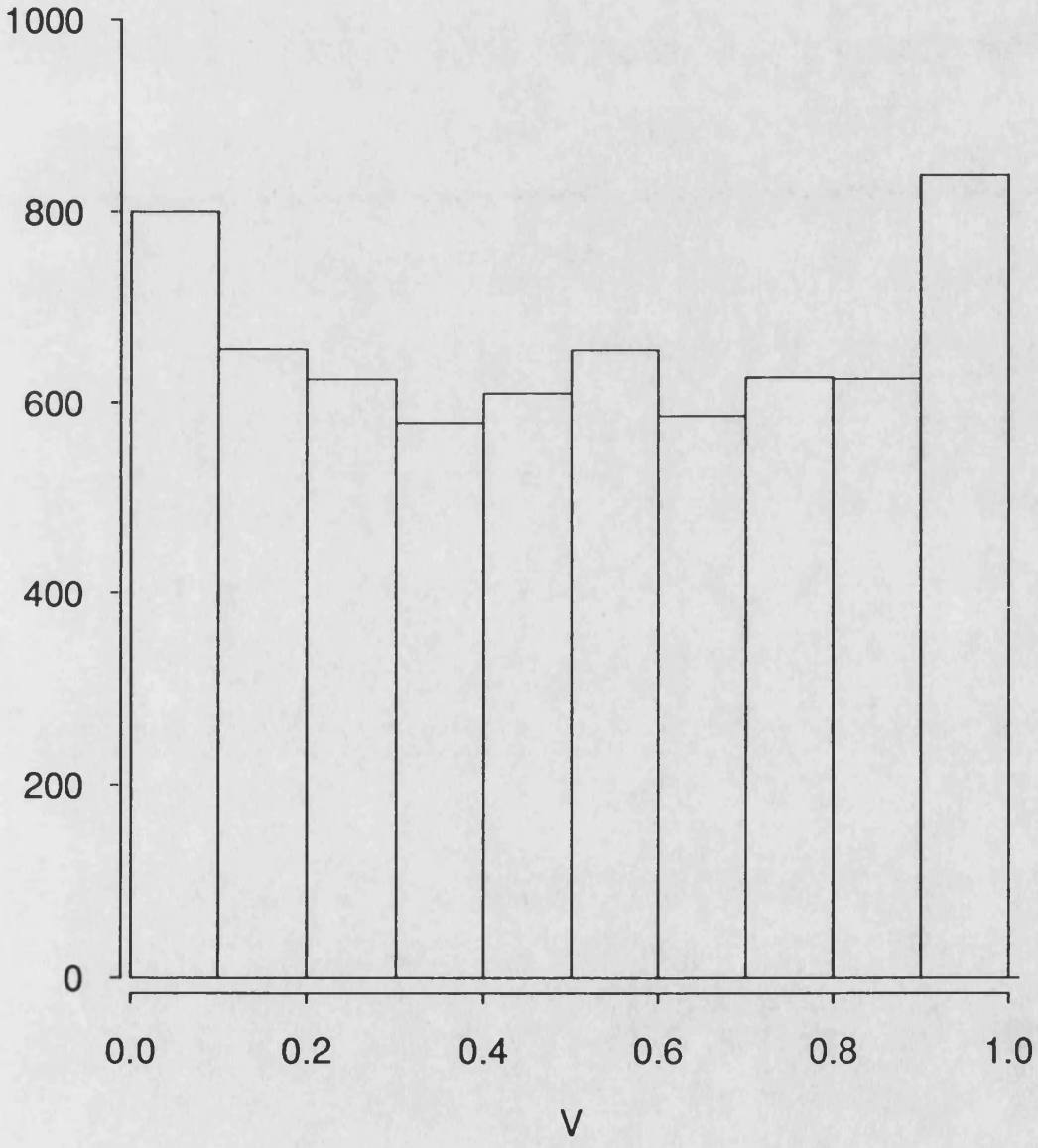

Figure 4

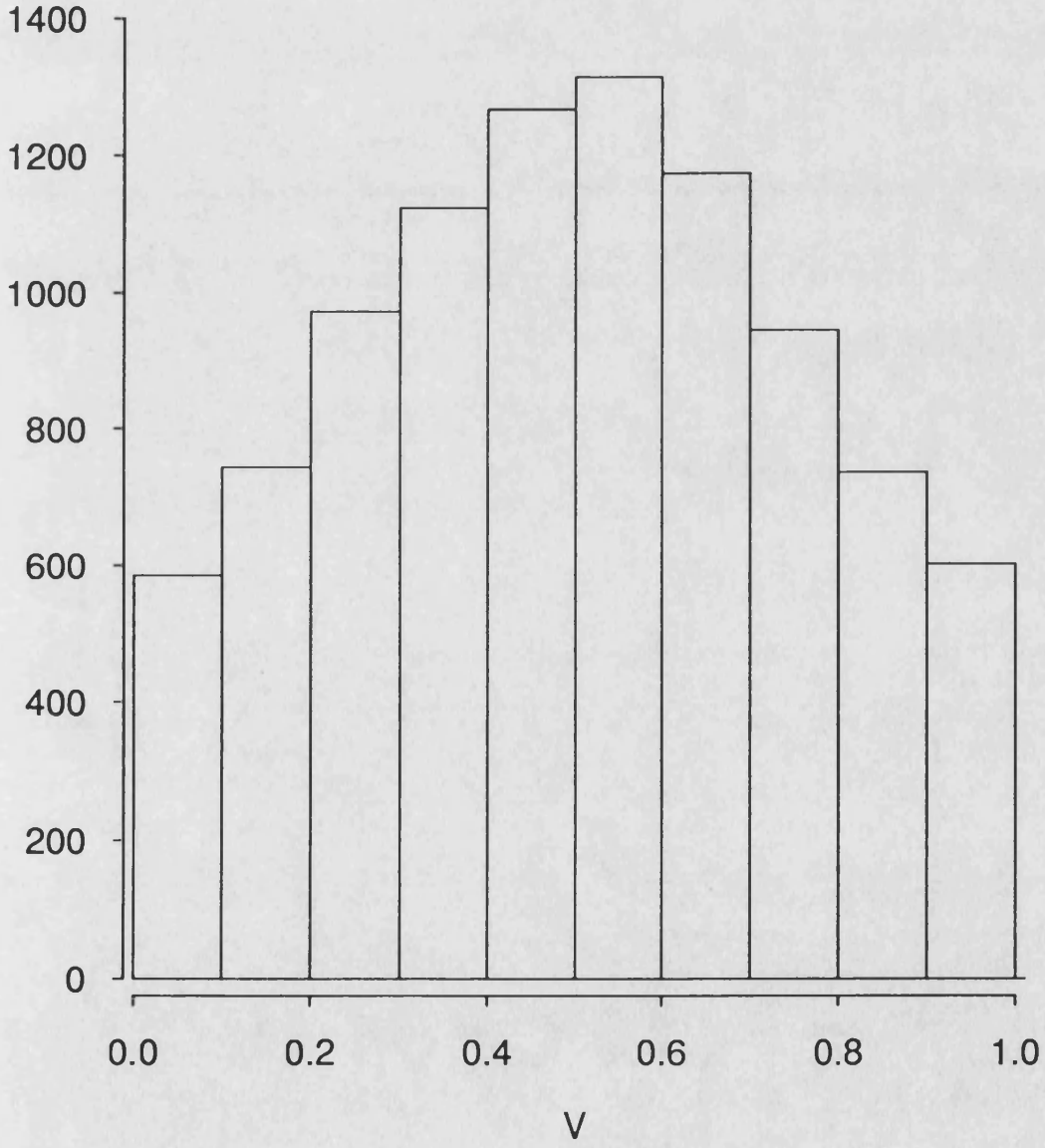

Figure 5

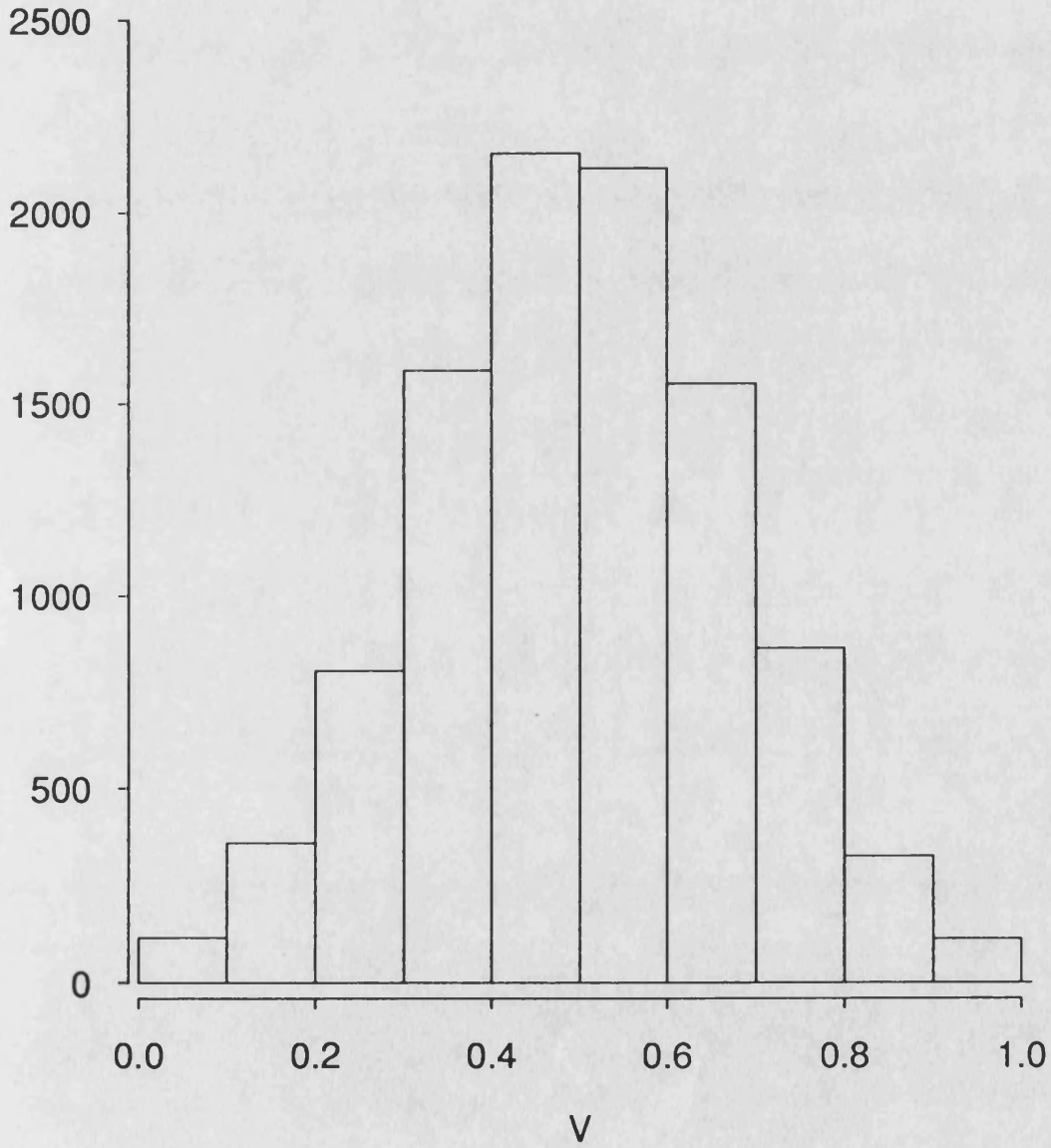

The Relationship between Plant Position and Yield

1. Introduction

This section is concerned with the spatial distribution of two species of plants, *Erophila verna* and *Poa annua*, in a plot measuring 361 mm by 213 mm. The plot was dug up in North-East England in the winter and cultivated in a seed tray. Various pieces of data about the plants were later collected. There were 204 Erophila plants and 25 Poa plants.

The Erophila plant is a winter annual and grows at ground level as a rosette, which is usually less than 10 mm in diameter but is occasionally larger. A stalk grows from the rosette and is usually less than 20 mm in height, On the stalk, there will anything up to 30 leaves growing. Beneath the ground the diameter of the roots is typically twice the rosette diameter. The data we have on the Erophila plants consists of a position for each plant and its seed number. We also have the rosette diameters of some of the Erophila plants.

The Poa plant which is a summer annual is a grass, each plant consisting of one rooted node. From each rooted node there will be anything from 3 to 10 branches growing, though 4 or 5 branches per plant was more usual for plants in our plot. Each plant can be up to 100 mm across and 100 mm high, but typical values for our plot were 30 mm across and 50 mm high. We only have the positions of each Poa plant.

Three topics for investigation naturally suggest themselves about the above data set with regard to the relationship between plant position and yield :

(i) the trend in positions of plants of each species ;

(ii) the dependence between plants of differing species ;

(iii) the relationship between plant spacing and yield.

These will be investigated by regarding the positions of the Erophila plants as a realisation of some planar point process, the "Erophila" process, and the positions of the Poa plants as a realisation of the "Poa" process. Much use will be made of the Dirichlet tessellations of these point processes, either regarded individually or jointly. The Dirichlet tessellations and some of the basic calculations concerned with tile parameters associated with them were calculated using the Tile4 computer package. The Tile4 package was also useful in helping to draw the following maps and tessellations of the plants. Figure 1 is a map of the positions

of the plants of both species and the Dirichlet tessellation of those points. Figures 2 and 3 show the same map for the Erophila and Poa plants respectively when considered alone. In these three maps, the number 1 represents the positions of Erophila plants, and the number 2 the positions of the Poa plants. Finally, figure 4 shows the seed number for each Erophila plant at its position, along with the Dirichlet tessellation. The Poa plants are marked by the number -1.

The trend in positions of plants of each species is considered in the next section. We are essentially asking whether either species, regarded as a point process, shows any evidence of departure from a stationary process. It is easier however to consider whether there is any evidence of departure from some particular type of stationary point process, generally the Poisson point process. Statistical tests for this fall into four types : quadrat-based tests, distance-based tests, second order tests, test set based tests. In particular, we shall be concentrating on the test set methods, in order to find distances at which the Poisson hypothesis breaks down for each plant process. We shall be concluding that section with a graphical method of comparing the Erophila and Poa processes with those from a given distribution.

The dependence between the positions of one species of plant and the other is considered in Section 3. Most of the tests for testing the dependence between two different point processes are generalisations of the tests for testing single type point processes. However, only the test set based methods seem to generalise naturally, and they allow us to find distances at which there is evidence of attraction or repulsion between the two species.

In the final section we investigate the relationship between plant spacing and yield (seed number) for the Erophila plants. The Dirichlet tessellation would seem to be a natural tool to use to do this, since it would appear that to a first approximation a plant could only obtain soil nutrients from those regions of soil nearer to it than to any other, its Dirichlet tile. However, a plant may be some distance away from some parts of its Dirichlet tile and so will be less successful in obtaining nutrients from those parts. We shall attempt to model this and to find the radius of some critical circle, from which the plant obtains its nutrients.

2. The Trend in the Positions of Plants of One Species

We are interested in whether there is any evidence of a trend in the positions of plants of a particular species. If we regard the positions of plants of a particular species as a planar point process, this is equivalent to asking whether there is any evidence to suggest that this process is non-stationary. Instead of

testing directly for stationarity, it is often easier to test whether the process is "random", that is a stationary planar Poisson point process. Recall that a process in the plane is a Poisson process with mean measure Λ, where Λ is a measure defined on Borel sets in the plane, if it satisfies the following two conditions :

(i) The number of points in any Borel set B has a Poisson distribution with mean $\Lambda(B)$;

(ii) The numbers of points in any two disjoint Borel sets are independent.

Thus a Poisson process is stationary if $\Lambda(B)$ is proportional to the area of B. There are of course many different types of stationary point processes which are not Poisson processes, for example the Cox or doubly stochastic Poisson processes. These are defined by taking a non-stationary Poisson process with mean measure Λ, where Λ is a realisation of a stationary stochastic process. Following Ripley (1977), tests for a stationary Poisson process can be divided into four categories :

(i) tests based on quadrat counts ;

(ii) distance-based tests ;

(iii) second order methods ;

(iv) tests based on some test set.

Under the null hypothesis of a Poisson process the number of plants in any two disjoint regions of equal area are independently and identically distributed. If the region is first divided up into quadrats, then the number of plants in each quadrat can be counted. To construct a test these can then be compared to a theoretical distribution for a Poisson process. Unfortunately the results of this test depend heavily on the choice of origin for the quadrats and the orientation of the quadrats. For example, a field of wheat ploughed in straight lines will give vastly different quadrat numbers depending on whether the quadrats are aligned along the line of ploughing or not. If we combine neighbouring quadrats into blocks, then we can construct a permutation test of any given size by permuting the quadrats within blocks. Details of this permutation test are given in Mead (1974) and Besag and Diggle (1977). Like permutation tests in general, this test is not very powerful against certain alternatives.

The second approach is to use distance-based methods, which are generally based on the distance between a point and its nearest neighbour. The best-known of these is the Clark-Evans test, in which the average nearest neighbour distance is compared to a normal distribution, Clark and Evans (1954). The Clark-Evans test

compared favourably with other tests for "randomness" in a study by Ripley (1979). Suppose that A is the area of the region, N the number of points and d_i the distance from the i^{th} point to its nearest neighbour, then

$$\bar{d} = \frac{1}{n} \sum_{i=1}^{n} d_i \tag{2.1}$$

denotes the empirical average interpoint distance, and

$$CE = \frac{\bar{d} - \mathrm{E}(d_i)}{[Var(\bar{d})]^{\frac{1}{2}}} \sim N(0,1) \ , \tag{2.2}$$

where

$$\mathrm{E}(d_i) \approx 0.5 \left[\frac{A}{N}\right]^{\frac{1}{2}} \quad \text{and} \quad Var(\bar{d}) \approx \frac{0.0683A}{N^2} \ .$$

In its original form the Clark-Evans test ignored edge effects and the interdependence of the d_i. Donelly (1978), in a simulation study, gave better approximations for $\mathrm{E}(d_i)$ and $Var(\bar{d})$ by making edge corrections,

$$\mathrm{E}(d_i) \approx 0.5 \left[\frac{A}{N}\right]^{\frac{1}{2}} + \left(0.514 + 0.412N^{-\frac{1}{2}}\right)\frac{P}{N} \ ,$$

where P is the perimeter, and

$$Var(\bar{d}) \approx \frac{0.070A}{N^2} + \frac{0.037PA^{\frac{1}{2}}}{N^{5/2}} \ .$$

The Clark-Evans statistic was calculated for the tray of Erophila and Poa. The Erophila plants alone had a Clark-Evans statistic of -9.4, the Poa plants alone had a statistic of -13.0, and both species of plants regarded together had a Clark-Evans statistic of -9.7. Under the hypothesis of a Poisson point process the Clark-Evans statistic is a standard normal random variable, so this is extremely strong evidence of departure from the Poisson point process hypothesis.

One of the problems with the types of test outlined above is that they are unable to test for interactions at different scales simultaneously. The tests given below involve estimating a function of distance and plotting it against distance. From this we are able to see the scales at which the Poisson hypothesis breaks down.

The first order properties of a point process are given by its intensity, λ say, which is the expected number of points in a unit area. By definition, for a stationary process in general and a Poisson process in particular, this is a constant. The second order properties of a point process are best summed up by the K function of Ripley (1976) and (1977). The K function has the following

properties.

(a) $\lambda^2 K(t)$ is the expected number of ordered pairs of distinct points less than a distance t apart.

(b) $\lambda K(t)$ is the expected number of further points within t of an arbitrary point of the process.

(c) Under additional assumptions, $g(t)=\lambda^2 \frac{dK}{dt} \frac{1}{c(t)}$ is a joint density for the occurrence of two points a distance t apart, where $c(t)=2\pi t$ for a planar process.

Ripley (1976) and (1977) gives an unbiased estimator for K, $\hat{K}$, which is a weighted empirical distribution function for inter-point distances. $\hat{K}$ can then be plotted against distance. If we can simulate a particular planar point process, then we can simulate $\hat{K}$ for this process and thus obtain confidence bands for K.

Test set procedures are based on some property of a test set placed at an arbitrary point in the plane. The p function of Ripley (1976) and (1977) uses a circular test set,

$$p(t) = \mathbf{P} \{ \text{ Disc of radius } t \text{ contains at least one point } \} \ . \qquad (2.3)$$

Ripley (1977) gives an unbiased estimator for p, $\hat{p}$. As above, if we let d_i denote the distance of $\mathbf{P}_i$ from its nearest neighbour, and r_i the distance of $\mathbf{P}_i$ from the boundary, then

$$\hat{p}(t) = \frac{\#\{ i \mid d_i \le t \le r_i \}}{\#\{ i \mid t \le r_i \}} \ , \qquad (2.4)$$

that is the proportion of points further than t away from the boundary that are also within t of another point. Its derivation is similar to the function $\hat{G}$ given below. As before, we can plot $\hat{p}$ against distance and obtain confidence bands by simulation. Baddeley (1980) showed that that $\hat{p}(t)$ was approximately normally distributed under the appropriate conditions, and that $\hat{p} \to p$ at a rate of $N^{-\frac{1}{2}}$.

The empty space function, G, of Lotwick (1981), for a circular test set, G, is defined by

$$G(t) = \mathbf{P} \{ \text{ Disc of radius } t \text{ contains no points } \} \ , \qquad (2.5)$$

so for a Poisson point process of intensity λ,

$$G(t) = \exp \{ -\lambda \pi t^2 \} \ .$$

Ripley's and Lotwick's approaches are clearly equivalent since

$$G(t) = 1 - p(t) \ .$$

Unlike the second order K function, the empty space function G, and Ripley's p

function, depend on correlations of all orders. The empty space function may thus be useful in detecting non-Poisson point processes which have the same K function as a Poisson process of similar intensity, Baddeley and Silverman (1984). The empty space function also generalises to planar process with more than one type of point as we shall see later.

The empty space function can be estimated by translating the circular test set throughout the region. In order to ensure that the test set is wholly within the region, we can constrain the centre of the test set to lie within a smaller region, or regard the region as a torus, that is with opposite edges of the region being identified. We shall adopt the former approach because some of the plants near the edge of the region may have been damaged or lost during transplantation. Suppose $D(\mathbf{u},t)$ is a disc of radius t centred at $\mathbf{u}$, and $N(A)$ is the number of points of the process in a bounded set A, then we can define an unbiased estimator $\hat{G}$ over a region R by

$$\hat{G}(t) = \frac{1}{|B|}\int_B I\{N[D(\mathbf{u},t)]=0\}\, d\mathbf{u} \quad , \tag{2.6}$$

$$\text{where } B = \{\, \mathbf{u}\in R \mid D(\mathbf{u},t)\subset B \,\} \quad ,$$

so B is the region R trimmed by t. Thus $\hat{G}(t)$ is the proportion of the region further than a distance t from any point.

The value of $\hat{G}(t)$ can be easily calculated by constructing the Dirichlet tessellation of the points. Suppose we wish to find to find the empty space statistic of a set of points $\{\mathbf{P}_i\}$ in some region R. If we construct the Dirichlet tessellation of $\{\mathbf{P}_i\}$, then the Dirichlet cell of $\mathbf{P}_i$ is the set of all points in the plane nearer to $\mathbf{P}_i$ than any other point $\mathbf{P}_j$. The contribution of the point $\mathbf{P}_i$ to $\hat{G}(t)$ is the area within the sampling region of the complement of the disc of radius t in the Dirichlet tile of $\mathbf{P}_i$.

Of course, we will be interested in a multivariate statistic,

$$\left[\hat{G}(t_1),\ldots,\hat{G}(t_n)\right] \text{ for } t_1<\ldots<t_n \quad ,$$

in order to give us information about the empty space statistic at different ranges. Lotwick (1981) showed that under certain conditions, which are satisfied by the Poisson point process, $\hat{G}(\mathbf{t})$ has asymptotically a multivariate normal distribution as the sampling window size increased to fill the whole plane. However, as before, we can obtain confidence bands for the null hypothesis of a Poisson process by simulation. A value of the empty space estimate above a confidence band would tend to indicate that there is more empty space than null hypothesis would suggest, so there is some attraction between the points at that range, and

conversely a value of the empty space estimate below the confidence band that there is inhibition at that range.

Lotwick (1981) showed that for a Poisson point process of intensity λ,

$$Var\ [\ \hat{G}(t)\ ] = 4\pi t^2\ e^{-2\lambda\pi t^2}\ \{\ \int_0^1 2u \exp\ [\ 2\lambda t^2(arcosu - u(1-u^2)^{\frac{1}{2}})\ ]\ du - 1\ \}\ ,$$

and so for small t,

$$Var\ [\ \hat{G}(t)\ ] \propto t^2\ .$$

Thus we shall be considering the statistic

$$\frac{\log\ [\ \hat{G}(t)\ ]}{t^2}\ . \tag{2.7}$$

The solid lines in figures 5 and 6 show (2.7) plotted against t for the Erophila and Poa processes respectively, and the broken lines are simulated 95% confidence bands, based on 200 simulations, for the Poisson point process. The tailing off of the lower band in figure 5 is due to the empty space statistic becoming small as the region becomes packed with discs. It can be seen that the statistic (2.7) for the Erophila process is below the 95% confidence band for values of t<8mm, implying that there is more inhibition than a Poisson point process up to that range. The Poa process is always above the 95% confidence band, implying that the Poa process is always more clumped than the Poisson process. This is to be expected since the Poa plants are growing mainly in two clumps, (figure 3).

The Erophila is a plant which grows as a rosette, and it is physically impossible for one rosette to grow on top of another. Figure 7 is a histogram of the diameters of a random sample of 106 of the Erophila plants. A first approximation to the Erophila process may be given by the hard-core point processes of Matern (1986). He proposed two hard-core models for point processes. In the first model, we sample from a Poisson point process and delete any point which is within a given distance, say R, of another point whether already deleted or not. In the second model, we again sample from a Poisson point process and assign each point a "birth time", that is to say an independent realisation of a $U(0,1)$ random variable. We then delete any point which is within a given distance, R, of another point with an earlier birth time. Matern's second model would seem to more appropriate for the process of Erophila growth. The solid line in figure 8 shows the statistic (2.7) plotted against t for the Erophila process and the broken lines simulated 95% confidence bands, based on 200 simulations, for the second Matern hard-core model with points constrained to be at least 6.6 *mm* apart, the mean rosette diameter. This Matern hard-core model will have maximal empty space for t<½6.6=3.3, but in order to calculate $\hat{G}(t)$, we trim the region by a distance t, so the broken lines are non-coincident. This is a

better fit than the Poisson model with the statistic (2.7) lying below the confidence bands only for t<4mm. This may be because some of the Erophila plants do grow within 6.6 *mm* of each other. Bartlett (1974) extended this model by taking R to be a realisation of some distribution. A better approximation to the Erophila process might be made by estimating the distribution of the Erophila diameters.

Another hard-core process that could be used is the hard-core Kelly-Ripley processes, see Kelly (1976). These processes have a joint density proportional to

$$\varphi(\mathbf{x}) = b^{\#(\mathbf{x})}\, c^{t_R(\mathbf{x})} \quad ,$$

where $t_R(\mathbf{x})$ denotes the number of pairs of points closer than a distance R. When c=0, then if $t_R(\mathbf{x})$=0, $c^{t_R(\mathbf{x})}$=1, otherwise $c^{t_R(\mathbf{x})}$=0. Hence the case c=0 gives a hard-core model which is a realisation of a Poisson process in which there are no pairs of points less than a distance R apart, and so is a model for non-overlapping spheres of radius $\frac{1}{2}R$.

A graphical method of seeing whether there is any trend in the positions of the Erophila and Poa plants would be to estimate the intensity functions of both the Erophila and Poa plants when regarded as a point process and seeing how flat they were. We can estimate the intensity functions non-parametrically by placing a "bump" centred on each point. More formally, suppose we have a realisation of a point process on some bounded set of area A, say $\{\mathbf{x}_i\}_{i=1}^{N}$, where N is the number of points in the realisation. For some smoothing parameter h>0, we can take

$$K_h(\mathbf{y}) = (2\pi h^2)^{-\frac{1}{2}} \exp\left[\frac{-|\mathbf{y}|^2}{2h^2}\right] \quad ,$$

to be a kernel density function. We can estimate the intensity of the point process at y by

$$I_h(\mathbf{y}) = \frac{A}{N} \sum_{i=1}^{n} K_h(\mathbf{y}-\mathbf{x}_i) \quad ,$$

so I_h assigns unit mass to unit areas. It only remains to choose h. There are many automatic methods for so doing, but for our graphical purposes it is good enough to plot some I_h for some values of h and choose the "best" one. Note that the value of any intensity function estimated in this way will tend to tail off near the boundary unless we impose some kind of periodic boundary conditions.

Figure 9 shows a contour map of the estimated intensity function of the Erophila process, and figure 10 shows the the estimated intensity of a realisation of a Poisson point process conditional on having the same number of points as the

Erophila process. Figures 11 and 12 show the same contour maps for the Poa process and the Poisson point process conditional on having the same number of points as the Poa process. Figure 13 shows the estimated intensity function for the second Matern hard-core model conditional on having the same number of points as the Erophila process.

Figures 9 and 10 are broadly similar, which suggests that the Erophila process is similar to a Poisson process. However, figure 10 has a higher maximum than figure 9, so the Poisson process may be more clustered than the Erophila process. Likewise, figure 13 is similar to figure 9, though the intensity function in figure 13 is flatter than that of figure 9, and it has a hole. Hence the Matern hard-core model may be used to model the Erophila process, though it may be less clustered. Clearly there is little similarity between figures 11 and 12, and so it would be better not to model the Poa process with a Poisson process.

3. The Relationship between the Positions of Plants of Different Species

In this section we consider the problem of deciding whether the positions of the plants of one species has any effect on the positions of the plants of another species. In the previous section we regarded the positions of plants of a particular species as a realisation of a spatial point process. In this formulation, the problem becomes one of testing whether one species exerts an influence over the other is just one of testing for the dependence or independence of one point process from another. Harkness and Isham (1983), in a paper investigating the positions of 32 nests of one species of ants with 17 of another species in a rectangular region, do just this, testing for independence by a number of different methods. As before, we can divide these tests into four categories :

(i) tests based on quadrat counts ;

(ii) distance-based tests ;

(iii) second order methods ;

(iv) tests based on some test set.

If we suppose that each point process is a Poisson point process, then the number of plants of each of the two species in the i^{th} quadrat will be Poisson random variables, say M_i and N_i, having means λ and μ say. By stationarity, for $i \neq j$, M_i and M_j are independent realisations of the same random variables, as are N_i and N_j. Under the null hypothesis of independence, M_i and N_i are independent random variables, so an extremely naive test for independence between the two processes can be constructed by estimating the covariance between M_i and N_i. If

we have Q quadrats, then we can define a test statistic C by

$$C = \frac{1}{Q} \sum_{i=1}^{Q} M_i N_i - \lambda\mu \ , \tag{3.1}$$

which has an expected value of zero under the null hypothesis. Positive values of C would indicate an attraction between the two point processes, whereas negative values would indicate a repulsion.

Harkness and Isham (1983) suggest such an approach with their Table 7 in which they give a joint distribution of quadrat counts. These give rise to a C-value of 1/16, agreeing with their conclusion that there is no evidence of dependence between the two sorts of nests. If we consider the Erophila and Poa data over an 8×4 array of quadrats, we obtain a C-value of -0.043, again giving no evidence of a dependence. It is possible to construct a permutation test to test for the significance of C. For example, if π denotes a permutation of the integers from 1 to Q, then

$$C_\pi = \frac{1}{Q} \sum_{i=1}^{Q} M_i N_{\pi(i)} - \lambda\mu \tag{3.2}$$

is a realisation of C under the null hypothesis that the two processes are independent stationary point processes. Unfortunately, this type of test based on quadrat counts suffers from the usual drawbacks, namely that the results of such a test depend upon the choice of origin and the orientation of the quadrats. Again, such a test is not very powerful against certain alternative hypotheses.

In order to show a dependence between the two types of nests, Harkness and Isham (1983) consider some distance-based statistics, concerning the nests of one species which have a neighbour nearer than the region boundary. In particular, they consider the number of such nests which have the same type of nest as nearest neighbour, and the number of such nests which have the other type of nest as nearest neighbour, for which they also consider the nearest-neighbour distance. These statistics are then compared with two kinds of simulated statistics, one by a generated by random simulation of one type of nest (assuming they form a Poisson process), and the other by a random toroidal shift of the nest positions.

One useful method of collecting data from a spatial point pattern is the *sparse–sampling* method, in which the distances from sampling origins to neighbouring points are measured. Such sampling methods naturally give rise to distance-based tests. Diggle and Cox (1983) compare the powers of some such tests for sparsely-sampled multitype spatial point processes.

As in the previous section, a major problem with these two types of test is that they are unable to test for interactions at different ranges simultaneously. In order to do this, we have to find analogues of tests based upon second moment functions and test sets. Recall that for a point process of intensity λ, the K function of Ripley (1976) and (1977), $\lambda K(t)$ is the expected number of further points within a distance of t of an arbitrary point of the process. Suppose we have r stationary point processes in the plane, with type i being of intensity λ_i, then we can define the second order point moment function, K_{ij}, in the manner of Lotwick and Silverman (1982), so K_{ij} is the second moment distribution function of j-type points with respect to i-type points. Thus we have K_{ii} is Ripley's K function and $K_{ij}=K_{ji}$. Note that a necessary, but not sufficient, condition for an i-type process to be independent of a j-type process is that

$$K_{ij}(t) = \pi t^2 \quad .$$

They then proceed to give estimators $\hat{K}_{ij}$ for K_{ij}, which are again extensions of $\hat{K}$ the estimator for K, and note that the variance of $\hat{K}_{ij}$ will be larger the more clustered the individual marginal processes are. Hence, acceptance regions based on the Poisson hypothesis will be too narrow if the marginal processes are clustered and vice-versa.

The method of testing which seems to generalise most naturally to more than one type of point process is the method based on some kind of test set, for example empty space methods. Recall that for a stationary point process X, we defined $G_X(t)$ to be the probability that there a disc of radius t contains no point of the process. Clearly, for independent stationary point processes X and Y,

$$G_{X\cup Y}(t) = G_X(t)\, G_Y(t) \quad . \tag{3.3}$$

Note that (3.3) extends naturally to processes with more than two types of points. Accordingly, Lotwick and Silverman (1982) defined

$$T_{XY}(t) = \log G_{X\cup Y}(t) - \log G_X(t) - \log G_Y(t) \tag{3.4}$$

as a statistic for investigating the dependence between the X and Y processes. Positive values of T_{XY} would indicate an attraction between the X and Y points at a range of t, whereas negative values would indicate a repulsion between the two types of points at that range.

We can use the estimates of $G_X(t)$, $\hat{G}_X(t)$ etc., introduced in the last section to obtain an estimate, $\hat{T}_{XY}(t)$, for $T_{XY}(t)$. Thus,

$$\hat{T}_{XY}(t) = \log \hat{G}_{X\cup Y}(t) - \log \hat{G}_X(t) - \log \hat{G}_Y(t) \quad . \tag{3.5}$$

Again we would be interested in a multivariate statistic to give us information about the dependence between the two species at different ranges,

$$\left[\hat{T}_{XY}(t_1),\ldots,\hat{T}_{XY}(t_n)\right] \text{ for } t_1<\ldots<t_n \ .$$

In the last section, we noted that Lotwick (1981) had shown that under certain conditions, $\hat{G}(t)$ has asymptotically a multivariate normal distribution as the sampling size increased to fill the whole plane, and he deduced that $\hat{T}(t)$ also has a multivariate normal distribution with zero mean and a covariance matrix depending on $t_1,\ldots,t_n$ and the marginal distributions of both the X and Y processes. If we knew the marginal distributions fo the X and Y processes, it would be possible to calculate theoretical confidence bands for $\hat{T}(t)$, but we could also simulate values for $\hat{T}(t)$ by simulating the X and Y processes.

If however we did not the marginal distribution of the X and Y processes, we could still simulate values of $\hat{T}(t)$ under the null hypothesis, by using the independence (under the null hypothesis) and the stationarity of the X and Y processes. Suppose we regard the region as a torus, that is to say with opposite edges identified. If we choose a random translation of the torus, then we can obtain a new process Y' by "moving" Y by this translation. Because Y is a stationary process, Y' will have the same marginal distribution as Y, and the point process Y' will be independent of the process X. Thus we can simulate values of $\hat{T}(t)$ under the null hypothesis.

Lotwick (1981) showed that under the double Poisson hypothesis, that is both the X and Y are Poisson point processes,

$$Var\ [\hat{T}(t)] \propto t^3 \ , \tag{3.6}$$

for small t, so we shall consider the statistic

$$\frac{10000\ \hat{T}(t)}{t^3} \ . \tag{3.7}$$

The solid line in Figure 14 shows (3.7) plotted against t for the Erophila and Poa processes along with 95% confidence bands, based on 200 simulations, generated under the double Poisson hypothesis, and figure 15 shows (3.7) plotted against t with 95% confidence bands again based on 200 simulations but generated using random toroidal shifts. Both are similar, showing that there is inhibition between the two species up to a range of about 17mm, just over twice the root diameter of

the Erophila plants.

4. The Relationship between Plant Spacing and Yield

There are many quantities there may be regarded as the yield of a plant, for example its height, weight etc., but the quantity for which we have data for the Erophila plants are their seed numbers. Figure 16 is a histogram of seed numbers for the Erophila plants. From figure 16 it can be seen that just over half the Erophila plants are seedless, and figure 17 is a histogram of the Dirichlet tile areas of the seedless plants. In the following analysis, we shall sometimes be considering all the Erophila plants and sometimes just those plants that produced seeds.

One model that could be used where the yield takes a limited number of integral values is the proportional odds model. Suppose that $\gamma_j(\mathbf{x})$ denotes the probability that a plant with covariate $\mathbf{x}$ has a yield of j or less, then we can define the odds that a plant has a yield of more than j, the odds of "survival" beyond j to be

$$\lambda_j(\mathbf{x}) = \frac{1-\gamma_j(\mathbf{x})}{\gamma_j(\mathbf{x})} \quad .$$

The proportional odds model then gives us

$$\lambda_j(\mathbf{x}) = \lambda_j(\mathbf{x}_0) \exp\{ \beta^T(\mathbf{x}-\mathbf{x}_0) \} \qquad j=0,\ldots,k-1 \quad ,$$

where $\mathbf{x}_0$ is some arbitrary known value and $\lambda_j(\mathbf{x}_0)$ is a set of k nuisance parameters. McCullagh (1980) and others have used unconditional maximum likelihood to estimate simultaneously the k nuisance parameters $\lambda_j(\mathbf{x}_0)$ and the regression parameter vector β. McCullagh (1984) gives a method of eliminating the nuisance parameters when we have more than one "strata", (in our case, more than one seed tray), and β is constant across strata. Unfortunately, this model was not useful for the Erophila data, mainly because of the high value of the seed number for some plants, corresponding to high value of k, compared with the number of plants.

If we regard the positions of the plant as a point process in the plane, it is plausible that a plant obtains its nutrients entirely from its Dirichlet tile, its Dirichlet tile being that portion of the plane nearer to it than to any other plant. Thus it seems natural to use the Dirichlet tessellation to explore the relationship between plant spacing. Mead (1966) was the first paper to use the Dirichlet tessellation to try to explain the yield of a plant, by defining various explanatory variables in a linear regression for the yield in terms of the Dirichlet tessellation. Suppose the plant position is P, the vertices of its Dirichlet tile are V_i, and the

centroid of its tile is C. We can then define the mean distance of the centroid from the vertices, D, to be the weighted sum

$$D = \frac{1}{2\pi} \sum w_i \, |CV_i| \ ,$$

where w_i is the external angle of the Dirichlet tile at vertex V_i. Mead (1966) used three statistics based on a plant's Dirichlet tile as the explanatory variables in a linear regression for the yield.

(i) *Area*, A = area of the Dirichlet tile ;

(ii) *Eccircularity*, $\lambda = D \left[\frac{\pi}{A}\right]^{\frac{1}{2}}$;

(iii) *Abcentricity*, $v = \frac{|CP|}{D}$.

Eccircularity is a measure of how much the tile shape differs from being circular, and has a minimum value of 1. Abcentricity measures the departure of the centroid of the tile from the plant. It is zero when these two points coincide and tends to 1 as the plant tends to one vertex of a regular tile. For irregular tiles, abcentricity may be greater than 1 as the plant tends to a vertex of a tile.

Mead used regressions of the form

$$Y_i = \alpha + \beta_1 A_i + \beta_2 \lambda_i + \beta_3 v_i + \varepsilon_i \qquad (4.1)$$

and

$$Y_i = \alpha + \beta_1 \log(A_i) + \beta_2 \lambda_i + \beta_3 v_i + \varepsilon_i \ , \qquad (4.2)$$

where Y_i is the yield of plant i etc. and ε_i are independent normal errors. He attempted to estimate values of α and $\beta_{1,2,3}$ both for plants from a single block or across blocks. We can extend these ideas to try regressions of the form

$$\log(Y_i) = \alpha + \beta_1 A_i + \beta_2 \lambda_i + \beta_3 v_i + \varepsilon_i \qquad (4.3)$$

and

$$\log(Y_i) = \alpha + \beta_1 \log(A_i) + \beta_2 \lambda_i + \beta_3 v_i + \varepsilon_i \ . \qquad (4.4)$$

The minimum number of seeds for an Erophila plant which produced seeds is 23, so we cannot attempt to fit a regression model based on normal errors to the entire data set. However, when we attempt to fit these regressions to the Erophila data for the 94 plants with seeds, we obtain the following F-statistics on 3 and 90 degrees of freedom for the significance of the regression, and consequently the following p-value for the regressions :

(4.1) 3.82 0.013 ,

(4.2) 4.07 0.009 ,

(4.3) 3.48 0.019 ,

(4.4) 4.07 0.009 .

Thus, all the regressions (4.1)-(4.4) are significant. When we test the hypothesis that $\alpha, \beta_i = 0$ for each regression, we obtain the following t-statistics on 90 degrees of freedom :

α	β_1	β_2	β_3
1.01	3.14	0.20	1.12
-1.69	3.26	0.98	1.14
8.36	2.90	-0.06	1.16
2.09	3.18	0.75	1.20

where $\mathbf{P}[|t_{90}|<2.00]=0.05$. Hence abcentricity and eccirularity are not significant explanatory variables, so we shall consider regressions of the form

$$Y_i = \alpha + \beta_1 A_i + \varepsilon_i \ , \tag{4.5}$$

$$Y_i = \alpha + \beta_1 \log(A_i) + \varepsilon_i \ , \tag{4.6}$$

$$\log(Y_i) = \alpha + \beta_1 A_i + \varepsilon_i \ , \tag{4.7}$$

and

$$\log(Y_i) = \alpha + \beta_1 \log(A_i) + \varepsilon_i \ . \tag{4.8}$$

Attempting to fit the regressions (4.5)-(4.8) we obtain the following F-statistics on 1 and 92 degrees of freedom for the significance of the regressions and their corresponding p-values :

(4.5) 10.3 0.008 ,

(4.6) 10.3 0.014 ,

(4.7) 9.08 0.002 ,

(4.8) 10.5 0.003 .

Figures 18 and 19 show a plot of yield against tile area and the logarithm of tile area respectively for seeded Erophila plants, and figures 20 and 21 a plot of the logarithm of yield against tile area and the logarithm of tile area respectively.

A plant is obviously going to be more successful at capturing nutrients from some parts of its tile than from others, and the concepts of abcentricity and eccircularity are an attempt to model this. However, in our case and many others, the area or some function of it is by far the most significant explanatory variable. This is probably because abcentricity and eccircularity are artificial mathematical concepts and they are not commensurable with each other or with the area of a tile, that is to say it is unclear as to whether we should use abcentricity or, for example, the square of abcentricity in the regression.

It would appear that a plant will be more successful at extracting nutrients from the nearer parts of its tile than the other parts. Accordingly, Sibson (personal communication) introduced a model based on the area in a plant's tile within a certain distance of the plant. Thus, we can consider models of the form

$$Y_i = \alpha + \beta A_i(r) + \varepsilon_i \quad , \tag{4.9}$$

and

$$Y_i = \alpha + \beta \log[A_i(r)] + \varepsilon_i \quad , \tag{4.10}$$

where $A_i(r)$ denotes the area in the i^{th} plant's tile within a distance r of the plant. We can fit regressions of the form (4.9) and (4.10) for different values of r, and find a value of r that gives the best fit, both for an individual plot or across plots if we wish. Sibson did this with some success for the plant data in Mead (1966). Figures 22 and 23 are plots of the yield of seeded plants against the area within r for r=8 and 10*mm* respectively.

Unfortunately, as we can see from figures 22 and 23, there is no such simple linear trend between the area within r of a plant in its tile and the plant's yield. In order to test for a connection we can construct a non-parametric test of the correlation between the yield and the area within r.

Suppose we have n plants, then we can define a statistic C by

$$C(r) = \frac{1}{A\bar{Y}} \sum_{i=1}^{n} Y_i A_i(r) \quad , \tag{4.11}$$

where A is the area of the region and $\bar{Y}$ is the average yield. Clearly $C(r)>0$ for $r>0$, and is an increasing function of r. If Y_i and A_i are independent, then

$$\mathrm{E}[C(r)] = \frac{1}{A\bar{Y}} \sum_{i=1}^{n} \mathrm{E}[Y_i]\ \mathrm{E}[A_i(r)] \leq \frac{1}{A} \sum_{i=1}^{n} A_i \leq 1 \quad ,$$

where A_i is the area of the i^{th} tile. If we take our null hypothesis to be that there is no correlation between Y_i and $A_i(r)$, then we can simulate values of $C(r)$ under the null hypothesis by permuting the yields, Y_i, amongst the tiles, to obtain

$$C_\pi(r) = \frac{1}{A\bar{Y}} \sum_{i=1}^{n} Y_{\pi(i)} A_i(r) \quad ,$$

where π is a permutation of the integers from 1 to n. We can then plot $C(r)$ against r along with confidence bands to see at what values of r significant correlation occurs.

We are using a non-parametric test, so we can perform this test both on all the Erophila data and just on those Erophila plants which produced seeds. The solid line in figure 24 shows this function for all the Erophila plants along with 95% confidence bands obtained from 200 permutations, and figure 25 for just the seeded Erophila plants. In figure 24 the function $C(r)$ is above the confidence bands for values of r>12mm, about the root diameter, whereas in figure 25 it is not. This would imply that that there is a correlation between not producing any seed at all and having a small tile area within r, but given that a plant has produced seeds, its tile area within r is not correlated with its seed number. However this is not a very powerful test.

It can be seen from the triangular shape of the distribution of the points in figures 20-23 that the mean of the distribution of Y_i given $A_i(r)$, is roughly linearly dependent on $A_i(r)$, and it may be possible to postulate a model based on this and obtain an estimate of r dependent on the best fit. Again, bearing in mind the triangular shape of the distribution of points, we could attempt to fit an extremely simple model in which

$$Y_i \sim Uni\ [\ a, b+mA_i(r)\ ] \quad , \tag{4.12}$$

where a,b,m and r are parameters to be estimated. A model such as (4.12) would not be robust to outliers. Clearly, $a \leq Min(Y_i)$ and $b \geq a$, so a single plant with a small yield and large tile would give an unnecessarily small value of a. However this is not such a serious a problem as a single outlying plant with a large yield and a small tile as this will give a far too large value of m.

A more sensible approach is one which does not have a cut-off point for high values of the yield. Since we are dealing with integer values for the yield, we will attempt to fit a model based upon the Poisson distribution, but it would be possible to use the same argument for the exponential distribution for a continuous yield. Suppose

$$Y_i \sim Poi\ [\ \lambda A_i(r)\ ] \quad , \tag{4.13}$$

then

$$\mathbf{P}\,(\,Y_i=y_i\,) = \frac{e^{-\lambda A_i(r)}\,\lambda^{y_i}A_i^{y_i}}{y_i!}\quad .$$

It only remains to estimate the parameters λ and r, which can be done by the method of maximum likelihood. The likehood function is given by

$$L\,(\,\mathbf{y}\,;\,\lambda,r\,) = e^{-\lambda\sum A_i(r)}\,\lambda^{\sum y_i}\prod_{i=1}^{n}A_i(r)^{y_i}\left[\prod_{i=1}^{n}y_i!\right]^{-1}\quad ,$$

so the log likelihood is given by

$$\mathcal{L}\,(\,\mathbf{y}\,;\,\lambda,r\,) = -\lambda\sum_{i=1}^{n}A_i(r) + \log(\lambda)\sum_{i=1}^{n}y_i \qquad (4.14)$$

$$+\sum_{i=1}^{n}y_i\log[A_i(r)] - \sum_{i=1}^{n}\log(y_i!)\quad .$$

The function $A_i(r)$ is a differentiable function of r since it is a sum of areas of intersection between fixed triangles and a circle with a fixed centre and of radius r, so differentiating (4.14) gives us

$$\frac{\partial\mathcal{L}}{\partial\lambda} = -\sum_{i=1}^{n}A_i(r) + \frac{1}{\lambda}\sum_{i=1}^{n}y_i\quad , \qquad (4.15)$$

and

$$\frac{\partial\mathcal{L}}{\partial r} = -\lambda\sum_{i=1}^{n}A_i'(r) + \sum_{i=1}^{n}y_i\frac{A_i'(r)}{A_i(r)}\quad . \qquad (4.16)$$

Equating (4.15) and (4.16) to zero, we obtain the following equations for $\hat{r}$ and $\hat{\lambda}$, the maximum likelihood estimates of r and λ,

$$\sum_{i=1}^{n}y_i\,\frac{A_i'(\hat{r})}{A_i(\hat{r})} - \sum_{i=1}^{n}y_i\,\frac{\sum_{i=1}^{n}A_i'(\hat{r})}{\sum_{i=1}^{n}A_i(\hat{r})} = 0\quad , \qquad (4.17)$$

and

$$\hat{\lambda} = \frac{\sum_{i=1}^{n}y_i}{\sum_{i=1}^{n}A_i(\hat{r})}\quad . \qquad (4.18)$$

We can approximate values of A_i' by using

$$A_i'(r) \approx \frac{A_i(r+h)-A_i(r)}{h}\quad , \qquad (4.19)$$

for small h, and so we can find approximate solutions of (4.17) and (4.18) for $\hat{r}$ and $\hat{\lambda}$. These solutions can then be checked with (4.14) to see whether they

maximise the log-likelihood function, as one solution to (4.18) is $r>\frac{1}{2}d$, where d is the largest Dirichlet cell diameter.

If we attempt to fit such a model to those Erophila plants which produced seeds, we obtain maximum likelihood estimates for r and λ of $\hat{r}=9mm$ and $\hat{\lambda}=0.33$. It is interesting to note that this value of r is roughly the average root diameter of the Erophila plants.

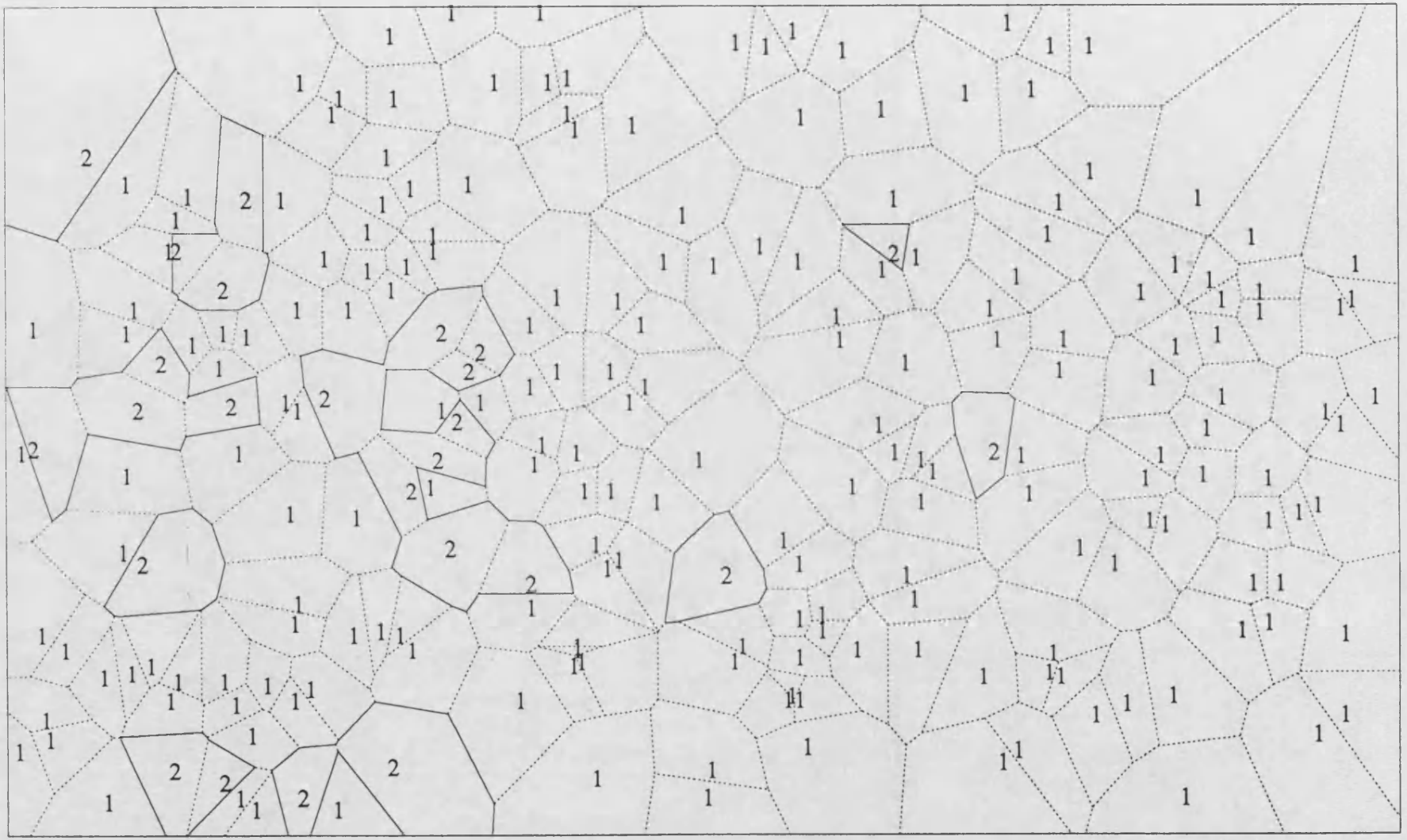

Figure 1

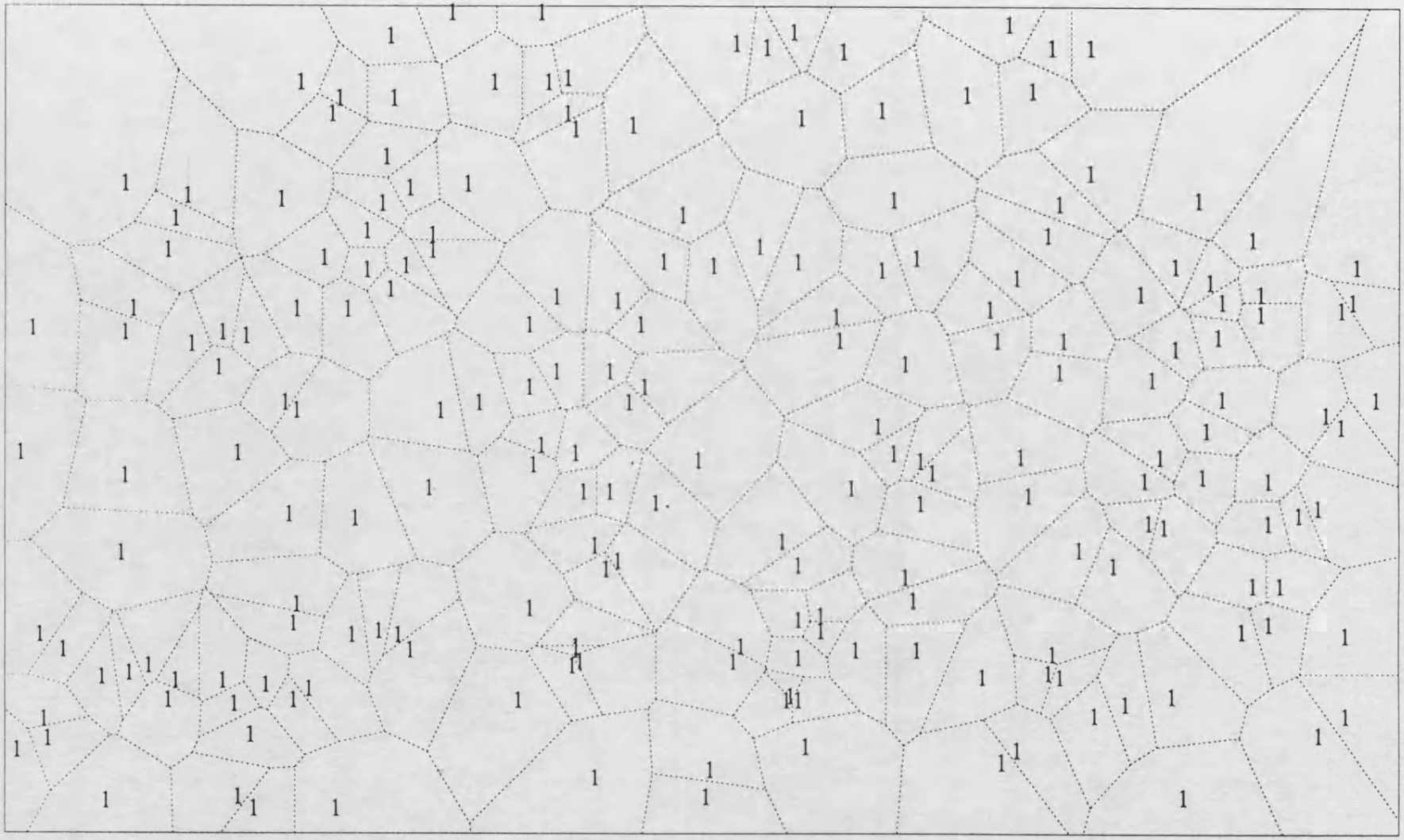

Figure 2

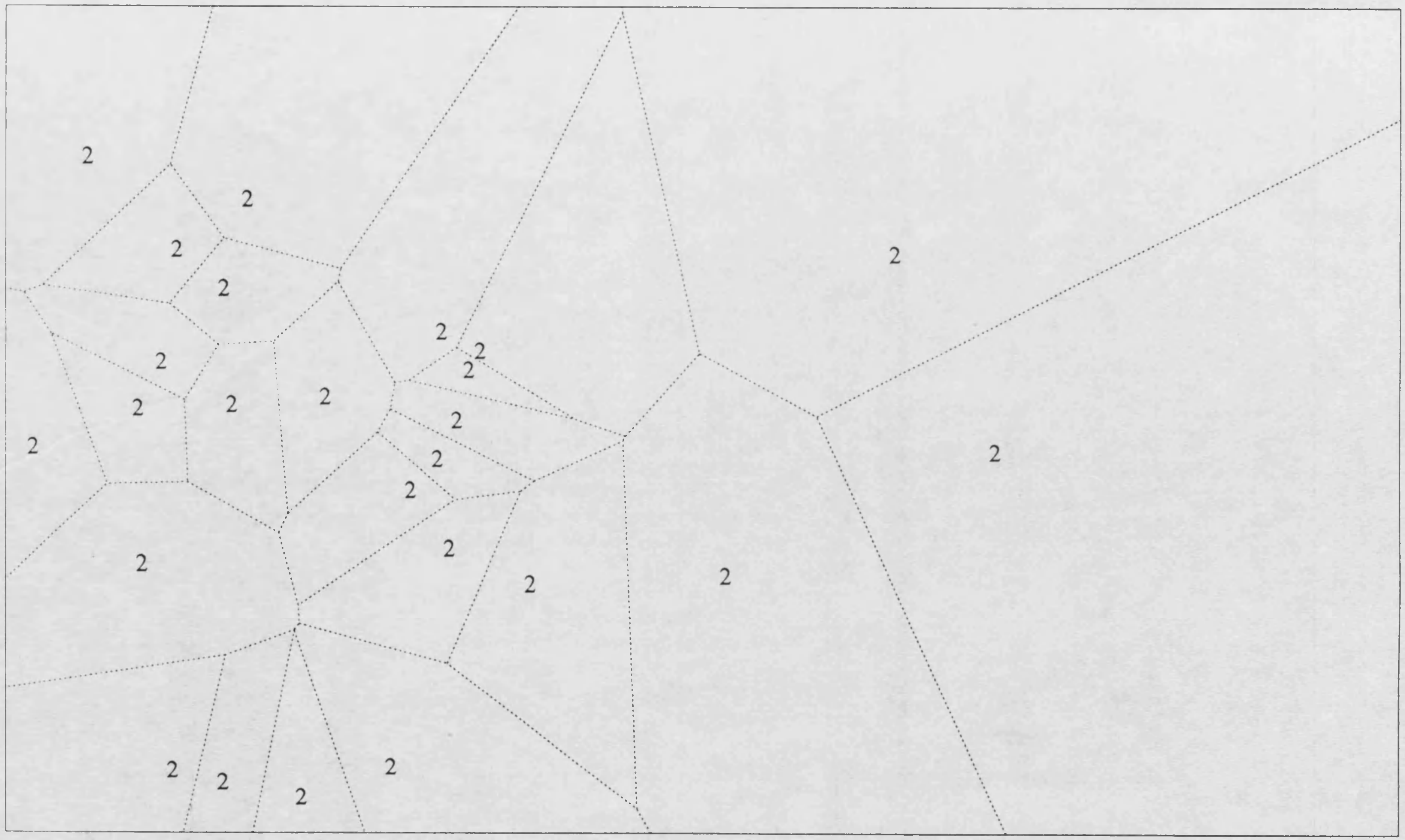

Figure 3

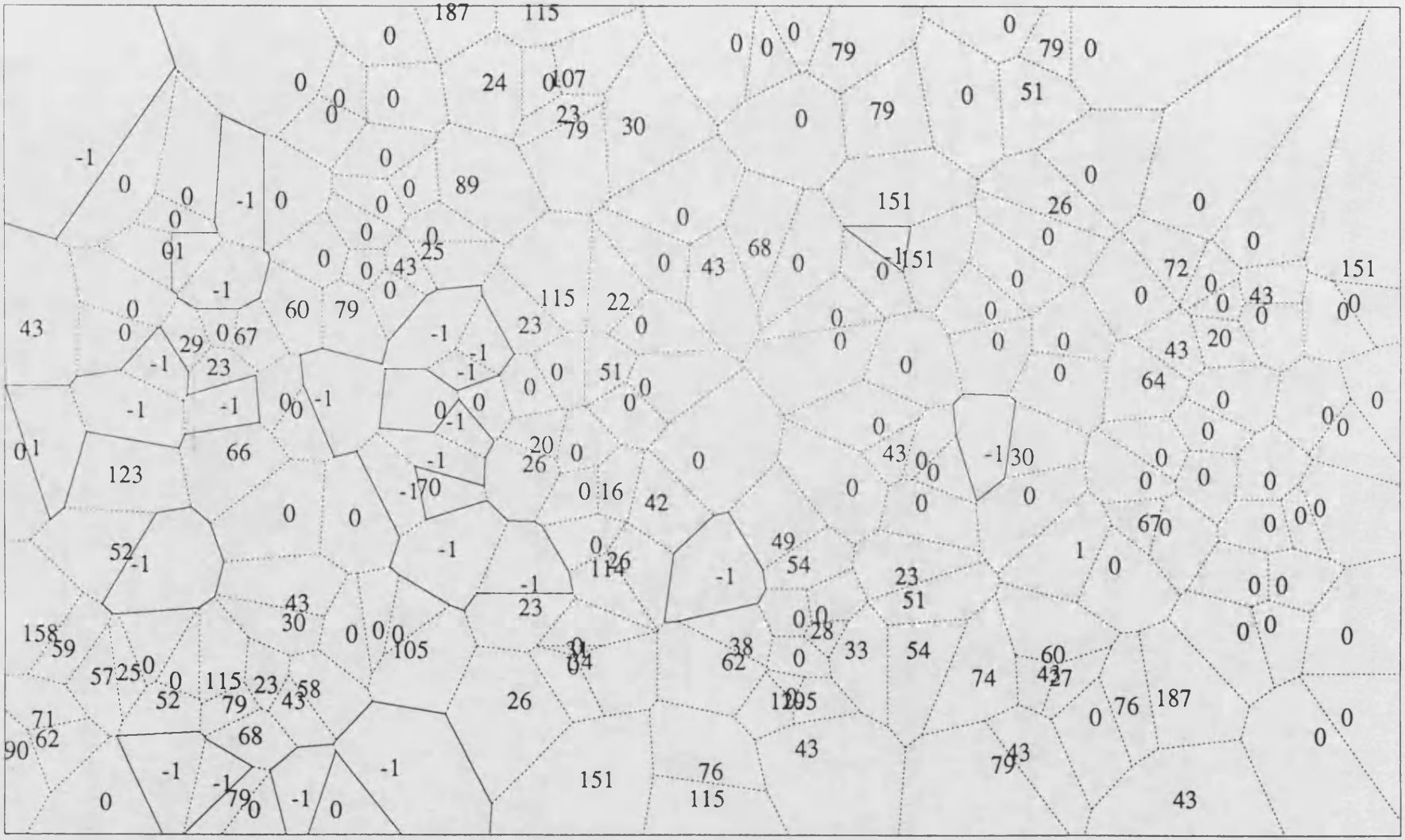

Figure 4

Figure 5

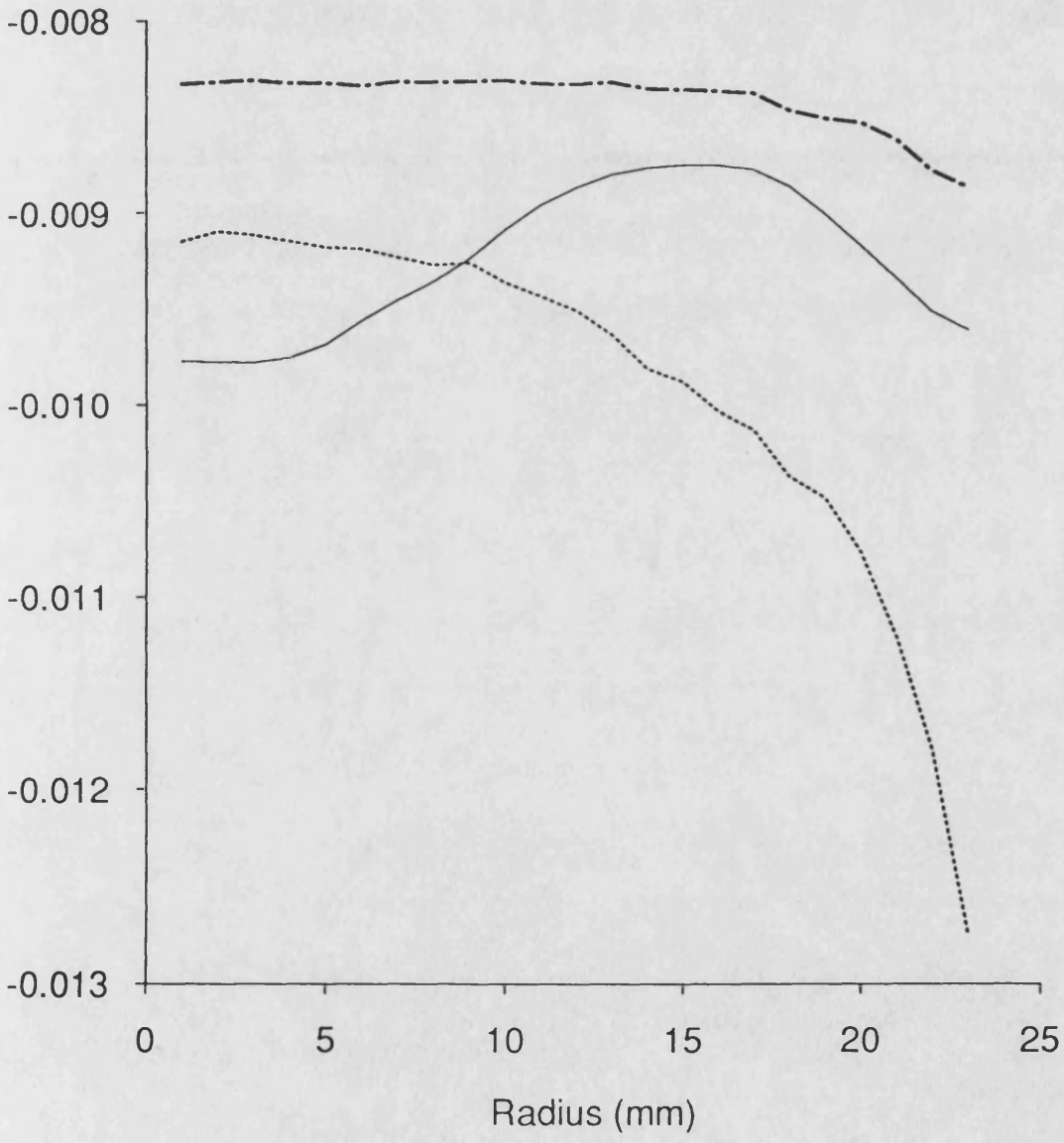

Figure 6

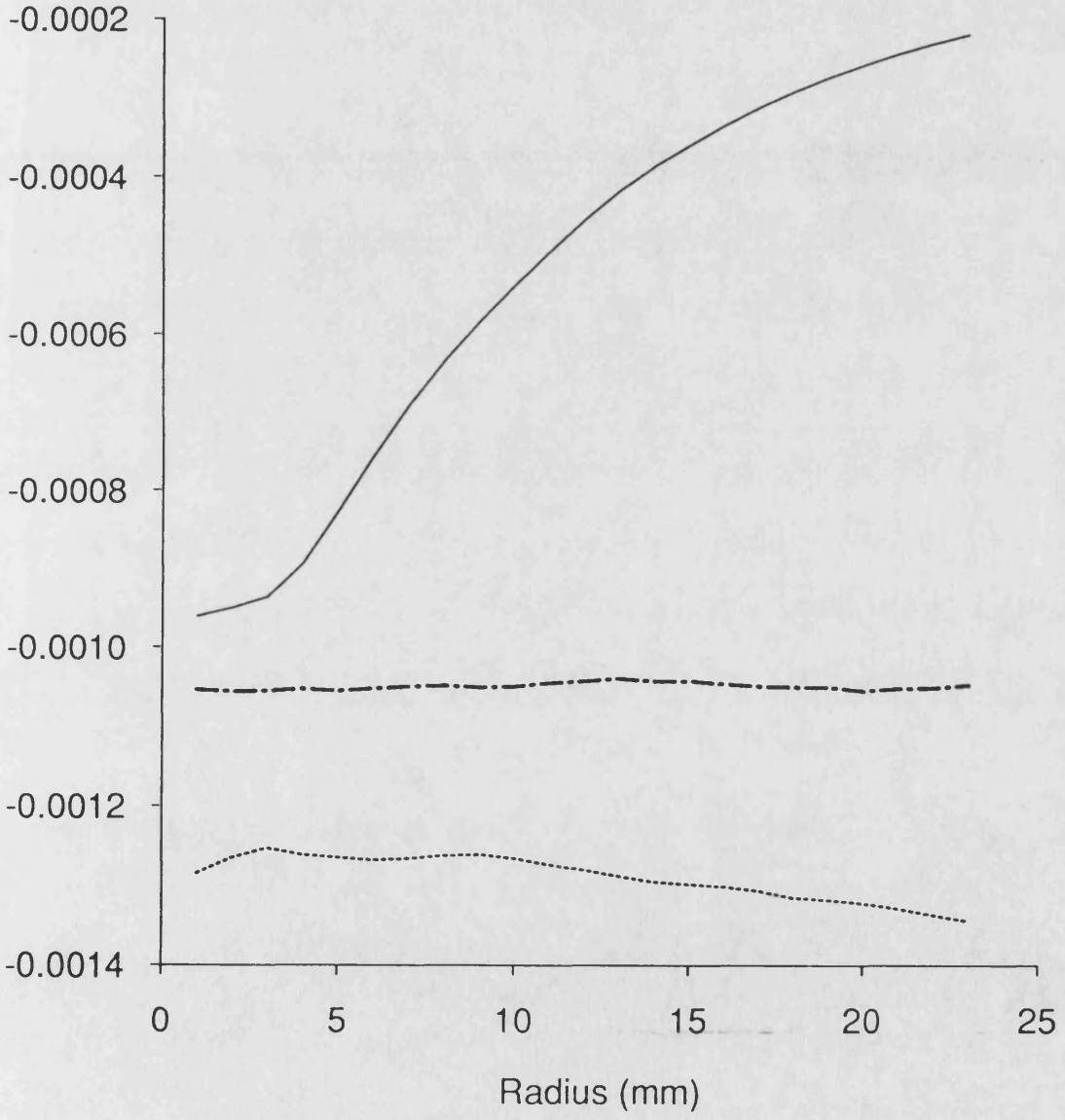
-0.0002
-0.0004
-0.0006
-0.0008
-0.0010
-0.0012
-0.0014
0
5
10
15
20
25
Radius (mm)

Figure 7

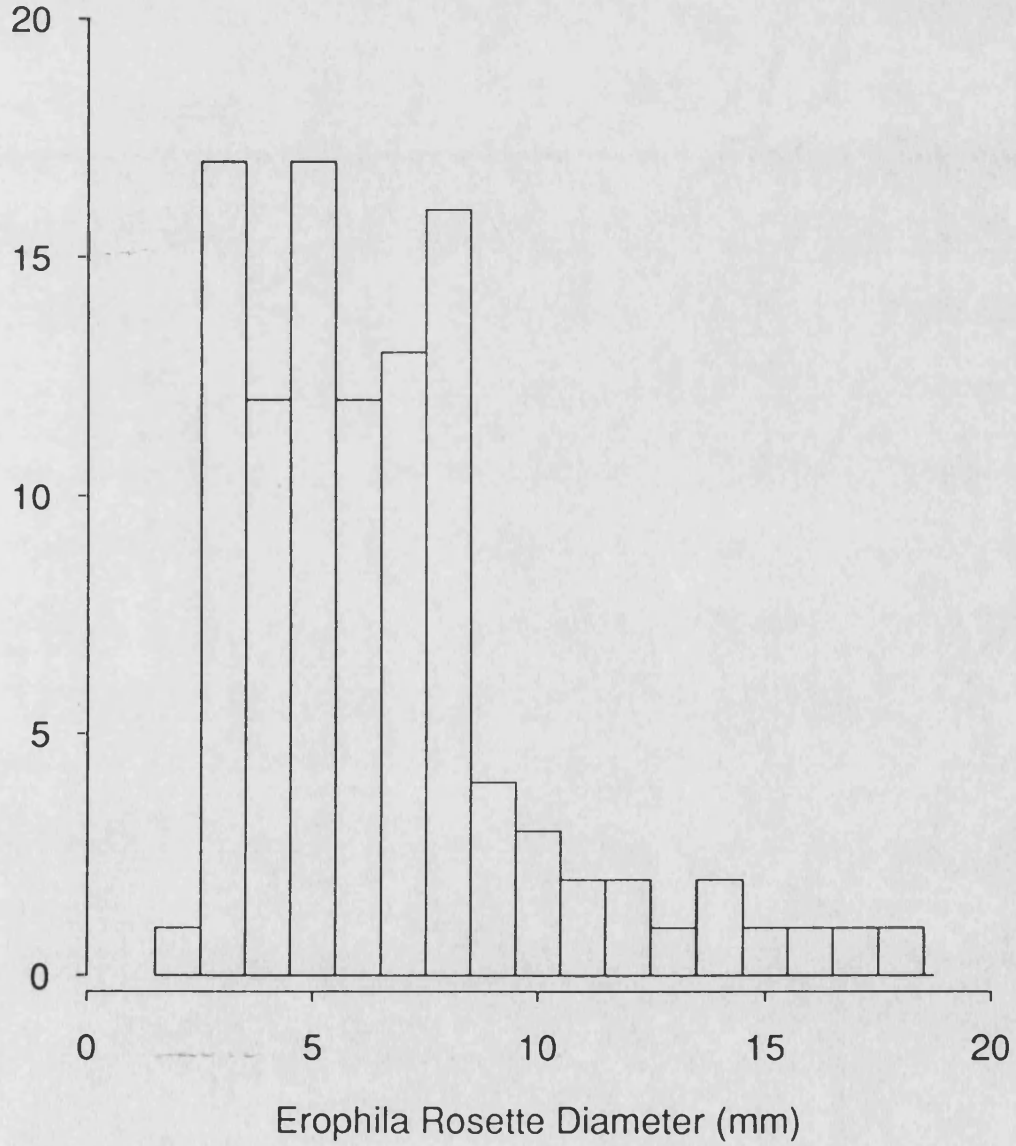

Figure 8

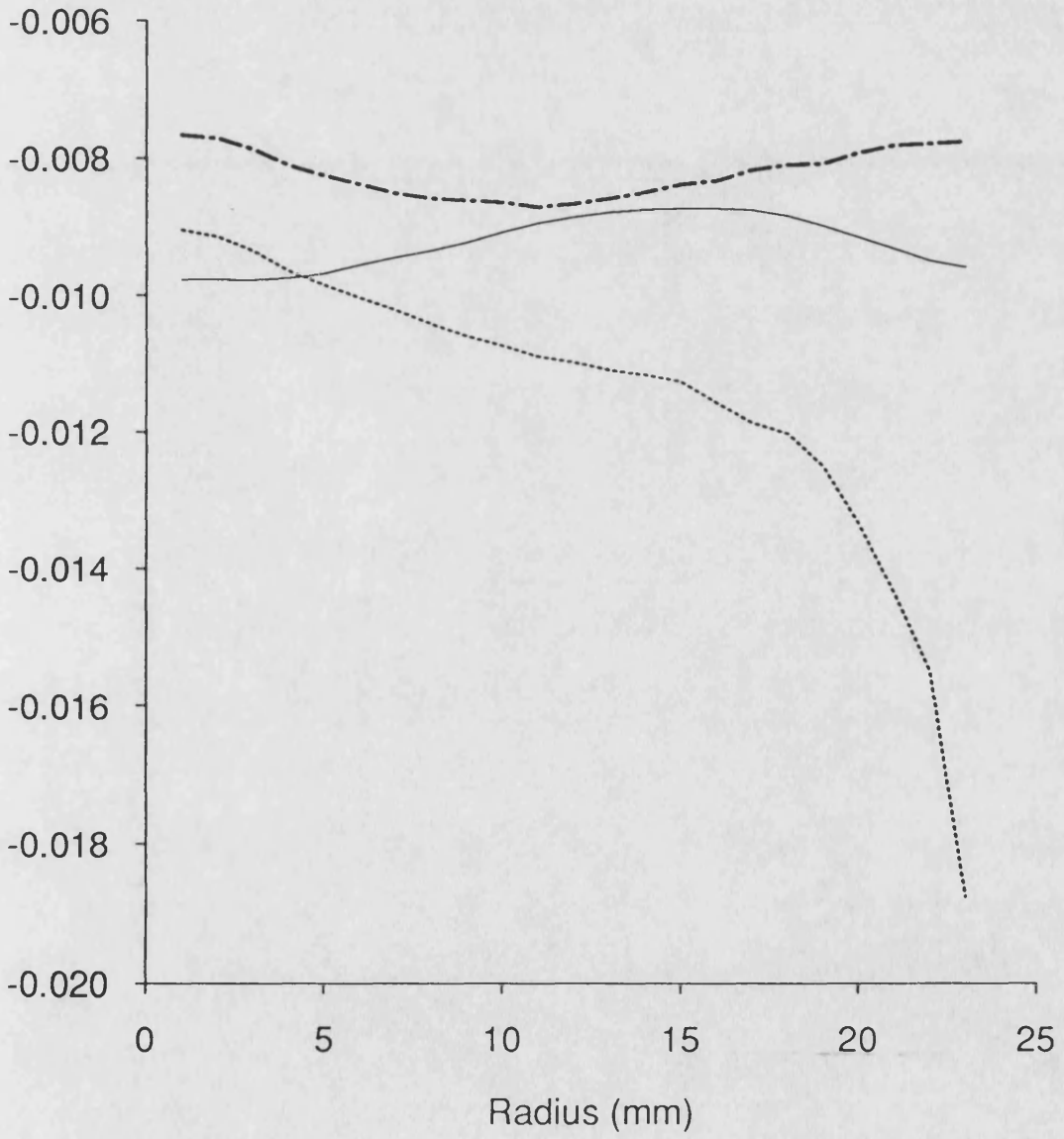
-0.006
-0.008
-0.010
-0.012
-0.014
-0.016
-0.018
-0.020
0
5
10
15
20
25
Radius (mm)

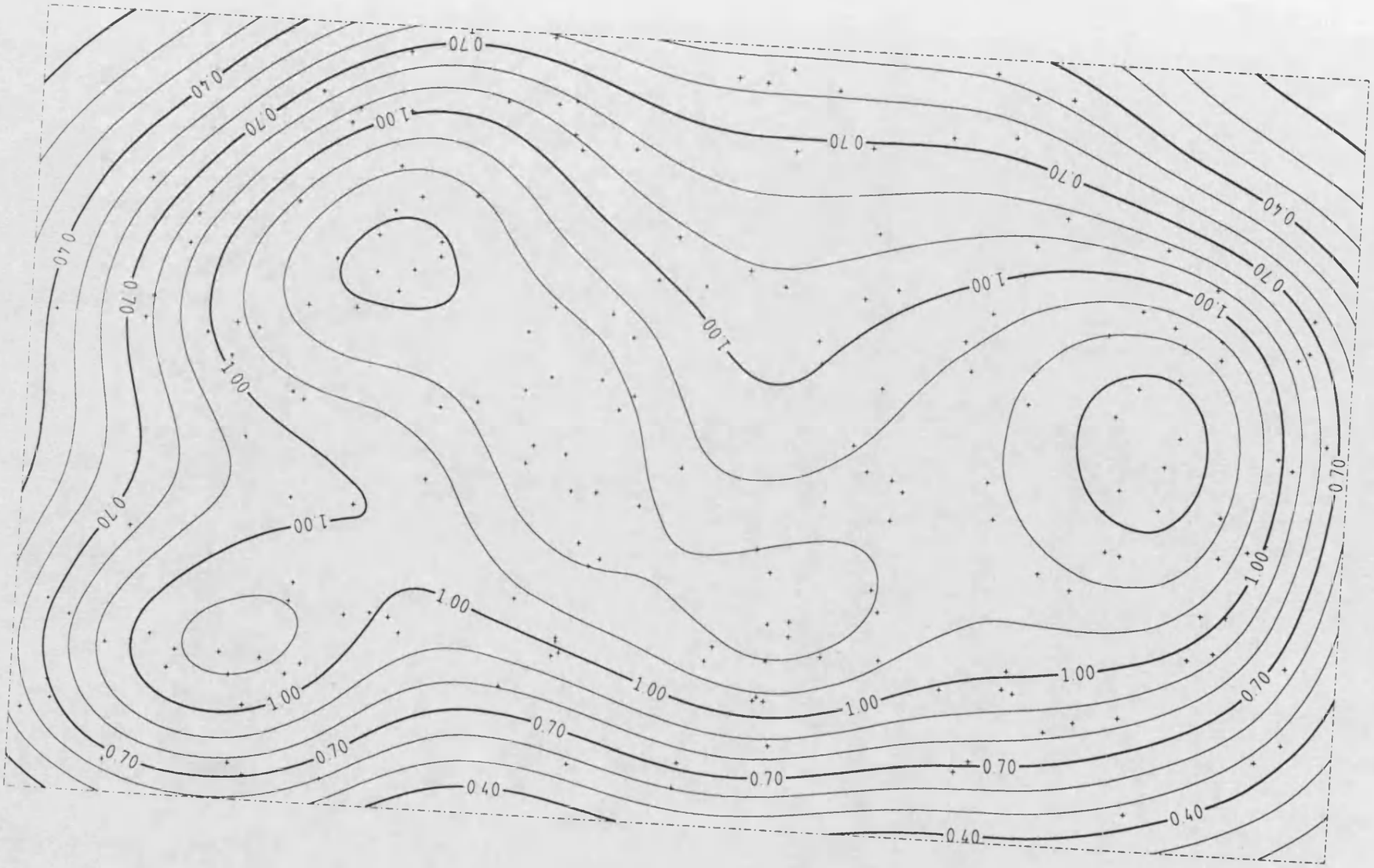
0.70
0.40
1.00
0.70
1.00
0.70
0.40
1.00
0.70
1.00
0.70
0.40
1.00
0.70
1.00
0.70
1.00
0.70
1.00
0.70
0.40
0.40

Figure 9

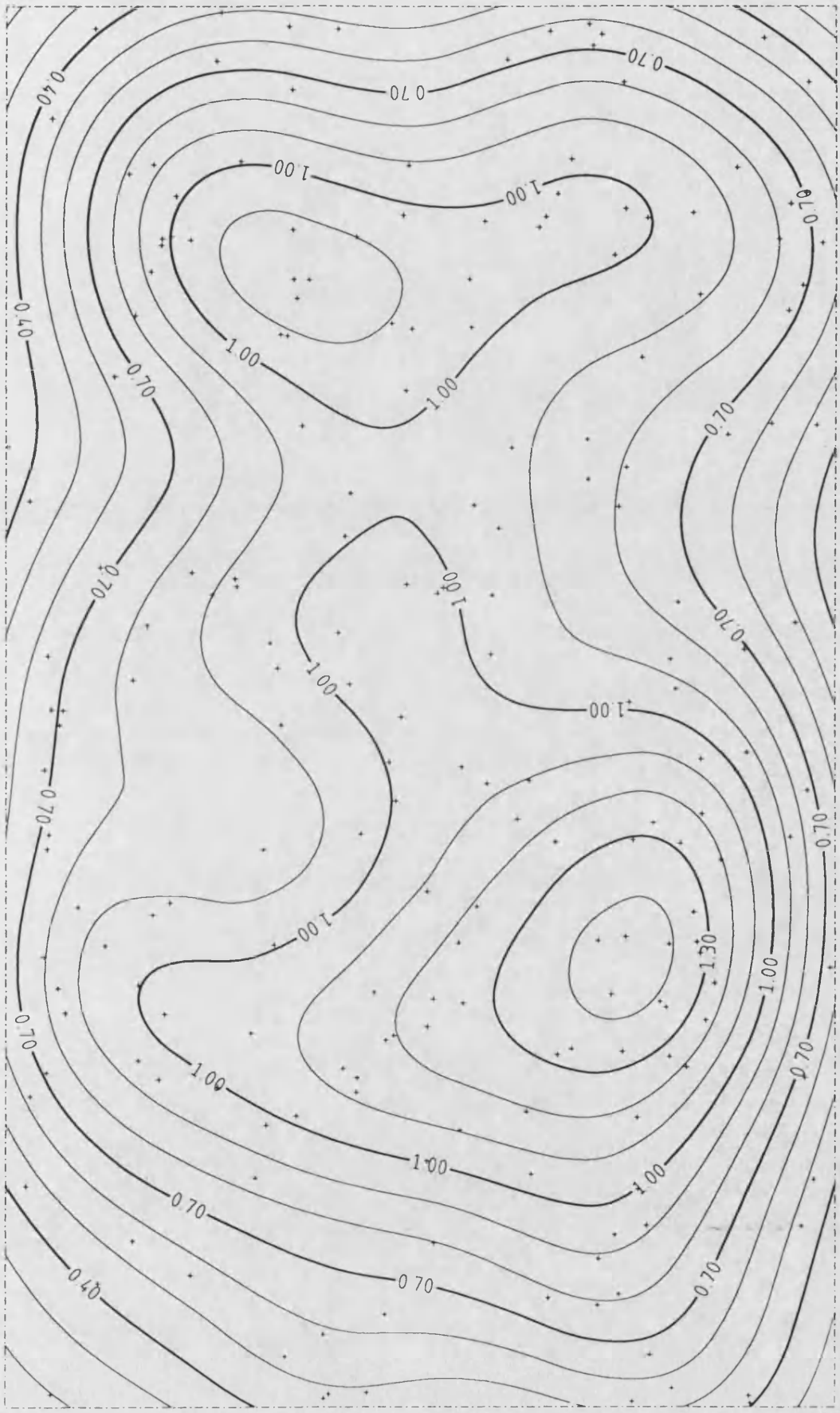

Figure 10

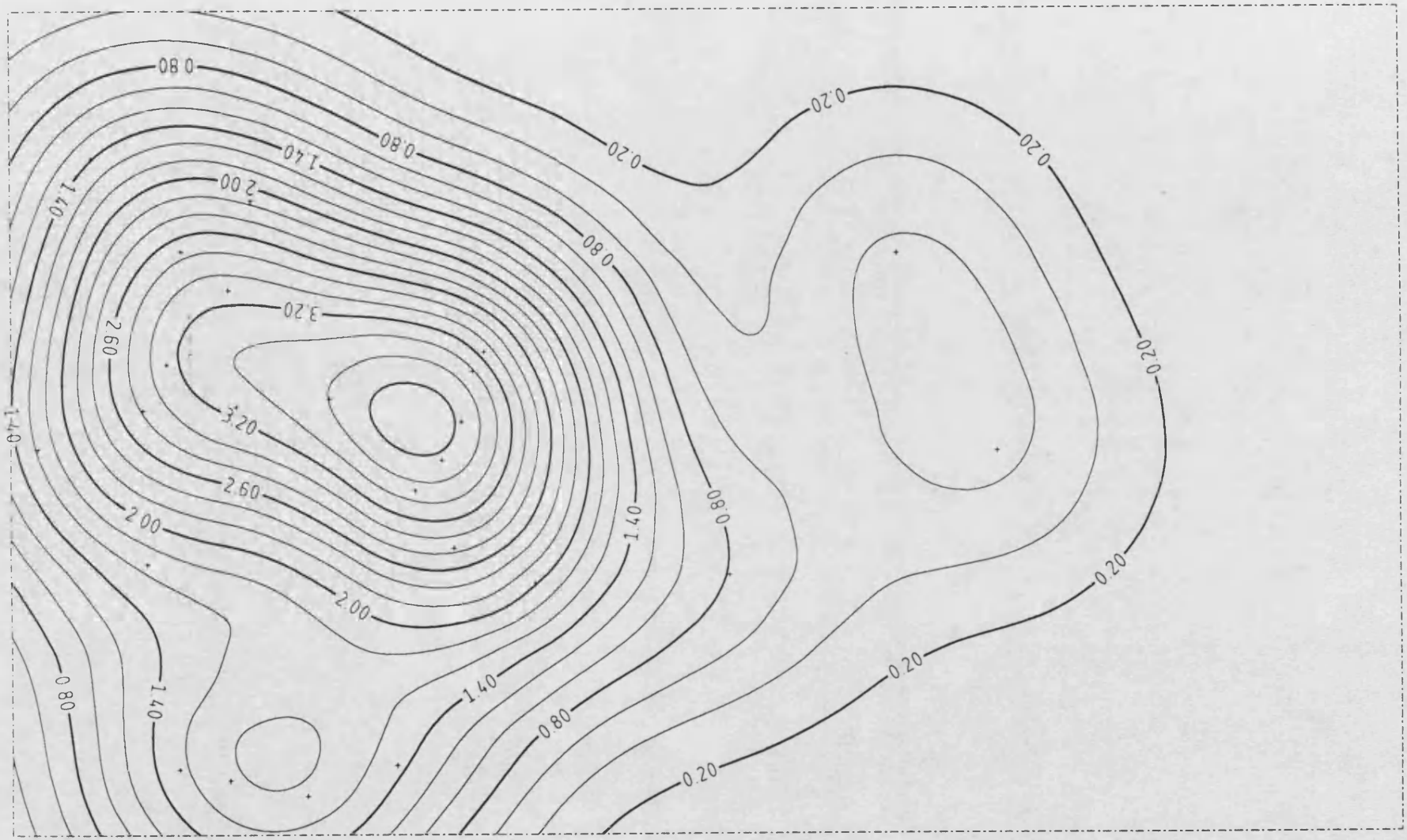
0.80
0.80
1.40
2.00
3.20
2.60
3.20
2.60
2.00
2.00
1.40
0.80
1.40
0.80
1.40
0.80
0.20
0.20
0.20
0.20
0.20
0.20
0.20

Figure 11

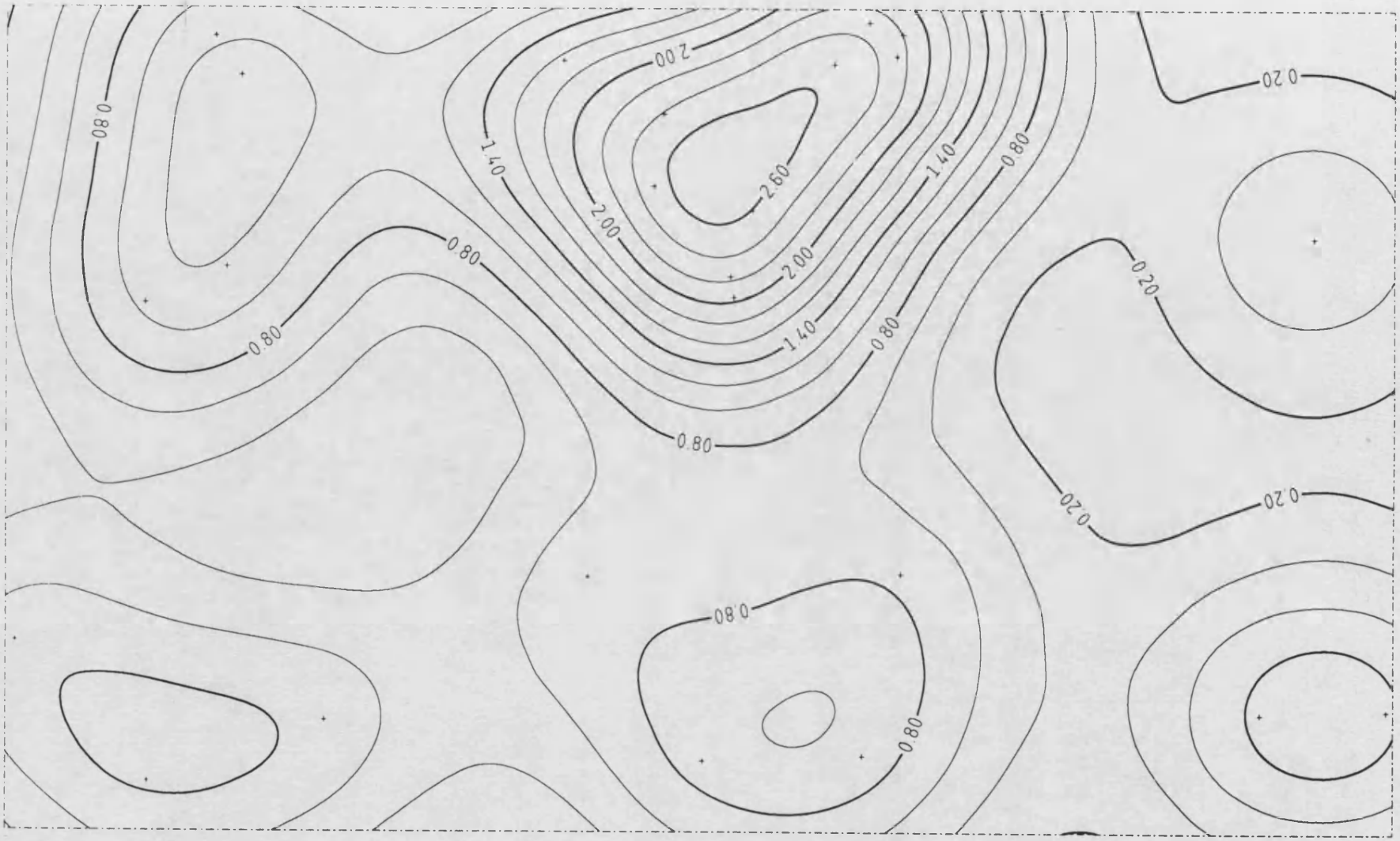

Figure 12

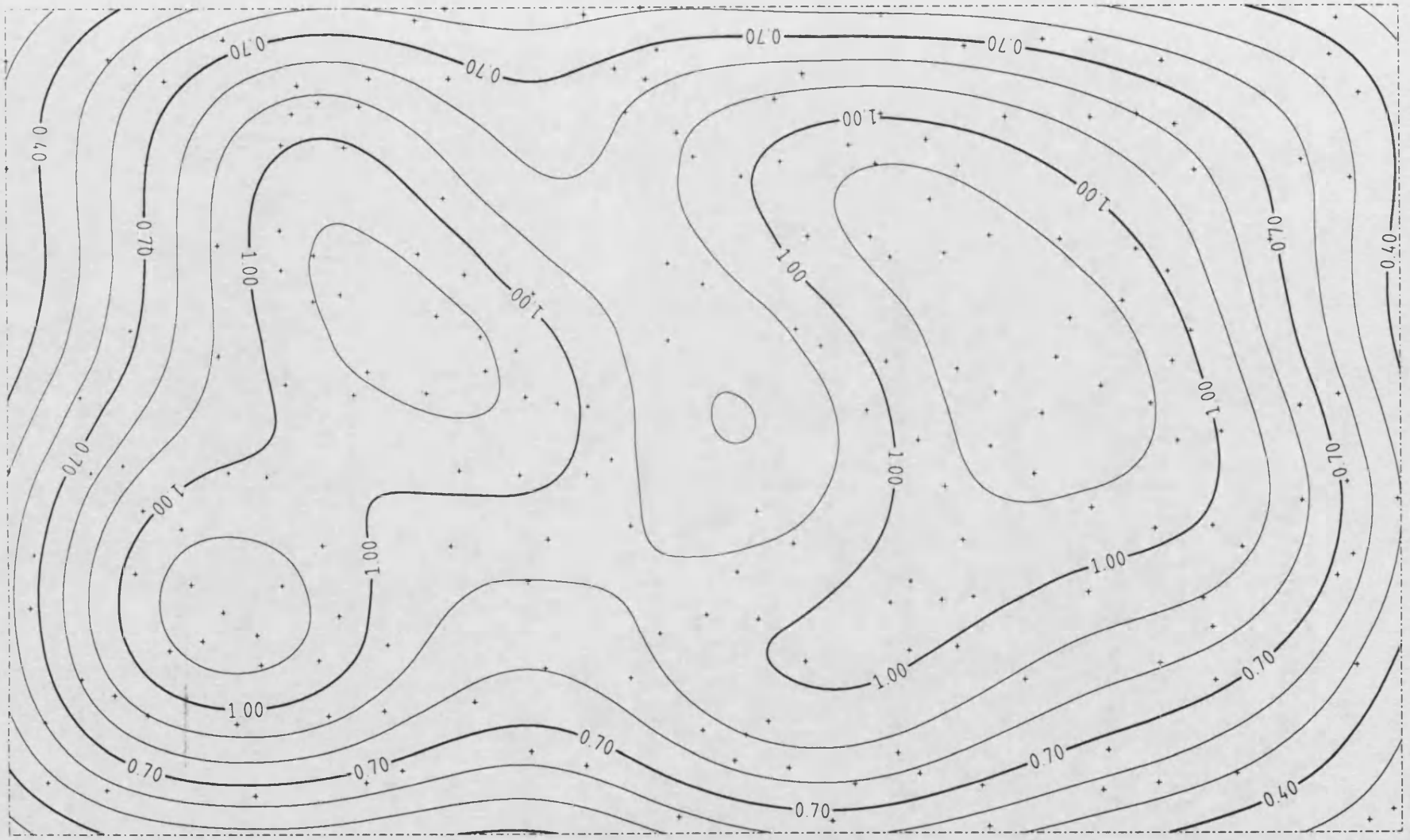

Figure 13

Figure 14

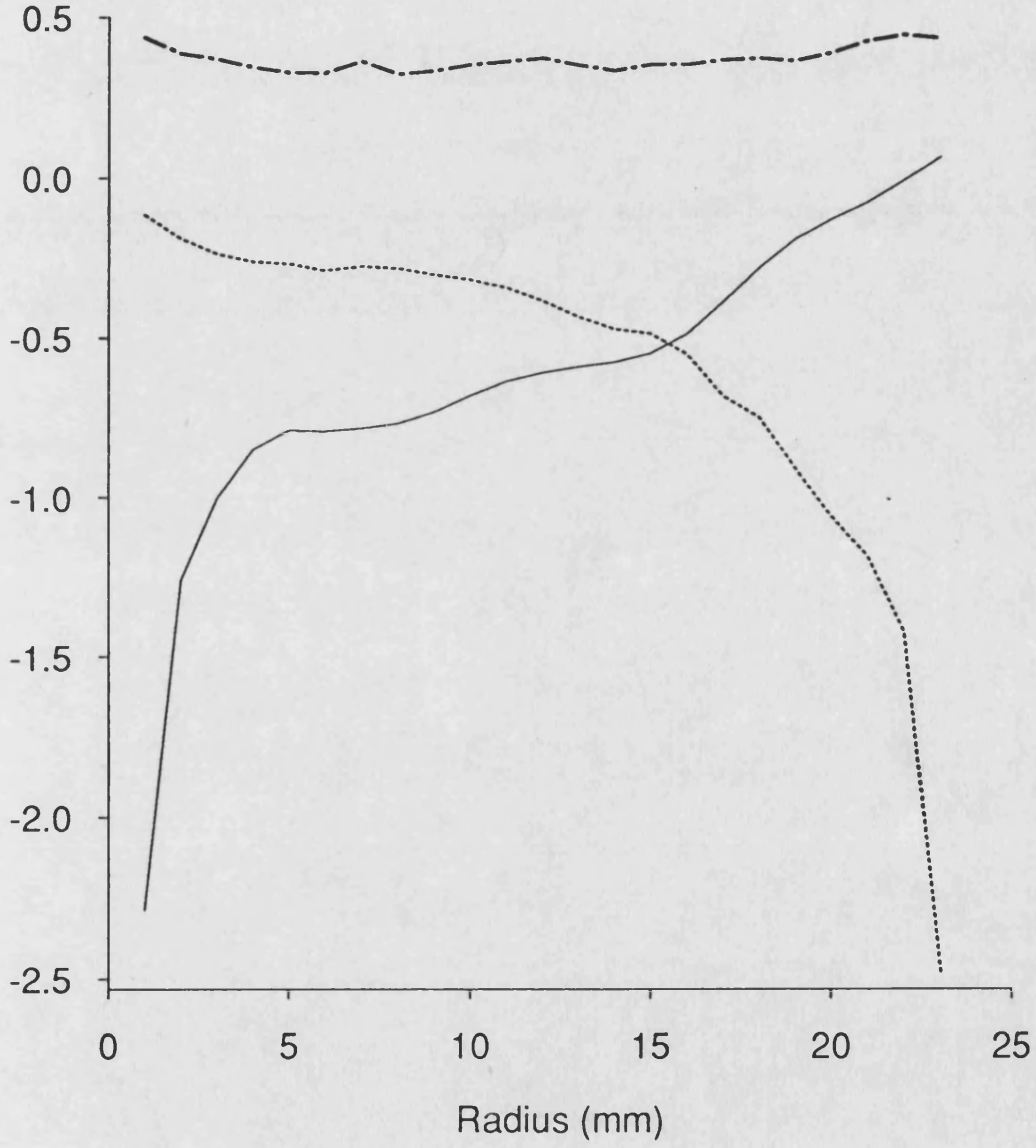

Figure 15

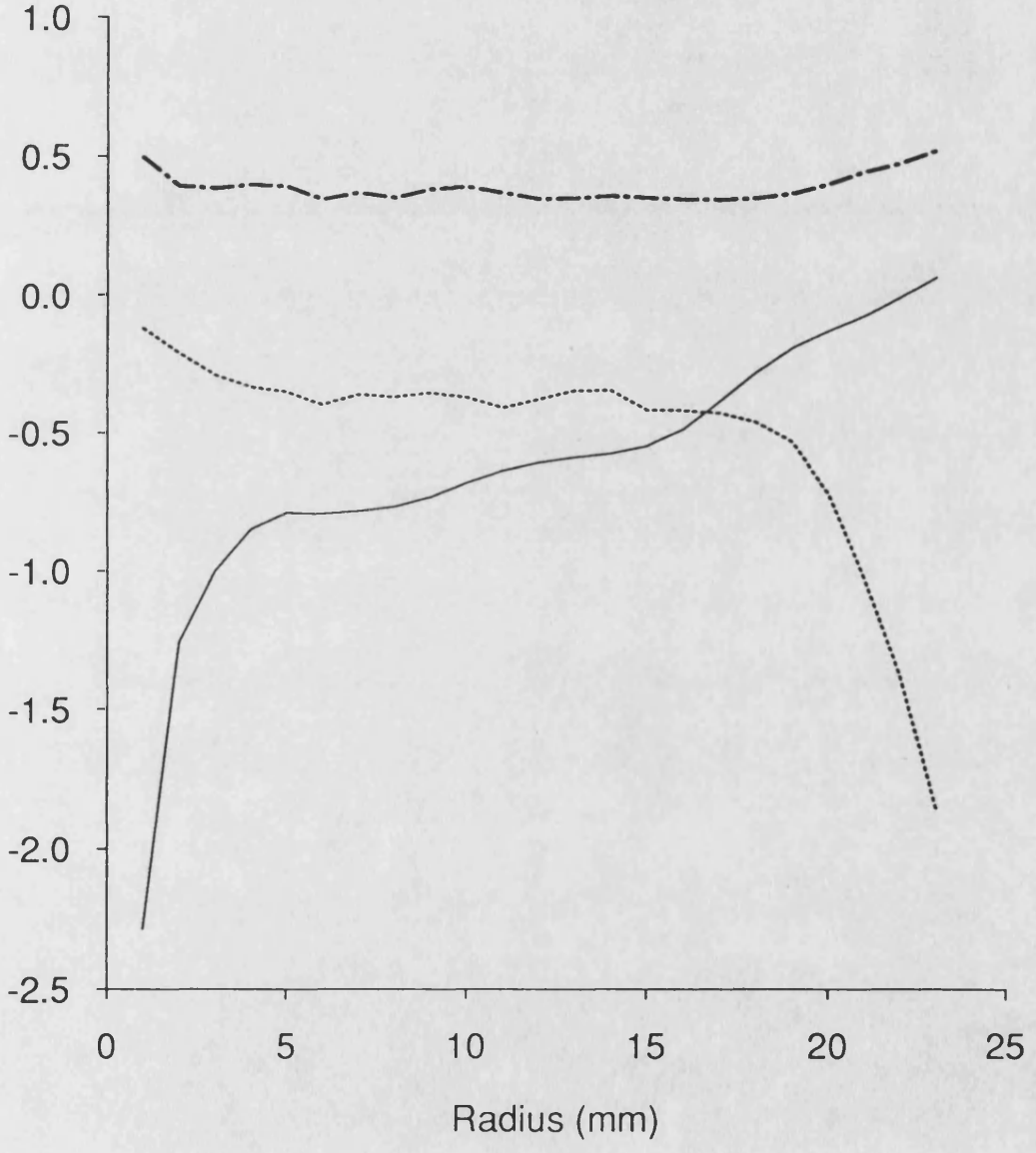

Figure 16

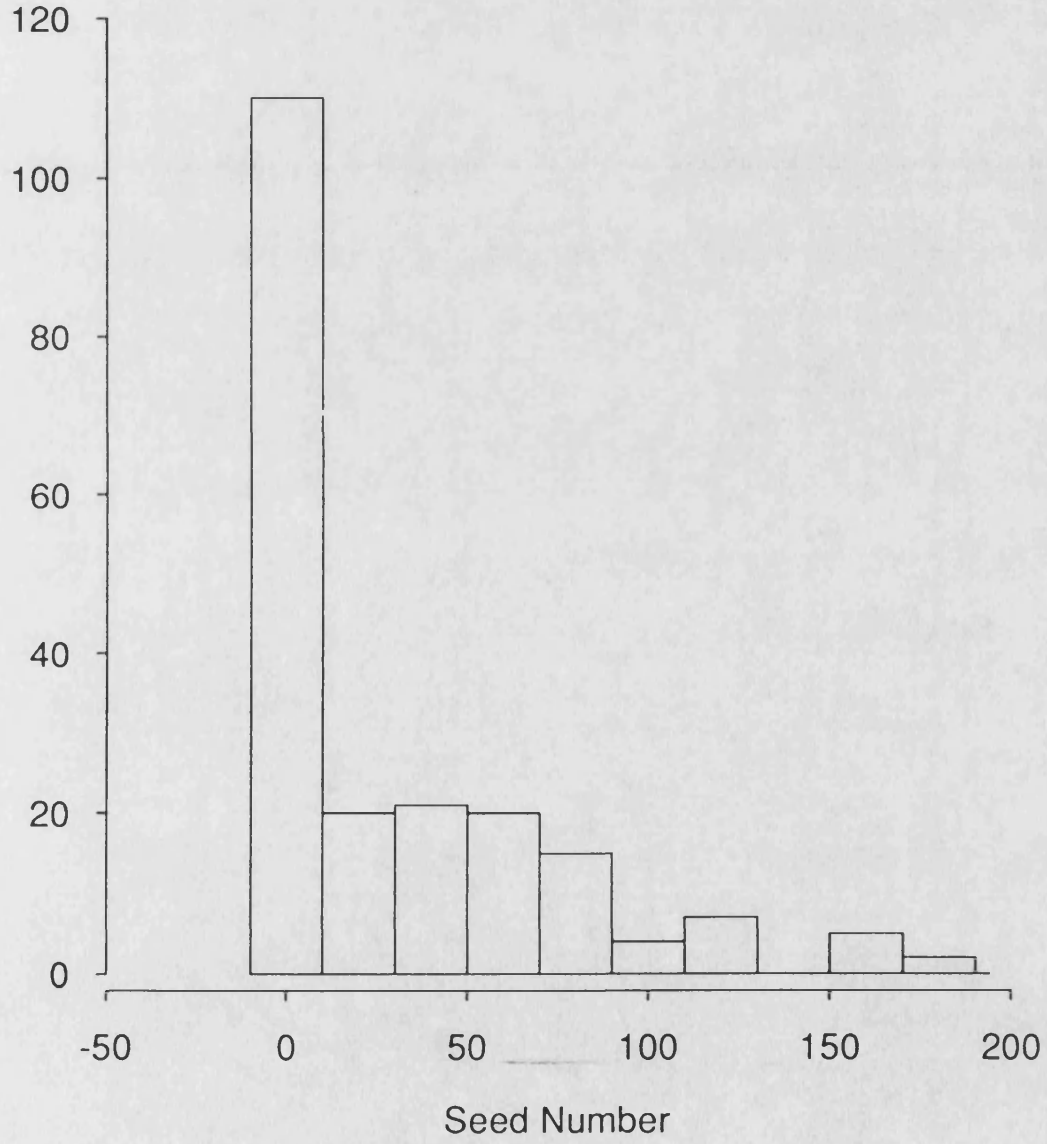

Figure 17

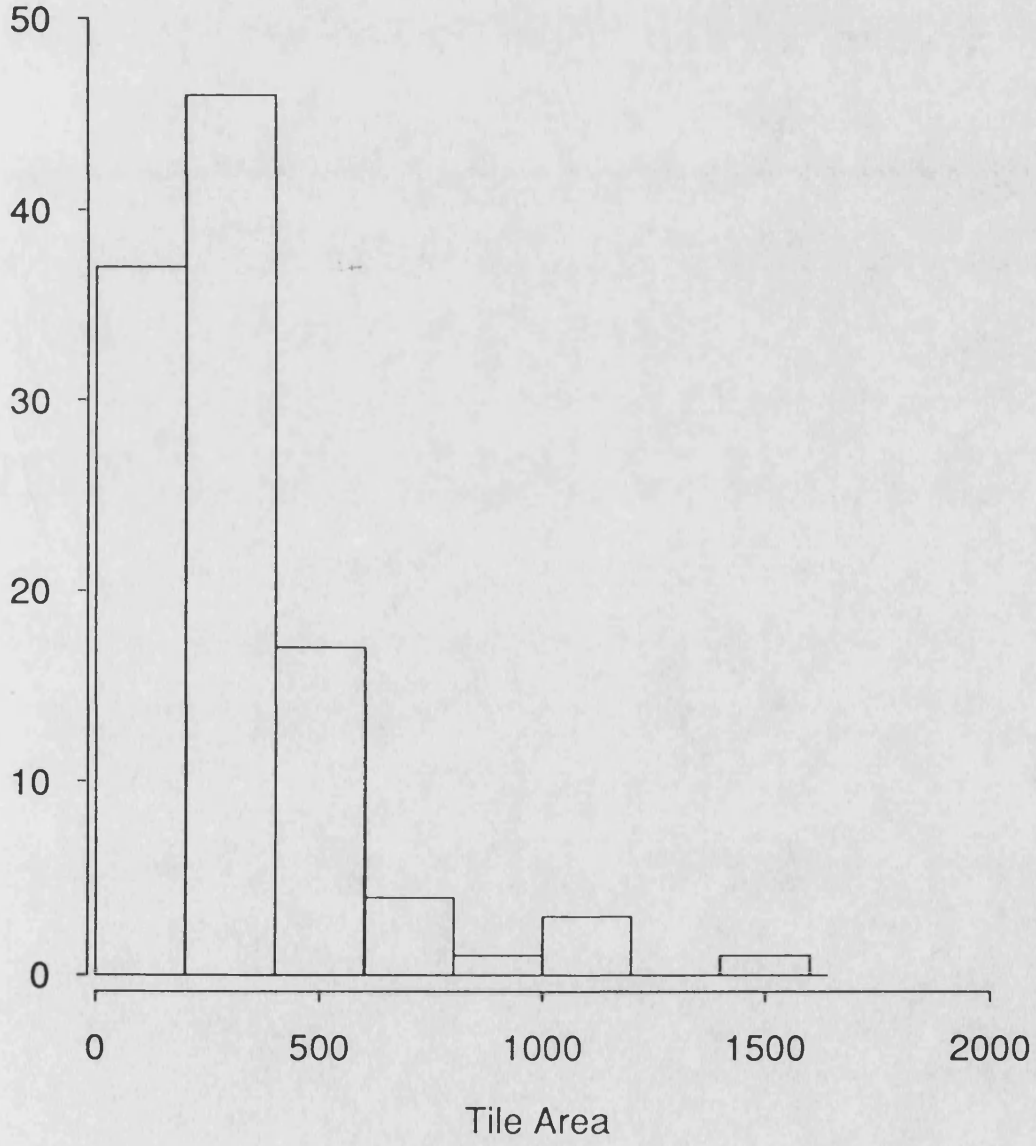

Figure 18

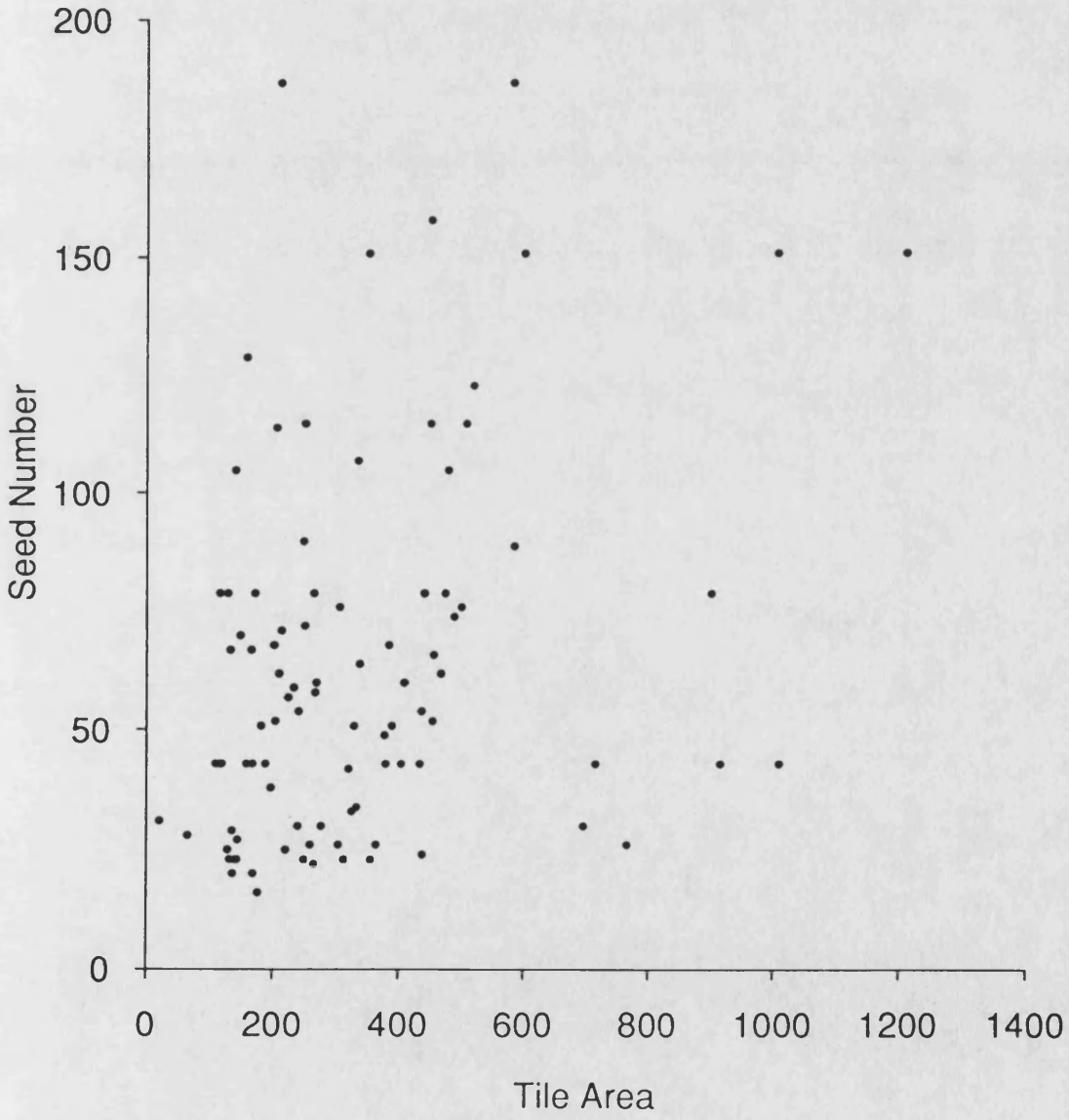
200
150
100
50
0
Seed Number
0
200
400
600
800
1000
1200
1400
Tile Area

Figure 19

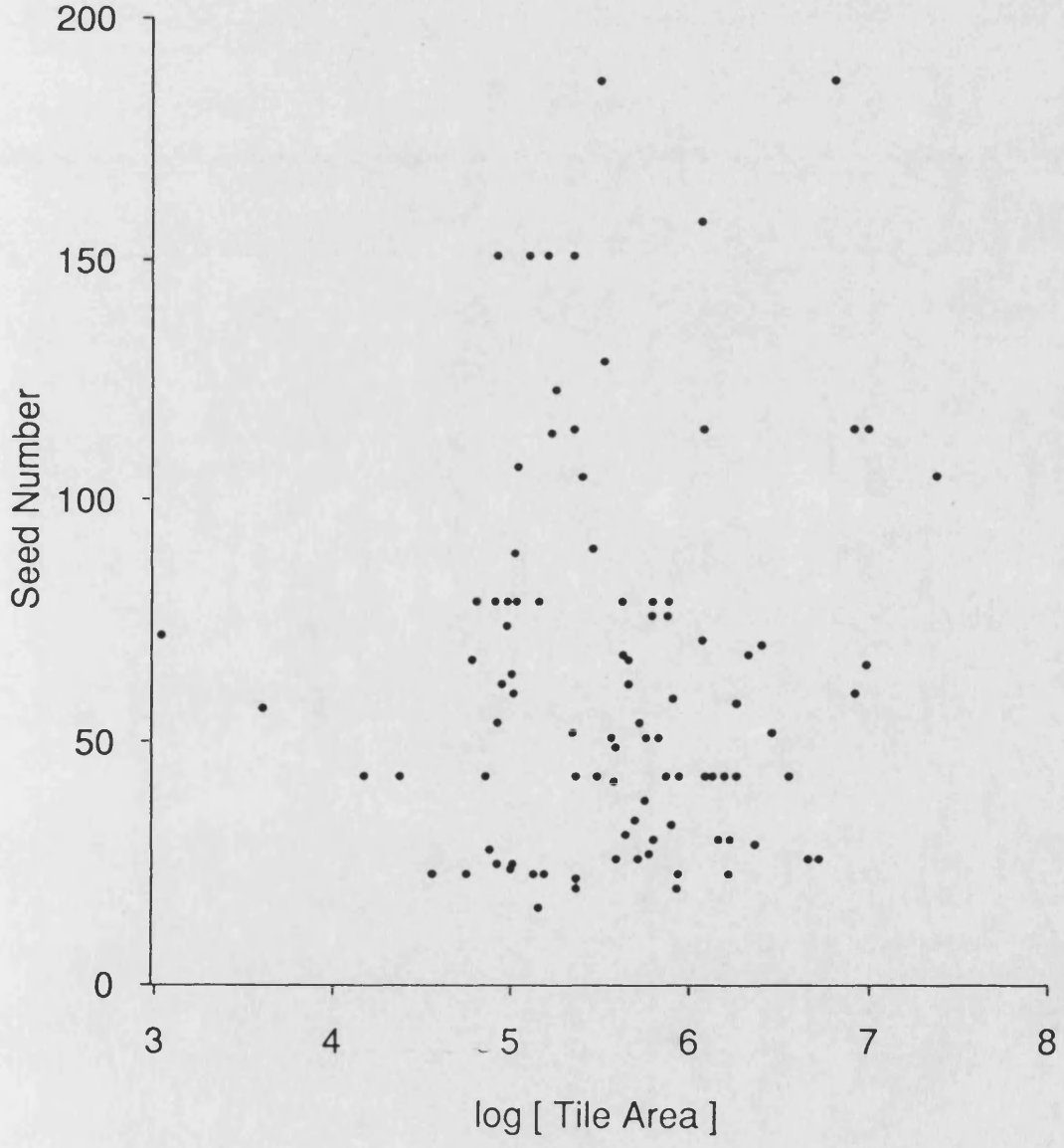

Figure 20

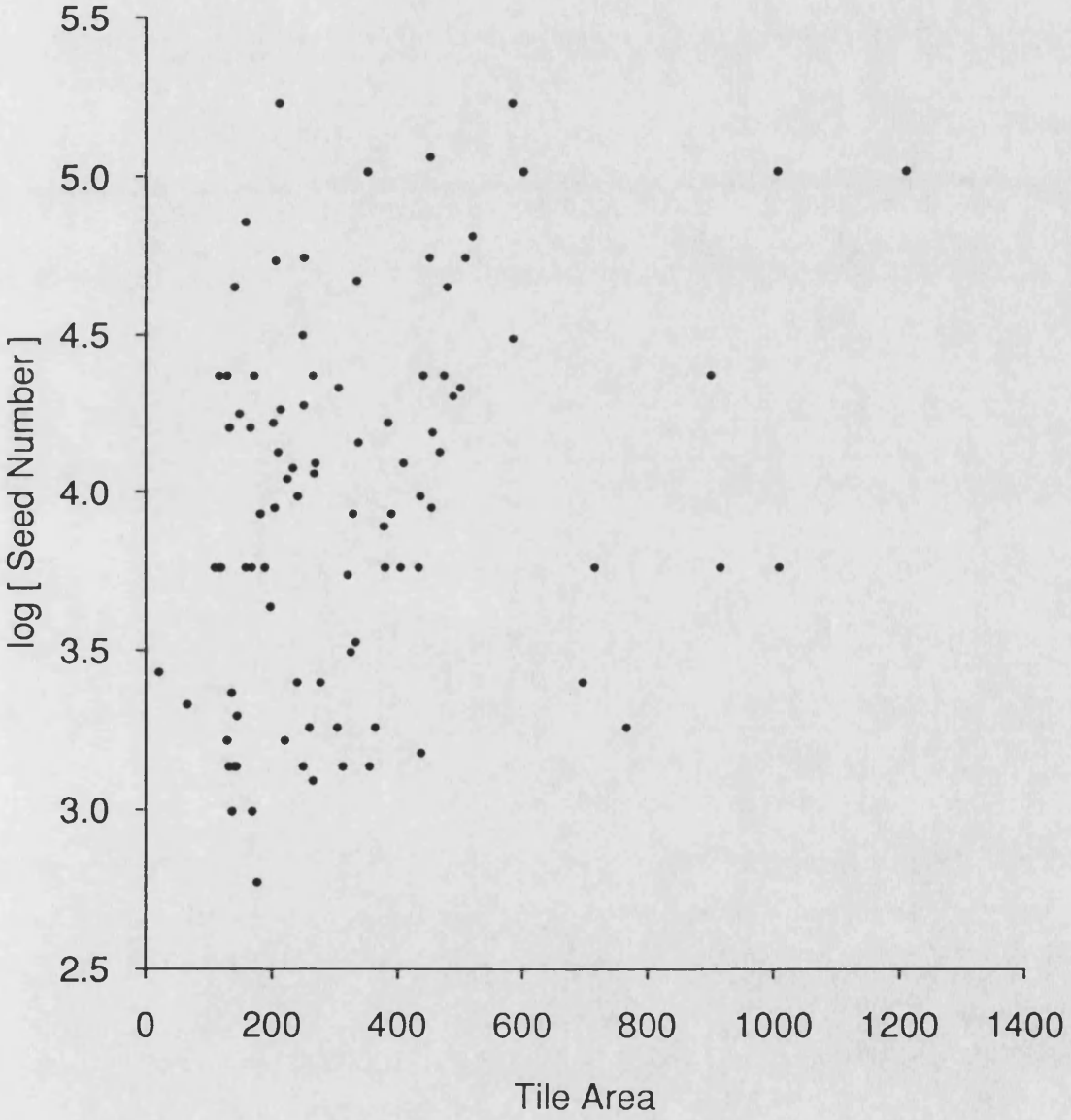
5.5
5.0
4.5
4.0
3.5
3.0
2.5
log [Seed Number]
0
200
400
600
800
1000
1200
1400
Tile Area

Figure 21

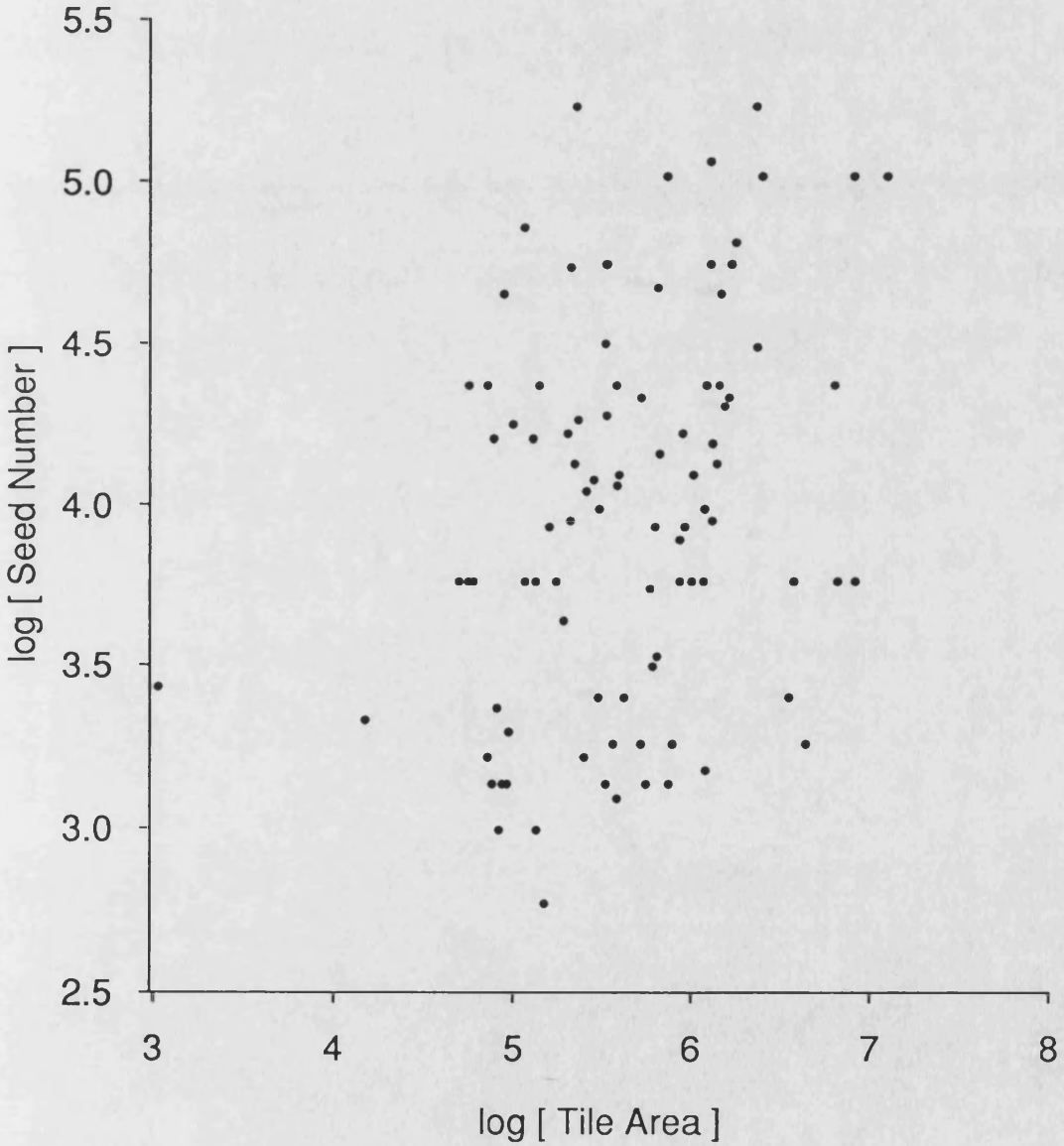

Figure 22

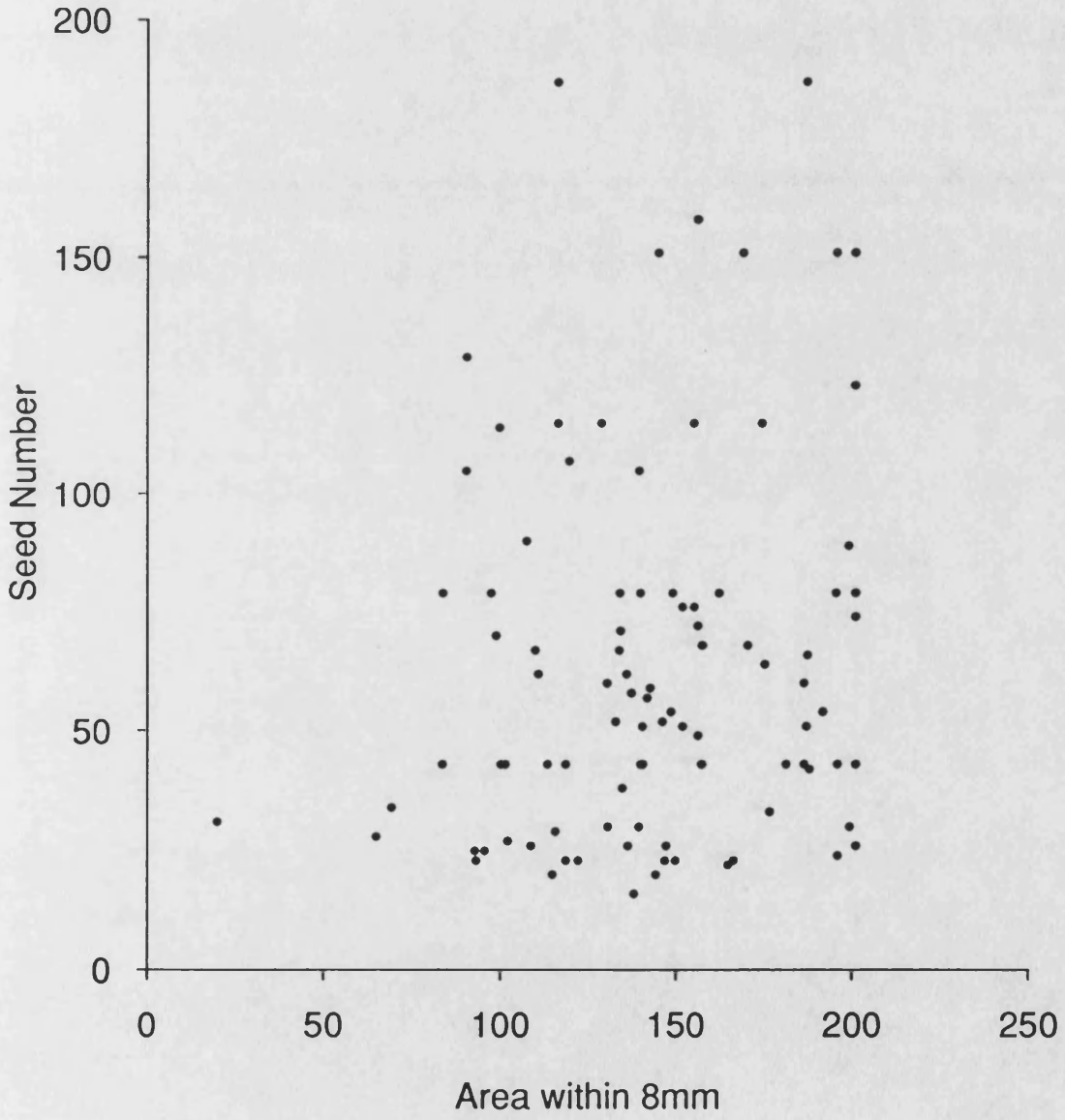
200
150
100
50
0
Seed Number
0
50
100
150
200
250
Area within 8mm

Figure 23

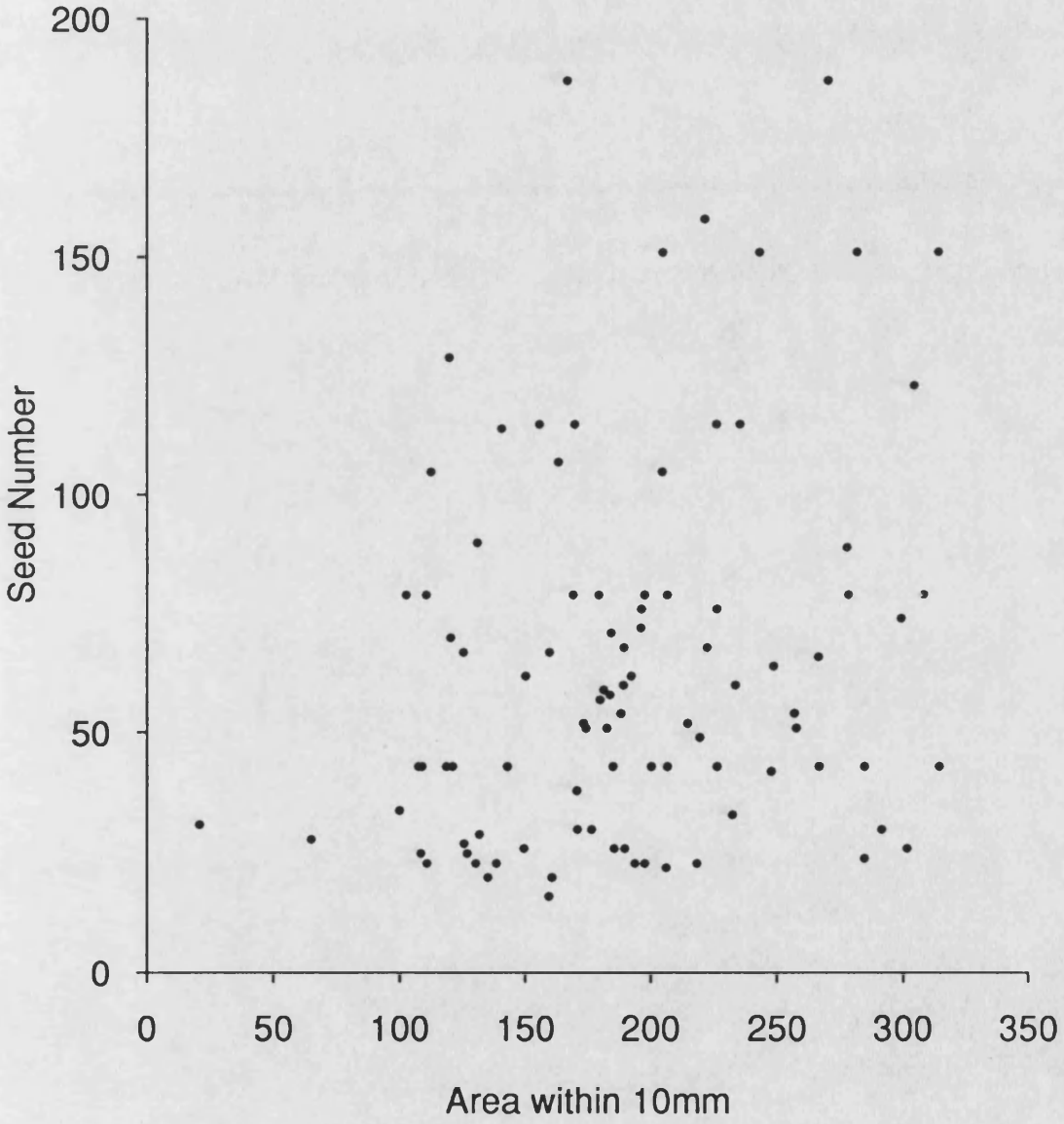
200
150
100
50
0
Seed Number
0
50
100
150
200
250
300
350
Area within 10mm

Figure 24

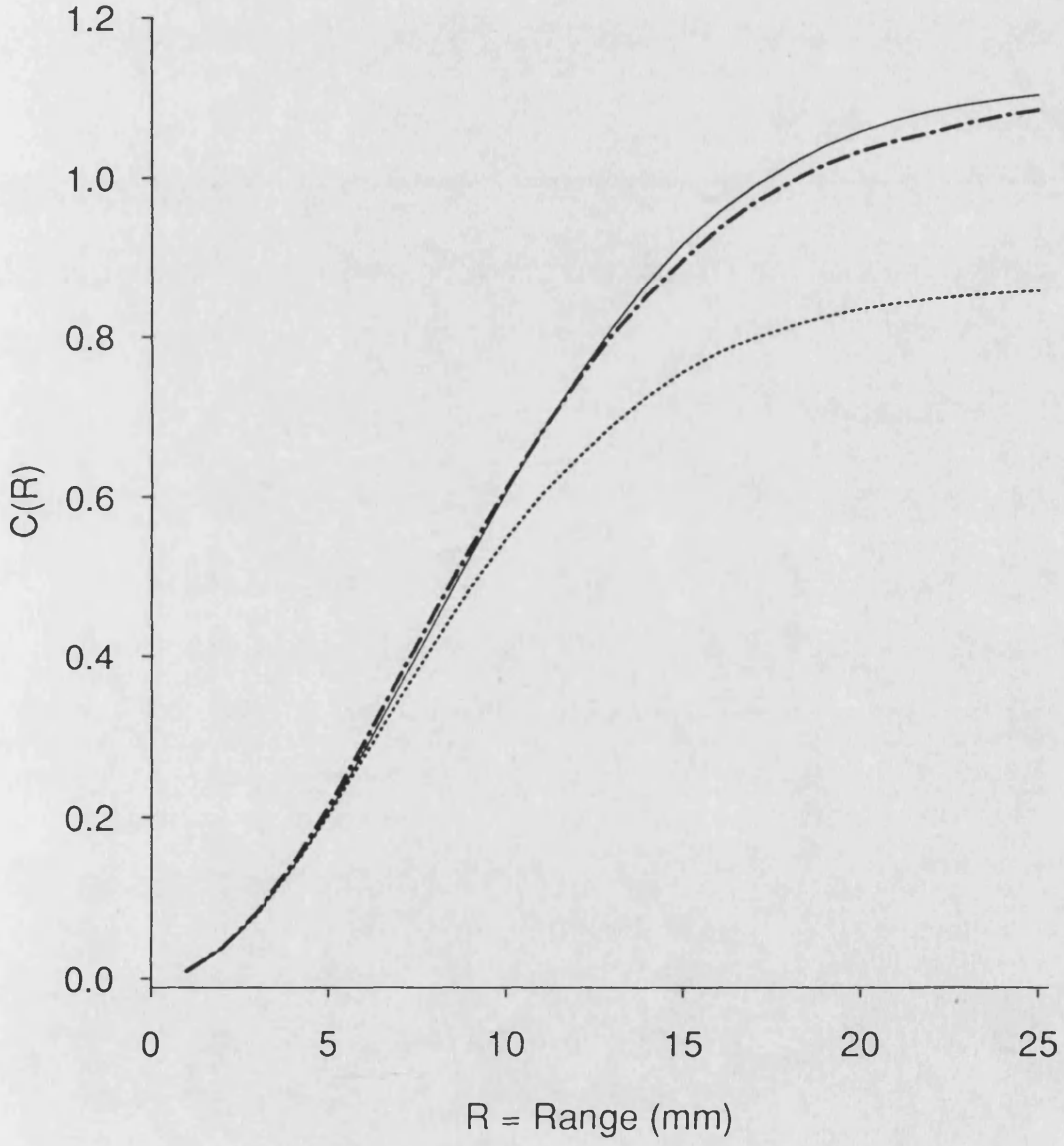

Figure 25

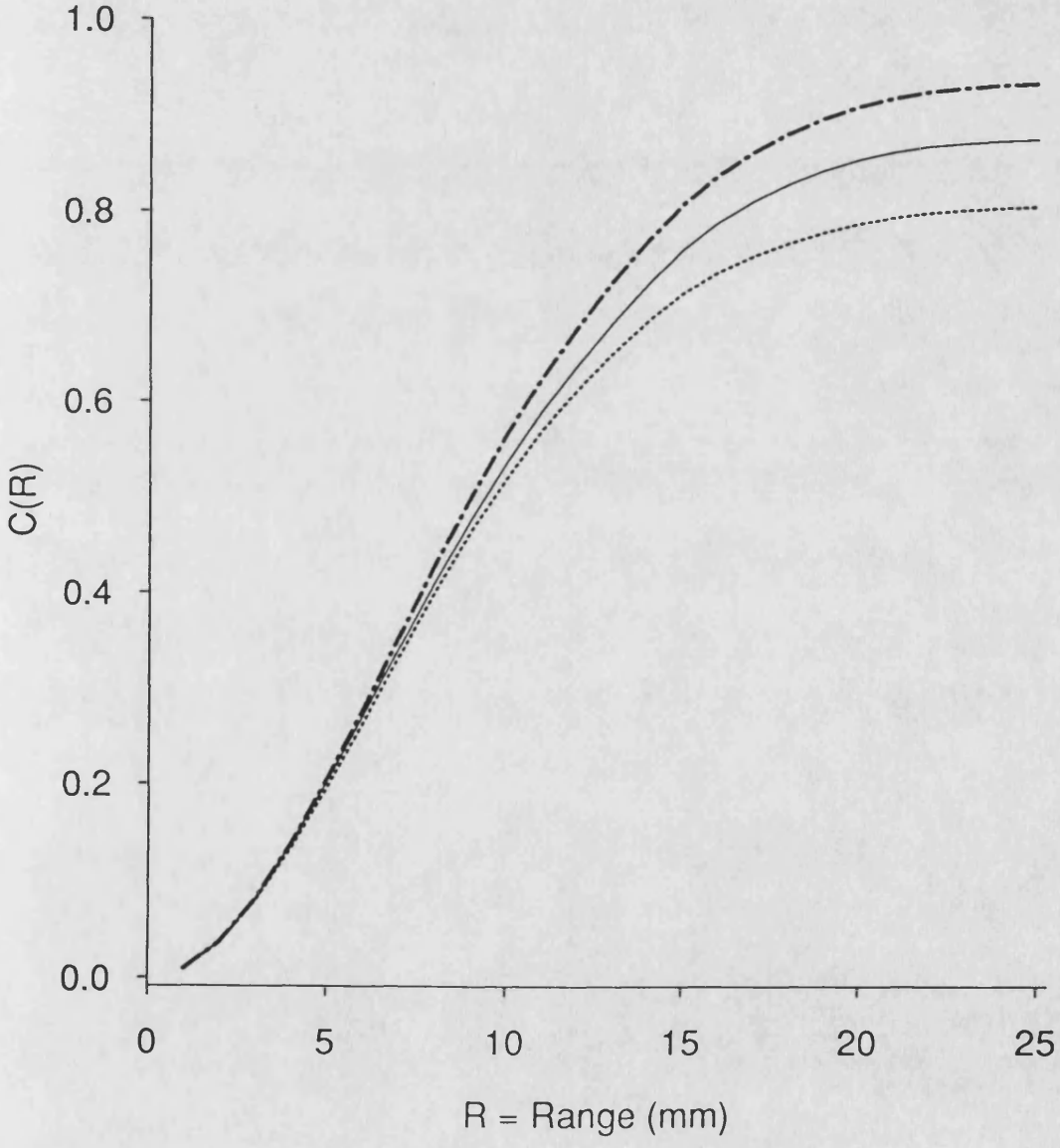

Simulation of Homogeneous Gaussian Random Fields

1. Introduction

A real-valued random field P on $\mathbf{R}^N$ is a suitably well-defined random function $P:\mathbf{R}^N \to \mathbf{R}$; the conditions for this will be given below. A realisation of P is therefore just a deterministic real-valued function on $\mathbf{R}^N$, and so we can make stochastic statements about the nature of real-valued random fields in the same way that we can make statements about real-valued functions. For example one class of random fields is the class of *discrete* random fields, that is those in which the random function can take values in a countable set. A map coloured with two colours is a realisation of a simple type of discrete random field in $\mathbf{R}^2$. Another class of random fields that is of particular interest in image analysis is the class of *Markov* random fields. In this class of random field, the distribution of the value of the field in one region is known conditional on the values of the field in some pre-determined set of neighbouring regions.

Another class of random fields of practical interest consists of those random fields that exhibit continuity in some stochastic sense. For example, the surface of this piece of paper, on a microscopic level, can be modelled as a two dimensional continuous random field. The surface of the sea at any particular time can also be modelled as a two dimensional continuous random field, but if we were interested in how the sea surface changed over time, we could model it as three dimensional continuous random field, having two spatial dimensions and one temporal dimension. Examples of such modelling include the modelling of metallic surfaces by Greenwood and Williamson (1966), and the modelling of sea surfaces by Longuet-Higgins (1957).

One of the most useful tools for studying real-valued random fields is that of the excursion set, $A_u(P,S)$, above a given level $u \in \mathbf{R}$, which is defined for any $S \subseteq \mathbf{R}^N$ by

$$A_u(P,S) = \{ t \in S \mid P(t) \geq u \} \ ,$$

the set of all points in S above u. There has been much work on excursion sets and related topics, such as the nature of maxima of a random field. Most of this work has been done in the area of Gaussian random fields, that is those for which the joint distribution of any collection of points is multivariate Gaussian. This is because Gaussian random fields can be used for practical purposes, for example modelling, and are among the easier random fields to handle analytically. Adler

(1981), summarises most of the theoretical results.

The random fields we shall deal with are Gaussian and for the most part differentiable. Continuous, non-differentiable fields do occur in reality, such as in the theory of fractals, see Mandelbrot (1977), but they are generally extremely rough surfaces having excursion sets composed of uncountably many components.

For a more formal definition of a random field, consider a collection of real-valued random variables, $P(\mathbf{t})$, indexed by points $\mathbf{t}$ in $\mathbf{R}^N$, along with a collection of measures,

$$F_{\mathbf{t}_1,\ldots,\mathbf{t}_n} \quad \text{for any } \mathbf{t}_i \in \mathbf{R}^N \text{ and } n=1,2,\ldots \ ,$$

on the Borel sets in $\mathbf{R}^n$ which satisfy

$$F_{\mathbf{t}_1,\ldots,\mathbf{t}_n}(B) = \mathbf{P}\,[\,(P(\mathbf{t}_1),\ldots,P(\mathbf{t}_n)) \in B\,] \quad \forall \text{ Borel sets } B \in \mathbf{R}^n. \qquad (1.1)$$

The Daniell-Kolmogorov Theorem gives us the following necessary and sufficient conditions on F for P to be a well-defined stochastic process on the points of $\mathbf{R}^N$, that is a *random field* on $\mathbf{R}^N$.

(a) *Symmetry.* If we write F as a distribution function $F_{\mathbf{t}_1,\ldots,\mathbf{t}_n}(\mathbf{x}_1,\ldots,\mathbf{x}_n)$, then F should remain invariant whenever $\{\mathbf{x}_i\}$ and $\{\mathbf{t}_i\}$ are acted on by the same permutation.

(b) *Consistency.* For every Borel set, B, on $\mathbf{R}^n$ and $n,m=1,2,\ldots,$

$$F_{\mathbf{t}_1,\ldots,\mathbf{t}_{m+n}}(B\times\mathbf{R}^m) = F_{\mathbf{t}_1,\ldots,\mathbf{t}_n}(B) \ .$$

Naturally, it would be of interest to know when real-valued random fields were stochastically equal, and, just as with random variables, there are many senses in which real-valued random fields could be said to be stochastically equal. The strictest type of stochastic equality occurs when two real-valued random fields P and Q satisfy

$$\mathbf{P}\,\{\,P(\mathbf{t}) = Q(\mathbf{t})\,\} = 1 \quad \forall\, \mathbf{t}\in\mathbf{R}^N \ ;$$

P and Q are then said to be *equivalent.*

For any realisation of P, the subset of $\mathbf{R}^{N+1}$ determined by $\{(\mathbf{t},P(\mathbf{t})):\mathbf{t}\in\mathbf{R}^N\}$. is called a *sample path* or *sample function* of P; this is clearly of importance in the simulation of P. It is not difficult to construct equivalent random fields which possess differing sample path behaviours, see Adler (1981), so the collection of finite dimensional measures (1.1) for P do not necessarily determine the behaviour

of the sample functions of P. Since we are essentially proposing to use the collection of finite dimensional measures (1.1) for P in order to simulate P we have to impose the technical condition of *separability*, see Adler (1981), on P. A separable field ensures that the sample function is determined by its value on an everywhere dense countable subset of $\mathbf{R}^N$, and thus by the collection of finite dimensional measures (1.1). For every stochastic process there is a corresponding equivalent separable stochastic process, see Adler (1981), so there is no loss in generality in assuming that a random field is separable.

One of the most basic basic properties a random field can possess is that of being independent of location or homogeneous. Suppose P is a well-defined random field on $\mathbf{R}^N$, then we say that P is *strictly homogeneous* (or *strictly stationary*) if, any k real numbers $x_1,\ldots,x_k$, and any $(k+1)$ points in $\mathbf{R}^N$, $\mathbf{t}_1,\ldots,\mathbf{t}_k,\tau$, satisfy

$$\mathbf{P}\,[\,P(\mathbf{t}_1)\le x_1,..,P(\mathbf{t}_k)\le x_k\,] = \mathbf{P}\,[\,P(\mathbf{t}_1+\tau)\le x_1,..,P(\mathbf{t}_k+\tau)\le x_k\,]$$

for $k=1,2,\ldots$. This condition is obviously equivalent to requiring that the distribution function, $F_{\mathbf{t}_1,\ldots,\mathbf{t}_n}$, be invariant under translations of the $\mathbf{t}_i$.

The first order moment function for a random field is given by $\mathbf{E}[P(\mathbf{t})]$, so for a strictly homogeneous random field

$$\mathbf{E}\,[\,P(\mathbf{t})\,] = \text{constant}\ , \tag{1.2}$$

and without loss of generality we can assume that this constant is zero. The second order moment, $R:\mathbf{R}^{2N}\to\mathbf{R}$, is defined by

$$R(\mathbf{s},\mathbf{t}) = \mathbf{E}\left\{\left[P(\mathbf{s})-\mathbf{E}[P(\mathbf{s})]\right]\left[P(\mathbf{t})-\mathbf{E}[P(\mathbf{t})]\right]\right\}\ ,$$

which, for a strictly homogeneous random field, reduces to

$$R(\mathbf{s},\mathbf{t}) = \mathbf{E}\,\{\,P(\mathbf{s})P(\mathbf{t})\,\} = \mathbf{E}\,\{\,P(\mathbf{s}-\mathbf{t})P(\mathbf{0})\,\}$$

$$= \text{function of } (\mathbf{s}-\mathbf{t}) \text{ alone.} \tag{1.3}$$

A random field that satisfies (1.2) and (1.3) is known as a *second-order homogeneous* or *stationary* random field, and clearly every strictly homogeneous random field is homogeneous. For a homogeneous random field, we can simplify our notation and considering $R:\mathbf{R}^N\to\mathbf{R}$, write

$$R(\mathbf{s}-\mathbf{t}) = \mathbf{E}\,\{\,P(\mathbf{s})P(\mathbf{t})\,\} = \mathbf{E}\,\{\,P(\mathbf{s}-\mathbf{t})P(\mathbf{0})\,\}\ . \tag{1.4}$$

The arguments outlined above, suitably modified, also hold for complex-valued random fields, X, on $\mathbf{R}^N$, with a covariance being defined by

$$R(\mathbf{s},\mathbf{t}) = \mathbf{E}\left\{ (X(\mathbf{s})-\mathbf{E}[X(\mathbf{s})]) \overline{(X(\mathbf{t})-\mathbf{E}[X(\mathbf{t})])} \right\} .$$

A further restrictive condition we can place on a homogeneous random field is that of *isotropy*, which requires that the covariance function is a function of the length of the argument alone :

$$R(\mathbf{t}) = R(|\mathbf{t}|) \quad . \tag{1.5}$$

Hence an isotropic random field is one in which the distribution functions, $F_{\mathbf{t}_1,\ldots,\mathbf{t}_n}$, are invariant under rotations, that is there are no preferred directions. Matern (1986) showed that the covariance function of an isotropic random field is bounded below in the following sense,

$$R(\mathbf{t}) \geq \inf_{u>0} \{ \Gamma(\tfrac{1}{2}N)(2/u)^{\frac{1}{2}(N-2)} J_{\frac{1}{2}(N-2)}(u) \} R(\mathbf{0}) \quad ,$$

where J_k denotes the Bessel function of the first kind of order k. If $R(\mathbf{0})=1$, then, for example, isotropic covariances are bounded below by -0.403 in $\mathbf{R}^2$ and -0.218 in $\mathbf{R}^3$.

A *Gaussian random field*, or Gaussian stochastic process, on $\mathbf{R}^N$ is a random field in which the distribution functions, $F_{\mathbf{t}_1,\ldots,\mathbf{t}_n}$, are all multivariate normal distribution functions, that is to say that for any $k=1,2,\ldots$ and $\mathbf{t}_1,\ldots,\mathbf{t}_k$, the vector $(P(\mathbf{t}_1),\ldots,P(\mathbf{t}_k))$ has a k-dimensional multivariate Gaussian distribution. If a Gaussian random field is homogeneous, then it has constant mean and $R(\mathbf{s},\mathbf{t})$ is a function of $(\mathbf{s}-\mathbf{t})$ alone, and it is easily seen from the form of the density function of a multivariate normal density that a Gaussian random field is also strictly homogeneous.

There are two main reasons why we are interested in simulating stochastic processes. Firstly, as an exploratory technique, we can simulate a model to see what it looks like, and secondly, we can use simulated data for inference for Monte-Carlo tests. In the latter case we may be interested in some statistic of the model. Each time we simulate the model, we can also calculate a simulated statistic conditional on the model and thus calculate an empirical distribution of the statistic conditional on the model. This empirical distribution can then be used for tests of statistical hypotheses.

There are various ways to simulate homogeneous Gaussian random fields. If we only wanted to simulate a homogeneous random field at a few pre-determined points for which we knew the covariance matrix, Σ, we could just treat the

simulation as the simulation of a multivariate normal random variable. Suppose $\xi_1,\ldots,\xi_n$ are independent $N(0,1)$ random variables and M is an $n\times n$ matrix, then $M\xi$ is an n-dimensional multivariate normal distribution with mean zero and covariance matrix MM^T. Thus, all that remains to be done is to find a matrix M such that $\Sigma=MM^T$. If we cannot calculate M analytically, then we can use the Cholesky decomposition which gives a lower triangular matrix L such that $\Sigma=LL^T$. Note that we can simulate a non-isotropic Gaussian random field by this method.

We may however need an algorithm to simulate a Gaussian random field at an arbitrary set of points Most methods for simulating a Gaussian random field with a given covariance function at an arbitrary set of points use a central limit approximation by taking the average of a number of homogeneous non-Gaussian random fields having the same covariance function.

One such method for the simulation of an isotropic Gaussian random field is the "random coin" method given by Sironvalle (1980), which is a generalisation of the "non-random coin" method of Zubrzycki (1957). Suppose we place on each point of a Poisson point process of parameter λ the centre of a disc or "coin" of radius R, where R is a random variable having distribution function F. Let $Z(\mathbf{x})$ be the number of coins covering the point $\mathbf{x}$, and suppose Z has covariance function $c:\mathbf{R}^+\rightarrow\mathbf{R}$. In the plane, for example, F and c are related by

$$1-F(r) = \frac{2}{\pi\lambda}\int_r^\infty c''(s)\,(s^2-r^2)^{-\frac{1}{2}}\,ds \quad . \tag{1.6}$$

If λ is chosen appropriately, this gives us a proper distribution function for many covariance functions c. Z is then a non-Gaussian process, but we can average several independent copies to obtain a Gaussian process. This is also equivalent to taking λ large, re-scaling the covariance function, and considering $\lambda^{-1}Z$.

The "turning band" method of Matheron (1973) gives another a method for isotropic Gaussian random fields by considering the rotations of linear processes along arbitrary lines. Suppose P_1 is a homogeneous process on $\mathbf{R}$ having covariance R_1. If θ is a random rotation in $\mathbf{R}^N$ and we take

$$P(\mathbf{t}) = P_1((\theta\mathbf{t})_1) \quad , \tag{1.7}$$

then R and R_1 are related by

$$R(|\mathbf{t}|) = \frac{2\Gamma(\frac{1}{2}N)}{\pi^{\frac{1}{2}}\Gamma[\frac{1}{2}(N-1)]}\int_0^1 R_1(v|\mathbf{t}|)\,(1-v^2)^{\frac{1}{2}(N-3)}\,dv \quad . \tag{1.8}$$

Given a covariance function R, we can invert (1.8) to obtain R_1 the covariance function of a Gaussian process on $\mathbf{R}$. If we can simulate such a process on $\mathbf{R}$, we

can then use (1.7) to simulate a non-Gaussian process on $\mathbf{R}^N$ having the correct covariance, and an average of a number of these processes gives us an approximately Gaussian random field having the correct covariance function.

To use the turning bands method, we need to produce a one dimensional homogeneous random field. One method given by Ripley, Ripley (1987), is to consider a generalised moving average process,

$$X(x) = \int k(x-y)\, dB(y) \quad , \tag{1.9}$$

where k is an integrable function and B denotes Brownian motion. This process has covariance function

$$R(x) = \int k(x-u)k(u)\, du \quad . \tag{1.10}$$

(1.10) is a convolution, so if $\hat{R}$ and $\hat{k}$ denote the Fourier transforms of R and k respectively, then

$$\hat{R}(t) = \hat{k}(t)^2 \quad .$$

We can therefore either calculate $\hat{R}$, and hence $\hat{k}$, analytically or by means of the fast Fourier transform. (1.9) is also a convolution and so the fast Fourier transform of X can easily be evaluated numerically and thus X. Details are given in Ripley (1987) and Davis, Hagan and Borgman (1981).

The method given below to simulate homogeneous, not necessarily isotropic, Gaussian random fields also depends on defining such a field in terms of a stochastic integral, which can then approximated in one of two methods. The formal definition of this integral is given in the next section. The first method, considered in Section 3, approximates the integral by its Riemann sum. This constrains the simulated field to be Gaussian and has the covariance function approaching the correct covariance function asymptotically. The second method involves a Monte-Carlo approach to the integral, which gives a simulated field with the correct covariance and is asymptotically Gaussian. This method is considered in Section 4 and an algorithm for its implementation is given in Section 5. In Section 6 we consider the χ^2 random field, which is a sum of squares of Gaussian random fields, and in the final section we give some contour maps of computer simulations of these fields.

2. Integral Representation of a Homogeneous Gaussian Random Field

In this section we shall give a representation of a homogeneous Gaussian random field with mean zero and unit variance in terms of Riemann-Stieltjes stochastic integral. Our treatment of stochastic integrals will be an expanded version of pages 28-30 of Adler (1981).

Suppose we have a complex-valued random field $\eta(t)$, $t\in\mathbf{R}^N$, which is mean square continuous and has finite variance for all t. In order to define the stochastic integral, we need to regard η as if it were an N-dimensional distribution function, but for a complex-valued measure. We can do this by first defining define a function, $\hat{\eta}$ on the intervals of $\mathbf{R}^N$. Suppose

$$I=(a_1,b_1]\times\ldots\times(a_N,b_N]$$

is an interval in $\mathbf{R}^N$, then we can define

$$g_N(x_1,\ldots,x_N) = \eta(x_1,\ldots,x_N) \ ,$$

$$g_{n-1}\left[x_1,\ldots,x_{n-1},(a_n,b_n],\ldots,(a_N,b_N]\right] =$$

$$g_n\left[x_1,\ldots,x_{n-1},b_n,(a_{n+1},b_{n+1}],\ldots,(a_N,b_N]\right]$$

$$-g_n\left[x_1,\ldots,x_{n-1},a_n,(a_{n+1},b_{n+1}],\ldots,(a_N,b_N]\right] \ ,$$

$$\hat{\eta}(I) = g_0\left[(a_1,b_1],\ldots,(a_N,b_N]\right] \ , \qquad (2.1)$$

so $\hat{\eta}(\varnothing)=0$.

We first show that if I is expressed as a finite disjoint union of subintervals, then $\hat{\eta}$ is finitely additive. If I is the disjoint union of two subintervals, so $I=I_1\bigcup I_2$, where, without loss of generality,

$$I_1 = (a_1,c_1]\times(a_2,b_2]\times\ldots\times(a_N,b_N] \ ,$$

$$I_2 = (c_1,b_1]\times(a_2,b_2]\times\ldots\times(a_N,b_N] \ ,$$

for some $a_1<c_1<b_1$. Then clearly,

$$\hat{\eta}(I) = \hat{\eta}(I_1) + \hat{\eta}(I_2) \ .$$

Therefore suppose inductively that any interval is additive with respect to a partition into n subintervals. Consider a partition into $n+1$ subintervals, $I=\bigcup_{i=1}^{n+1} J_i$, where

$$J_1 = (a_1,c_1]\times\ldots\times(a_N,c_N] \ ,$$

and $a_1<c_1<b_1$. If we define I_1,I_2 as above, then $I_2\bigcap J_1=\varnothing$, so I_2 is the disjoint union of $\{I_2\bigcap J_k\}_{k=2}^{n+1}$ and hence

$$\hat{\eta}(I_2) = \sum_{k=2}^{n+1}\hat{\eta}(I_2\bigcap J_k) = \sum_{k=1}^{n+1}\hat{\eta}(I_2\bigcap J_k) \ .$$

Suppose $(b_1,a_2,\ldots,a_N)\in\bar{J}_{n+1}$, where $\bar{J}_{n+1}$ is the closure of J_{n+1}, then

$I_1 \cap J_{n+1} = \emptyset$, and so we have

$$\hat{\eta}(I_1) = \sum_{k=1}^{n} \hat{\eta}(I_1 \cap J_k) = \sum_{k=1}^{n+1} \hat{\eta}(I_2 \cap J_k) \quad .$$

Thus,

$$\begin{aligned} \hat{\eta}(I) &= \hat{\eta}(I_1) + \hat{\eta}(I_2) \\ &= \sum_{k=1}^{n+1} \hat{\eta}(I_1 \cap J_k) + \hat{\eta}(I_2 \cap J_k) \\ &= \sum_{k=1}^{n+1} \hat{\eta}(J_k) \quad , \end{aligned}$$

and the inductive proof is complete.

Thus $\hat{\eta}$ is finitely additive for any any partition of an interval into subintervals. We can extend this definition to the class $\mathcal{A}^N$ of sets which are finite unions of disjoint intervals by

$$\hat{\eta}\left(\bigcup_{i=1}^{n} I_i\right) = \sum_{i=1}^{n} \hat{\eta}(I_i) \quad ,$$

for any collection $\{I_i\}_{i=1}^{n}$ of disjoint intervals. $\hat{\eta}$ is then well-defined as a random additive set function on $\mathcal{A}^N$, for suppose we have two collections of disjoint intervals, $\{I_i\}_{i=1}^{n}$ and $\{J_j\}_{j=1}^{m}$ with $\bigcup_{i=1}^{n} I_i = \bigcup_{j=1}^{m} J_j$, then

$$\begin{aligned} \hat{\eta}\left[\bigcup_{i=1}^{n} I_i\right] &= \sum_{i=1}^{n} \hat{\eta}(I_i) \\ &= \sum_{i=1}^{n}\sum_{j=1}^{m} \hat{\eta}\left[I_i \cap J_j\right] \\ &= \sum_{j=1}^{m} \hat{\eta}(J_j) = \hat{\eta}\left[\bigcup_{j=1}^{n} J_j\right] \quad . \end{aligned}$$

Now, $\mathrm{E}[|\hat{\eta}(I)|^2]$ is finite for all intervals I, so we can define η to be a field with *orthogonal increments* if

$$\mathrm{E}\left[\hat{\eta}(I)\overline{\hat{\eta}(J)}\right] = 0 \quad , \tag{2.2}$$

for all pairs of disjoint intervals I,J. For such a field, we can define an additive finite set function, $\hat{F}$ on $\mathcal{A}^N$ by

$$\hat{F}(S) = \mathrm{E}\left[|\hat{\eta}(S)|^2\right] \quad . \tag{2.3}$$

for any $S \in \mathcal{A}^N$, so $\hat{F}(\emptyset)=0$. In order to show that $\hat{F}$ is a measure on $\mathcal{A}^N$, it only remains to show that $\hat{F}$ is countably additive on $\mathcal{A}^N$, that is to say suppose $\{S_i\}$ is a collection of disjoint members of $\mathcal{A}^N$, with $\bigcup_{i=1}^{\infty} S_i \in \mathcal{A}^N$, then

$$\hat{F}\left[\bigcup_{i=1}^{\infty} S_i\right] = \sum_{i=1}^{\infty} \hat{F}(S_i) \quad .$$

If $A_1 \supseteq A_2 \supseteq \ldots$ is a decreasing sequence of sets with $\bigcap_{i=1}^{\infty} A_i = \emptyset$, then we can say $A_i \to \emptyset$ as $i \to \infty$. Suppose $\{I_i\}$ is a sequence of intervals such that $I_i \to \emptyset$ as $i \to \infty$ then $\hat{\eta}(I_i) \to 0$ in mean square as η is mean square continuous. Thus for any $\{T_i\}$ a collection of members of $\mathcal{A}^N$, with $T_i \to \emptyset$, $\hat{\eta}(T_i) \to 0$ in mean square, and hence $\hat{F}(T_i) \to 0$.

Let $T_n = \bigcup_{i=n+1}^{\infty} S_i \in \mathcal{A}^N$, then $T_i \to \emptyset$ as $\{S_i\}$ is a collection of disjoint members of $\mathcal{A}^N$. Now,

$$\hat{F}\left[\bigcup_{i=1}^{\infty} S_i\right] = \sum_{i=1}^{n} \hat{F}(S_i) + \hat{F}(T_n) \quad ,$$

so

$$\hat{F}\left[\bigcup_{i=1}^{\infty} S_i\right] - \sum_{i=1}^{n} \hat{F}(S_i) = \hat{F}(T_n) \to 0 \quad \text{as } n \to \infty \quad ,$$

and hence $\hat{F}$ is countably additive on $\mathcal{A}^N$. Thus $\hat{F}$ defines a measure on $\mathcal{A}^N$. $\hat{F}$ also defines, up to a constant, a point function on $\mathbf{R}^N$, say F. If we set $F(-\infty,\ldots,-\infty)=0$, then F is a scaled multivariate distribution function.

For such random fields, we can define mean square stochastic integrals. Suppose $A>0$, then we can define $\mathbf{A}^N=(-A,A]^N$. If we divide $\mathbf{A}^N$ into A_n disjoint I_{n_j} for $1 \le j \le A_n$ with $z_{n_j} \in I_{n_j}$ and

$$\sup_{1 \le j \le A_n} Vol(I_{n_j}) \to 0 \quad \text{as } n \to \infty \quad ,$$

We can now use Adler's Theorem 2.3.1 to define the stochastic integral.

Theorem.

If η is a complex-valued random field with orthogonal increments, then the Riemann-Stieltjes integral

$$\int_{\mathbf{R}^N} g(\mathbf{z})\, d\eta(\mathbf{z})$$

is well-defined as the mean square limit

$$\lim_{A\to\infty}\lim_{n\to\infty}\sum_{j=1}^{A_n} g(\mathbf{z}_{n_j})\,\hat{\eta}(I_{n_j})$$

for all g for which

$$\int_{\mathbf{R}^N} |g(\mathbf{z})|^2\, dF(\mathbf{z}) \quad \text{exists} \ \square$$

In particular,

$$\int_{\mathbf{R}^N} e^{i\mathbf{t}.\mathbf{z}}\, d\eta(\mathbf{z})$$

is a well-defined Riemann-Stieltjes integral converging in mean square for all $\mathbf{t}\in\mathbf{R}^N$.

Suppose Y is a homogeneous complex-valued random field on $\mathbf{R}^N$ with mean zero and finite variance, and having covariance function R_Y. If Y is continuous in mean square, then

$$R_Y(\mathbf{t})-R_Y(\mathbf{t}+\mathbf{h}) = \mathbf{E}\left[|Y(\mathbf{t}+\mathbf{h})-Y(\mathbf{0})|^2\right] - \mathbf{E}\left[|Y(\mathbf{t})-Y(\mathbf{0})|^2\right] \to 0 \ \text{ as } \ \mathbf{h}\to\mathbf{0} \ ,$$

so $R_Y(\mathbf{t})$ is continuous for all $\mathbf{t}\in\mathbf{R}^N$. Hence, by Bochner's Theorem, R_Y has a representation of the form

$$R_Y(\mathbf{t}) = \int_{\mathbf{R}^N} e^{i\mathbf{t}.\mathbf{z}}\, dF(\mathbf{z}) \ , \tag{2.4}$$

where F is the *spectral distribution function* of Y. We can now use the Spectral Representation Theorem, (Adler's Theorem 2.4.1) to define a random field in terms of a stochastic interval.

Spectral Representation Theorem.

> For every mean square continuous homogeneous random field $Y(\mathbf{t})$ with zero mean, there exists a mean square continuous field $\eta(\mathbf{t})$ with orthogonal increments, such that, for each $\mathbf{t}$, $Y(\mathbf{t})$ can be represented as a mean square integral as follows :
>
> $$Y(\mathbf{t}) = \int_{\mathbf{R}^N} e^{i\mathbf{t}.\mathbf{z}}\, d\eta(\mathbf{z}) \ . \tag{2.5}$$

The field $\eta(\mathbf{t})$ is defined up to an additive constant. If this is fixed by setting $\eta(-\infty,\ldots,-\infty)=0$, then we have

$$\mathbf{E}[\eta(\mathbf{t})]=0 \ , \ \mathbf{E}\left[|\eta(\mathbf{t})|^2\right]=F(\mathbf{t}) \ , \ \mathbf{E}\left[|\hat{\eta}(\mathbf{t})|^2\right]=\hat{F}(I) \ , \tag{2.6}$$

where I is any interval and F is determined by (2.4)

We are now in a position to use this theory to simulate an N-dimensional Gaussian random field P which has mean zero and covariance function R_P. Without loss of generality, we can assume that $R_P(\mathbf{0})=1$. If P and Q are independent and identically distributed random fields, then $R_P=R_Q$, and we can

define a complex-valued Gaussian random field X by

$$X(\mathbf{t}) = P(\mathbf{t}) + iQ(\mathbf{t}). \tag{2.7}$$

Now,

$$R_X(\mathbf{t}) = \mathbf{E}\,[\,P(\mathbf{0})P(\mathbf{t})\,] + \mathbf{E}\,[\,Q(\mathbf{0})Q(\mathbf{t})\,]$$

$$= R_P(\mathbf{t}) + R_Q(\mathbf{t}) = 2R_P(\mathbf{t}) \ ,$$

and hence $R_X(\mathbf{0})=2$. We know from (2.4) that

$$R_X(\mathbf{t}) = \int_{\mathbf{R}^N} e^{i\mathbf{t}.\mathbf{z}}\, dF(\mathbf{z}) \ ,$$

where F is the spectral distribution function of X. However,

$$R_X(\mathbf{0}) = \int_{\mathbf{R}^N} dF = 2 \ ,$$

so $F=2F_{\mathbf{W}}$, where $F_{\mathbf{W}}$ is the distribution function of some random variable $\mathbf{W}$ on $\mathbf{R}^N$. In particular, $R_X(\mathbf{t}) = 2\varphi_W(\mathbf{t}) = 2R_P(\mathbf{t})$, where φ_W is the characteristic function of W. However P is a real-valued random field, thus $R_P=\varphi_W$ is real-valued, and so W is a symmetric random variable.

For $\mathbf{z}\in\mathbf{R}^N$, suppose we let $\mu(\mathbf{z}) \sim N[0,F_{\mathbf{W}}(\mathbf{z})]$, with

$$\mathbf{E}\,[\,\mu(\mathbf{z})\mu(\mathbf{z}')\,] = F_{\mathbf{W}}\,[\,Min(\mathbf{z}_1,\mathbf{z}'_1),\ldots,Min(\mathbf{z}_N,\mathbf{z}'_N)\,] \ ,$$

then μ is a well-defined real-valued random process on $\mathbf{R}^N$ with mean zero. As before, we can extend this definition so $\hat{\mu}$ is also a random additive set function on $\mathcal{A}^N$. If we let $I(\mathbf{x})$ denote the semi-infinite interval $(-\infty,\mathbf{x}_1)\times\ldots\times(-\infty,\mathbf{x}_N)$, then $\mu(\mathbf{x})=\hat{\mu}(I(\mathbf{x}))$, so

$$\mathbf{E}\left[\hat{\mu}(I(\mathbf{x}))\hat{\mu}(I(\mathbf{y}))\right] = \mathbf{E}[\mu(\mathbf{x})\mu(\mathbf{y})] = \mathbf{P}\left[\mathbf{W}\in I(\mathbf{x})\bigcup I(\mathbf{y})\right] \ .$$

By expressing any interval as the appropriate unions and complements of semi-infinite intervals, we can show that for two intervals I and J, $\mathbf{E}[\hat{\mu}(I)\hat{\mu}(J)]=\mathbf{P}[\mathbf{W}\in I\bigcap J]$. In particular, $\mathbf{E}\,[\,|\hat{\mu}(I)|^2\,] =\mathbf{P}(\mathbf{W}\in I)$, and also $\mathbf{E}[\hat{\mu}(I)\hat{\mu}(J)]=0$, if I and J are disjoint, Hence μ is a field with orthogonal increments. Suppose μ and ν are independent and identically distributed random fields, then we can define a complex-valued random field λ by

$$\lambda(\mathbf{t}) = \mu(\mathbf{t}) + i\nu(\mathbf{t}) \ ,$$

and we can extend this definition as before to give a random field with orthogonal complements, and so

$$\mathbf{E}[\lambda(\mathbf{t})]=0 \ , \ \mathbf{E}[|\lambda(\mathbf{t})|^2]=2F_{\mathbf{W}}(\mathbf{t}) \ , \ \mathbf{E}[|\hat{\lambda}(\mathbf{t})|^2]=2\mathbf{P}(\mathbf{W}\in I) \ . \tag{2.8}$$

Consider the following mean square convergent Riemann-Stieltjes integral, which defines a complex-valued homogeneous random field $X'=P'+iQ'$ on $\mathbf{R}^N$,

$$X'(\mathbf{t}) = \int_{\mathbf{R}^N} e^{i\mathbf{t}.\mathbf{z}}\, d\lambda(\mathbf{z}) = \lim_{A\to\infty} \lim_{n\to\infty} e^{\mathbf{z}_{n_j}}\, \hat{\lambda}(I_{n_j})$$

$$= \lim_{A\to\infty} \lim_{n\to\infty} X'_{A_n}(\mathbf{t}) \text{ say.} \tag{2.9}$$

For any A and n, the real and imaginary parts of $X'_{A_n}(\mathbf{t})$ are the finite sums of independent normal random variables and hence are normally distributed, and so the real and imaginary parts of $X'(\mathbf{t})$, P' and Q', are mean square limits of normal random variables and hence are normally distributed. Now,

$$\mathbf{E}[X'(\mathbf{t})X'(\mathbf{0})] = i\mathbf{E}[P'(\mathbf{t})Q'(\mathbf{0})+P'(\mathbf{0})Q'(\mathbf{t})] = 2i\mathbf{E}[P'(\mathbf{t})Q'(\mathbf{0})]$$

$$= \mathbf{E}\left[\int_{\mathbf{R}^N}\int_{\mathbf{R}^N} e^{i\mathbf{t}.\mathbf{z}}\, d\lambda(\mathbf{z})d\lambda(\mathbf{y})\right]$$

$$= \mathbf{E}\left[\int_{\mathbf{R}^N}\int_{\mathbf{R}^N} e^{i\mathbf{t}.\mathbf{z}}\, d\theta(\mathbf{z},\mathbf{y})\right] = 0 \ ,$$

where $d\theta(\mathbf{z},\mathbf{y}) = d\mu(\mathbf{z})d\mu(\mathbf{y}) - dv(\mathbf{z})dv(\mathbf{y}) + id\mu(\mathbf{z})dv(\mathbf{y}) + idv(\mathbf{z})d\mu(\mathbf{y})$.

P' and Q' are therefore independent Gaussian random fields. The spectral representation theorem tells us that X has an integral representation and from (2.8), it must be of the form of (2.9). Thus X and X' are the same random field, and we haver the following integral representations for P and Q,

$$P(\mathbf{t}) = \int_{\mathbf{R}^N} \cos(\mathbf{t}.\mathbf{z})\, d\mu(\mathbf{z}) - \int_{\mathbf{R}^N} \sin(\mathbf{t}.\mathbf{z})\, dv(\mathbf{z}) \ , \tag{2.10}$$

$$Q(\mathbf{t}) = \int_{\mathbf{R}^N} \sin(\mathbf{t}.\mathbf{z})\, d\mu(\mathbf{z}) + \int_{\mathbf{R}^N} \cos(\mathbf{t}.\mathbf{z})\, dv(\mathbf{z}) \ . \tag{2.11}$$

We can also give expressions for the j^{th} partial derivatives of X, X_j, where they exist, as

$$X_j(\mathbf{t}) = \frac{\partial X}{\partial \mathbf{t}_j} = \int_{\mathbf{R}^N} i\mathbf{z}_j e^{i\mathbf{t}.\mathbf{z}}\, d\lambda(\mathbf{z}) \ , \tag{2.12}$$

$$\text{so } P_j(\mathbf{t}) = -\int_{\mathbf{R}^N} \mathbf{z}_j \sin(\mathbf{t}.\mathbf{z})\, d\mu(\mathbf{z}) - \int_{\mathbf{R}^N} \mathbf{z}_j \cos(\mathbf{t}.\mathbf{z})\, dv(\mathbf{z}) \ , \tag{2.13}$$

$$\text{and } Q_j(\mathbf{t}) = \int_{\mathbf{R}^N} \mathbf{z}_j \cos(\mathbf{t}.\mathbf{z})\, d\mu(\mathbf{z}) - \int_{\mathbf{R}^N} \mathbf{z}_j \sin(\mathbf{t}.\mathbf{z})\, dv(\mathbf{z}) \ . \tag{2.14}$$

Clearly P_j and Q_j are uncorrelated and therefore asymptotically independent. These integrals converge if and only if

$$\mathbf{E}\,[\ |\mathbf{W}_j|^2\ ] \text{ exists,}$$

that is if and only if

$$\frac{\partial^2 \varphi_W}{\partial t_j^{\,2}}_{\,t=0} \quad \text{exists.}$$

Equations (2.10) and (2.11) define Gaussian random fields with zero mean and covariance R_P. There are two obvious ways in which to use (2.10) and (2.11) to simulate a random field. The first method, considered in the next section is to approximate the integrals (2.10) and (2.11) by their Riemann sums, and then simulate those sums. The second method involves a Monte-Carlo integration approach and is considered in Section 4.

3. Riemann Sum Simulation

As outlined above, one method of simulating a Gaussian Random Field is to approximate the integrals (2.10) and (2.11) by their Riemann-Stieltjes sum. Let P_{A_n} and Q_{A_n} denote these Riemann sums, so for example,

$$P_{A_n}(\mathbf{t}) = \sum_{j=1}^{A_n} \cos(\mathbf{t}.\mathbf{z}_{n_j})\hat{\mu}(I_{n_j}) + \sin(\mathbf{t}.\mathbf{z}_{n_j})\hat{\nu}(I_{n_j}) \quad , \tag{3.1}$$

and let $X_{A_n}=P_{A_n}+iQ_{A_n}$. Thus P_{A_n} is a finite sum of independent normal random variables, so

$$P_{A_n}(\mathbf{t}) \sim N\left[0\ ,\ \sum_{j=1}^{A_n} \mathbf{P}(I_{n_j})\right] \quad . \tag{3.2}$$

Hence P_{A_n} is easily simulated and

$$\lim_{A\to\infty}\lim_{n\to\infty} P_{A_n}(\mathbf{t}) = P(\mathbf{t}) \quad .$$

The covariance function of P_{A_n} is given by

$$R_{P_{A_n}} = \mathbf{E}\left\{P_{A_n}(\mathbf{0})P_{A_n}(\mathbf{t})\right\} = \sum_{j=1}^{A_n} \cos(\mathbf{t}.\mathbf{z}_{n_j})\ \mathbf{P}[\mathbf{W}\in I_{n_j}] \quad ,$$

so asymptotically the covariance is given by the integral

$$\int_{\mathbf{R}^N} \cos(\mathbf{t}.\mathbf{z})\ dF_{\mathbf{W}}(\mathbf{z}) = \varphi_W(\mathbf{t}) = R_P(\mathbf{t}) \quad ,$$

the covariance function of P. The correlation between P_{A_n} and Q_{A_n} is given by

$$\mathbf{E}\,[P_{A_n}(\mathbf{0})Q_{A_n}(\mathbf{t})] = \sum_{j=1}^{A_n} \sin(\mathbf{t}.\mathbf{z}_{n_j})\mathbf{P}[\mathbf{W}\in(I_{n_j}] \quad ,$$

so if we choose I_{n_j} and z_{n_j} in a symmetric manner, then P_{A_n} and Q_{A_n} are uncorrelated and hence independent. In any case the asymptotic correlation is given by

$$\int_{R^N} \sin(\mathbf{t}.\mathbf{z})\, dF_{\mathbf{W}}(\mathbf{z}) = 0 \ ,$$

so P_{A_n} and Q_{A_n} are asymptotically uncorrelated and thus are asymptotically independent.

If we can calculate the "elements of measure", $\hat{\mu}(I_{n_j})$ in (3.1), then we can simulate a Gaussian random field having asymptotically the correct covariance function.

We are naturally interested in how closely the Riemann sum simulation approximates to a Gaussian random field. One good estimate of this will be given by the mean square error in approximating P by P_{A_n}. Now,

$$\mathbf{E}\left[\, |P(\mathbf{t})-P_{A_n}(\mathbf{t})|^2 \,\right] = \tfrac{1}{2}\,\mathbf{E}\left[\, |X(\mathbf{t})-X_{A_n}(\mathbf{t})|^2 \,\right] \ ,$$

so the mean square error in approximating P by P_{A_n} is half the mean square error in approximating X by X_{A_n}. If we define

$$X_A(\mathbf{t}) = \int_{A^N} e^{i\mathbf{t}.\mathbf{z}}\, d\lambda(\mathbf{z}) \ ,$$

then

$$\mathbf{E}\left[\, |X(\mathbf{t})-X_A(\mathbf{t})|^2 \,\right] = \int_{R^N \setminus A^N} |e^{i\mathbf{t}.\mathbf{z}}|^2\, d[2F_{\mathbf{W}}(\mathbf{z})]$$

$$= 2\,\mathbf{P}\left[\, \mathbf{W} \in \mathbf{R}^N \setminus \mathbf{A}^N \,\right] \ .$$

If we take

$$h = N^{\frac{1}{2}N} \operatorname*{Sup}_{1 \le j \le A_n} Vol(I_{n_j}) \ ,$$

then h bounds the largest distance between two points in the same box. So

$$\mathbf{E}\left[\, |X_A(\mathbf{t})-X_{A_n}(\mathbf{t})|^2 \,\right] = 2 \sum_{j=1}^{A_n} \int_{I_{n_j}} |e^{i\mathbf{t}.\mathbf{z}}-e^{i\mathbf{t}.\mathbf{z}_{n_j}}|^2\, F_{\mathbf{W}}(\mathbf{z})$$

$$\le 2|\mathbf{t}|^2 h^2\, \mathbf{P}\,(\mathbf{W} \in \mathbf{A}^N) \le 2|\mathbf{t}|^2 h^2 \ .$$

Now

$$\mathbf{E}\left[\, |X(\mathbf{t})-X_{A_n}(\mathbf{t})|^2 \,\right] \le \mathbf{E}\left\{ (\, |X(\mathbf{t})-X_A(\mathbf{t})| + |X_A(\mathbf{t})-X_{A_n}(\mathbf{t})|\,)^2 \right\}$$

$$\le 2\,\mathbf{E}\,[\, |X(\mathbf{t})-X_A(\mathbf{t})|^2\,]$$

$$+ 2\,\mathbf{E}\,[\,|X_A(\mathbf{t})-X_{A_n}(\mathbf{t})|^2\,]\ .$$

Thus the mean square error is given by

$$\mathbf{E}\,[\,|P(\mathbf{t})-P_{A_n}(\mathbf{t})|^2\,] \le 2\,\mathbf{P}\,(\,\mathbf{W}\in\mathbf{R}^N\backslash\mathbf{A}^N\,) + 2\,|\mathbf{t}|^2h^2\ . \qquad (3.3)$$

Similar estimates for the mean square error can be obtained for the Riemann sum simulation of the integrals for the derivatives of P and Q.

Figures 1 and 2 of Section 7 are contour maps of Gaussian random fields simulated by using this method.

4. Monte-Carlo Simulation

As mentioned at the end of Section 2, we can use a Monte-Carlo type of approach in order to evaluate the integrals that give rise to a homogeneous Gaussian random field. We can do this by simulating from the random variable **W** in Section 2 in order to give us realisations of the random measures μ and ν. In this section we shall give the theoretical arguments behind this idea and in the next section an algorithm for implementing it.

Let **W** be a symmetric random variable on $\mathbf{R}^N$ with probability measure **P**, distribution function $F_{\mathbf{W}}$ and real characteristic function φ_W. If we let M be a positive integer, then we can define the following random variables :

(i) $\mathbf{w}_1,\ldots,\mathbf{w}_M$ independently from **W** ;

(ii) $u_1,\ldots,u_M$ and $v_1,\ldots,v_M$ independently from an $N(0;1/M)$ distribution.

Let **B** denote the set of Borel sets in $\mathbf{R}^N$ then, for $I\in\mathbf{B}$, define

$$S(I) = \{\ k\ |\ \mathbf{w}_k\in I\ \}\ ,$$

$$\text{and } n(I) = |S(I)|\ ,$$

so $S(I)$ is an index set for I and $n(I)$ the number of realisations of **W** in I. Suppose

$$\hat{\mu}(I) = \sum_{k\in S(I)} u_k \text{ and } \hat{\nu}(I) = \sum_{k\in S(I)} v_k\ ,$$

then $\hat{\mu}(I)$ and $\hat{\nu}(I)$ are independently distributed as a $Bin(M,\mathbf{P}(\mathbf{W}\in I))$ mixture of $N(0;n(I)/M)$ distributions and hence have mean zero. Thus $\hat{\mu}$ and $\hat{\nu}$ are almost surely finite real measures on **B**, the set of Borel sets in $\mathbf{R}^N$. In particular, μ and ν both satisfy the orthogonality condition of Section 2 :

$$\mathbf{E}[\hat{\mu}(I)\hat{\mu}(J)] = \mathbf{E}[\hat{\mu}(I)\hat{\mu}(J)] = 0 \quad \forall \text{ disjoint } I,J\in\mathbf{B}\ .$$

The characteristic function of an $N(0;n/M)$ distribution is

$$\exp\left[-\frac{n\theta^2}{2M}\right] ,$$

so the characteristic function of $\hat{\mu}(I)$ is given by

$$\begin{aligned}
\varphi_{\hat{\mu}(I)}(\theta) &= \sum_{n=0}^{M} \binom{M}{n} \exp(-n\theta^2/2M)\, \mathbf{P}(\mathbf{W}\in I)^n\, \mathbf{P}(\mathbf{W}\notin I)^{N-m} \\
&= \left[\mathbf{P}(\mathbf{W}\notin I) + \exp(-\frac{\theta^2}{2M})\, \mathbf{P}(\mathbf{W}\in I) \right]^M \\
&= \left[1 - \mathbf{P}(\mathbf{W}\in I)\, [\, 1-\exp(\frac{-\theta^2}{2M}) \,] \right]^M \\
&= \left[1 - \frac{\theta^2 \mathbf{P}(\mathbf{W}\in I)}{2M} + O(1/M^2) \right]^M \\
&= \exp\, [\, -\tfrac{1}{2}\mathbf{P}(\mathbf{W}\in I)\theta^2 \,] + O(1/M) \quad \text{as } M\to\infty \ . \qquad (4.1)
\end{aligned}$$

Differentiating twice gives us

$$\mathbf{E}\, [\, \hat{\mu}(I)^2 \,] = \mathbf{E}\, [\, \hat{\nu}(I)^2 \,] = \mathbf{P}(\mathbf{W}\in I) \quad \text{for any } M>0 \ ,$$

and so the continuity theorem tells us that

$$\hat{\mu}(I), \hat{\nu}(I) \sim N[\, 0, \mathbf{P}(\mathbf{W}\in I) \,] \quad \text{as } M\to\infty \ .$$

The definitions of μ and ν can be extended to give a field with orthogonal increments on $\mathbf{R}^N$ by defining, for any $\mathbf{x}\in\mathbf{R}^N$,

$$I(\mathbf{x}) = (-\infty,x_1)\times\ldots\times(-\infty,x_N) \in \mathbf{B} \ ,$$

and taking $\mu(\mathbf{x})=\hat{\mu}(I(\mathbf{x}))$ and $\nu(\mathbf{x})=\hat{\nu}(I(\mathbf{x}))$.

Let g be a real-valued function on $\mathbf{R}^N$, so if

$$\int_{\mathbf{R}^N} g(\mathbf{z})^2\, dF_{\mathbf{W}}(\mathbf{z}) = \mathbf{E}\, [\, g(\mathbf{W})^2 \,] \quad \text{exists,}$$

then the random variable

$$\int_{\mathbf{R}^N} g(\mathbf{z})\, d\mu(\mathbf{z}) \qquad (4.2)$$

is well-defined as a Riemann-Stieltjes integral converging in mean-square with mean zero and variance

$$\int_{\mathbf{R}^N} g(\mathbf{z})^2\, dF_{\mathbf{W}}(\mathbf{z}) \ .$$

From (4.1) and the orthogonality condition, the characteristic function, ψ_{A_n}, of the Riemann sum of (4.2), S_{A_n} say, is given by

$$\psi_{A_n}(\theta) = \mathbf{E}\,[\,\exp(i\theta S_{A_n})\,] = \mathbf{E}\left[\exp\left(\,i\theta\sum_{j=1}^{A_n} g(\mathbf{z}_{n_j})\hat{\mu}(I_{n_j})\,\right)\right]$$

$$= \prod_{j=1}^{A_n} \mathbf{E}\left[\exp\left(\,i\theta g(\mathbf{z}_{n_j})\hat{\mu}(I_{n_j})\,\right)\right]$$

$$= \prod_{j=1}^{A_n}\left\{\exp\left(\,-\tfrac{1}{2}\theta^2 g(z_{n_j})\mathbf{P}[\mathbf{W}\in I_{n_j}]\,\right) + O(1/M)\right\}$$

$$= \exp\left[\,-\tfrac{1}{2}\theta^2\sum_{j=0}^{A_n} g(z_{n_j})\mathbf{P}(\mathbf{W}\in I_{n_j})\,\right] + O(1/M) \quad \text{as } M\to\infty \ .$$

Asymptotic normality as $M\to\infty$ follows from the continuity theorem, so

$$\int_{\mathbf{R}^N} g(\mathbf{z})\, d\mu(\mathbf{z}) \sim N\left[0\,,\ \int_{\mathbf{R}^N} g(\mathbf{z})^2\, dF_{\mathbf{W}}(\mathbf{z})\right] \quad \text{as } M\to\infty \ . \tag{4.3}$$

As in Section 2 we can define a complex-valued additive set function λ by

$$\hat{\lambda}(I) = \hat{\mu}(I) + i\hat{\nu}(I) \ ,$$

and again extend this definition to obtain a complex-valued field on $\mathbf{R}^N$ with orthogonal increments.

As before we can define a complex-valued random field X^* on $\mathbf{R}^N$ as the Riemann-Stieltjes integral

$$X^*(\mathbf{t}) = \int_{\mathbf{R}^N} e^{i\mathbf{t}.\mathbf{z}}\, d\lambda(\mathbf{z}) \ , \tag{4.4}$$

and its real and imaginary parts, P^* and Q^*, as

$$P^*(\mathbf{t}) = \int_{\mathbf{R}^N} \cos(\mathbf{t}.\mathbf{z})\, d\mu(\mathbf{z}) - \int_{\mathbf{R}^N} \sin(\mathbf{t}.\mathbf{z})\, d\nu(\mathbf{z}) \ , \tag{4.5}$$

$$Q^*(\mathbf{t}) = \int_{\mathbf{R}^N} \sin(\mathbf{t}.\mathbf{z})\, d\mu(\mathbf{z}) + \int_{\mathbf{R}^N} \cos(\mathbf{t}.\mathbf{z})\, d\nu(\mathbf{z}) \ . \tag{4.6}$$

However we can re-write (4.5) and (4.6) as

$$P^*(\mathbf{t}) = \sum_{k=1}^{M} \cos(\mathbf{t}.\mathbf{w}_k)u_k - \sin(\mathbf{t}.\mathbf{w}_k)v_k \ , \tag{4.7}$$

$$Q^*(\mathbf{t}) = \sum_{k=1}^{M} \sin(\mathbf{t}.\mathbf{w}_k)u_k + \cos(\mathbf{t}.\mathbf{w}_k)v_k \ , \tag{4.8}$$

From Section 2 we know that $P^*(\mathbf{t})$ and $Q^*(\mathbf{t})$ have mean zero and variance

$$\int_{\mathbf{R}^N} \left[\sin^2(\mathbf{t}.\mathbf{z}) + \cos^2(\mathbf{t}.\mathbf{z})\right] dF_{\mathbf{W}}(\mathbf{z}) = 1 \ ,$$

and, from (4.3), that $P^*(\mathbf{t})$ and $Q^*(\mathbf{t})$ are asymptotically normally distributed as $M \to \infty$.

Now

$$\mathbf{E}\,[\,P^*(\mathbf{0})Q^*(\mathbf{t})\,] = \mathbf{E}\,[\,\int_{\mathbf{R}^N}\int_{\mathbf{R}^N} \sin(\mathbf{t}.\mathbf{z})\,d\mu(\mathbf{y})d\mu(\mathbf{z})\,]$$

$$+\,\mathbf{E}\,[\,\int_{\mathbf{R}^N}\int_{\mathbf{R}^N} \cos(\mathbf{t}.\mathbf{z})\,d\mu(\mathbf{y})dv(\mathbf{z})\,]$$

$$= \int_{\mathbf{R}^N} \sin(\mathbf{t}.\mathbf{z})\,dF_{\mathbf{W}}(\mathbf{z}) = \mathrm{Im}(\varphi_W(\mathbf{t})) = 0\ ,$$

so $P^*(\mathbf{s})$ and $Q^*(\mathbf{t})$ are uncorrelated for all $\mathbf{s},\mathbf{t}\in\mathbf{R}^N$, and are therefore asymptotically independent as $M \to \infty$.

The covariance function of X^*, R_X^*, is given by

$$R_X^*(\mathbf{t}) = \mathbf{E}\left[X^*(\mathbf{0})\overline{X^*(\mathbf{t})}\right] = \int_{\mathbf{R}^N} e^{i\mathbf{t}.\mathbf{z}}\,dF(\mathbf{z}) = 2\varphi_W(\mathbf{t})\ ,$$

$$\text{but}\ \ R_X^*(\mathbf{t}) = R_P^*(\mathbf{t}) + R_Q^*(\mathbf{t})\ ,$$

$$\text{so}\ \ R_P^*(\mathbf{t}) = \varphi_W(\mathbf{t})\ . \tag{4.9}$$

Of course we can also give expressions for the j^{th} partial derivatives of X^*, X^{*j}, where they exist, as

$$P^{*j}(\mathbf{t}) = \sum_{k=1}^{M} -\mathbf{w}_k^{(i)}\sin(\mathbf{t}.\mathbf{w}_k)u_k - \mathbf{w}_k^{(i)}\cos(\mathbf{t}.\mathbf{w}_k)v_k\ , \tag{4.10}$$

$$Q^{*j}(\mathbf{t}) = \sum_{k=1}^{M} \mathbf{w}_k^{(i)}\cos(\mathbf{t}.\mathbf{w}_k)u_k - \mathbf{w}_k^{(i)}\sin(\mathbf{t}.\mathbf{w}_k)v_k\ , \tag{4.11}$$

where $\mathbf{w}_k^{(i)}$ denotes the i^{th} component of of the vector w_k. Clearly P^{*j} and Q^{*j} are uncorrelated, and from Section 2 we know that these integrals converge if and only if

$$\mathbf{E}\,[\,|\mathbf{W}_j|^2\,]\ \text{exists},$$

that is if and only if

$$\frac{\partial^2 \varphi_W}{\partial t_j^{\,2}}_{\mathbf{t}=\mathbf{0}}\ \text{exists.}$$

Thus the Monte Carlo simulation gives a random field that has the required covariance function and is asymptotically Gaussian. In the next section we shall give an algorithm for implementing this method for an arbitrary covariance

function.

5. An Algorithm for the Monte-Carlo Simulation

We can use equations (4.7) and (4.8) as a means of simulating a Gaussian Random Field with a given covariance function. We shall give details of this simulation of a two dimensional field, the extension to a higher dimensional field is obvious. Without loss of generality we can consider a field with zero mean and unit variance.

In order to simulate a field having covariance function R, we need to find a random variable $\mathbf{W}$ on $\mathbf{R}^2$ that has a characteristic function φ_W equal to R. The density of $\mathbf{W}$, $f_{\mathbf{W}}$, is related to the covariance function by the two dimensional Fourier transform

$$R(\mathbf{t}) = \varphi_W(\mathbf{t}) = \int_{\mathbf{R}^2} f_{\mathbf{W}}(\mathbf{z})\, e^{i\mathbf{t}.\mathbf{z}}\, d\mathbf{z} \quad . \tag{5.1}$$

Thus, to obtain a density function for $\mathbf{W}$ we have to invert a two dimensional Fourier transform. Obviously if we can perform this inversion analytically, we can easily obtain a density function ; if not, we will have to perform the inversion numerically. The inversion formula for a two dimensional Fourier transform gives us

$$f_{\mathbf{W}}(\mathbf{z}) = \frac{1}{4\pi^2} \lim_{R_1\to\infty} \lim_{R_2\to\infty} \int_{-R_1}^{R_1}\int_{-R_2}^{R_2} \varphi_W(\mathbf{t})\, e^{-i\mathbf{t}.\mathbf{z}}\, d\mathbf{t} \quad . \tag{5.2}$$

If we choose R_1 and R_2 such that the integral of φ_W is negligible outside the rectangle

$$S(R_1,R_2) = [-R_1,R_1]\times[-R_2,R_2] \quad ,$$

then we can approximate $f_{\mathbf{W}}$ by

$$\frac{1}{4\pi^2} \sum_{\mathbf{t}\in G} R(\mathbf{t})\, e^{-i\mathbf{t}.\mathbf{z}} \quad , \tag{5.3}$$

where the grid G consists of $2N_1$ by $2N_2$ regularly spaced points over the rectangle $S(R_1,R_2)$,

$$\text{ie.} \quad G = \left\{ \left[\frac{k_1R_1}{N_1}, \frac{k_2R_2}{N_2} \right] : k_i=-(N_i-1),\ldots,N_i \right\} \quad ,$$

because

$$f_{\mathbf{W}}(\mathbf{z}) \approx \frac{1}{4\pi^2} \int_{S(R_1,R_2)} \varphi_W(\mathbf{t})\, e^{-i\mathbf{t}.\mathbf{z}}\, d\mathbf{t}$$

$$= \frac{1}{4\pi^2} \int_{S(R_1,R_2)} R(\mathbf{t})\, e^{-i\mathbf{t}.\mathbf{z}}\, d\mathbf{t}$$

$$\approx \frac{1}{4\pi^2} \sum_{\mathbf{t}\in G} R(\mathbf{t})\, e^{-i\mathbf{t}.\mathbf{z}} \quad . \tag{5.4}$$

If we define another grid, H, by

$$H = \left\{ \left[\frac{l_1 N_1}{R_1}, \frac{l_2 N_2}{R_2} \right] : l_i = -(N_i - 1), \ldots, N_i \right\} ,$$

then for $l_1, l_2 = -(N_i - 1), \ldots, N_i$, and

$$\mathbf{z} = \left[\frac{l_1 N_1}{R_1}, \frac{l_2 N_2}{R_2} \right] \in H ,$$

we have

$$f_{\mathbf{W}}(\mathbf{z}) \approx \frac{1}{4\pi^2} \sum_{k_i = -(N_i-1)}^{N_i} R\left[\frac{k_1 R_1}{N_1}, \frac{k_2 R_2}{N_2} \right] \exp[-i(k_1 l_1 + k_2 l_2)] , \tag{5.5}$$

which is just a two dimensional inverse fast Fourier transform of the function

$$R\left[\frac{\mathbf{t}_1 R_1}{N_1}, \frac{\mathbf{t}_2 R_2}{N_2} \right]$$

for $\mathbf{z} \in H$. If the values of R at points of the grid G are written as a matrix, then the two dimensional fast Fourier transform (5.5) is obtained by applying a fast Fourier transform firstly to each row of the matrix and then to each column of the row-transformed matrix.

We can therefore define a function $\hat{f}_{\mathbf{W}} : \mathbf{R}^2 \to \mathbf{R}$ to estimate $f_{\mathbf{W}}$ by first requiring $\hat{f}_{\mathbf{W}}$ to be equal to the fast Fourier transform (5.5) on the grid H. If $\overline{H}$ denotes the convex hull of H, that is the smallest rectangle containing H, we can define $\hat{f}_{\mathbf{W}}$ by interpolation between the values of $\hat{f}_{\mathbf{W}}$ at the four nearest grid points and set $\hat{f}_{\mathbf{W}}$ equal to zero outside of $\overline{H}$. $\hat{f}_{\mathbf{W}}$ then estimates the density function of $\mathbf{W}$ over the whole plane. Though it is not crucial that

$$\int_{\mathbf{R}^2} \hat{f}_{\mathbf{W}} = 1 ,$$

since we will using $\hat{f}_{\mathbf{W}}$ to simulate from $\mathbf{W}$ by rejection sampling, this is a good test for the convergence of the fast Fourier transform.

If we let K be the maximum value of the density, so

$$K = \operatorname*{Sup}_{\mathbf{z}\in\mathbf{R}^2} \hat{f}_{\mathbf{W}}(\mathbf{z}) = \operatorname*{Max}_{\mathbf{z}\in H} \hat{f}_{\mathbf{W}}(\mathbf{z}) ,$$

then we can sample from $\mathbf{W}$ by rejection sampling. This is performed in the following manner. Let

$$\mathbf{W}_i \sim U(\bar{H}) \text{ , and } U_i \sim U(0,1) \text{ ,}$$

then we accept $\mathbf{W}_i$ as a realisation of $\mathbf{W}$ with probability $\frac{\hat{f}_{\mathbf{W}}(\mathbf{W}_i)}{K}$, that is if

$$\frac{\hat{f}_{\mathbf{W}}(\mathbf{W}_i)}{K} \geq U_i \text{ .}$$

Whether analytically or by the numerical method outlined above, we can simulate M independent realisations of $\mathbf{W}$, relabelled as $\mathbf{W}_1,\ldots,\mathbf{W}_M$, and also simulate the normal random variables

$$u_1,\ldots,u_M,v_1,\ldots,v_M \sim N(0;1/M) \text{ independently.}$$

It is then just a case of doing the sums (4.7) and (4.8) to obtain simulations for a Gaussian random field, and (4.10) and (4.11) for their derivatives.

Of course, we can also use this method to estimate a density for $f_{\mathbf{W}}$, which we can then use to simulate a homogeneous Gaussian random field using the Riemann Sum approach outlined in Section 3.

All the contour maps in Section 7, with the exception of figures 1 and 2, are of Gaussian or related random fields simulated using the Monte-Carlo approach.

6. The χ^2 Random Field

The χ^2 random field is a random field that is derived from the squares of random fields. In one dimension, they have both been studied, for example by Sharpe (1978), and used to model wind loads in engineering, but have not been much studied in higher dimensions.

Suppose we have n independent realisations of a homogeneous Gaussian random field with mean zero and unit variance, $X^{(1)}(\mathbf{t}),\ldots,X^{(n)}(\mathbf{t})$ each having covariance function R_X. We can then define a random field Y by

$$Y(\mathbf{t}) = [X^{(1)}(\mathbf{t})]^2 + \ldots + [X^{(n)}(\mathbf{t})]^2 \text{ ,} \qquad (6.1)$$

so clearly $Y(\mathbf{t})$ is a χ^2 random variable with n degrees of freedom, and hence the random field Y is known as a χ^2 random field with n degrees of freedom. If the covariance function of Y is denoted by R_Y, then, from Adler's (7.14), Adler (1981), we know that

$$R_Y(\mathbf{z}) = 2nR_X{}^2(\mathbf{z}) \text{ ,} \qquad (6.2)$$

so Y is a homogeneous random field. Given that we can simulate homogeneous Gaussian random fields and, where they exist, their derivatives, it is easy to simulate a χ^2 random field from (6.1), (6.2) and

$$Y_j(t) = 2X^{(1)}(t)X_j^{(1)}(t) + \ldots + 2X^{(n)}(t)X_j^{(n)}(t) \quad . \tag{6.3}$$

Figures 11 to 14 are contour maps of χ^2 random fields with one, five, ten and twenty degrees of freedom respectively, and covariance function

$$R_Y(t) = \exp\left[-\tfrac{1}{2}|t|^2\right] \quad .$$

7. Some Contour Maps of Simulated Random Fields

In this section, we present some contour maps of simulated random fields. These have been drawn using Conicon 3 based on a 13×13 grid of values and gradients. Conicon 3 employs a "heads-up" annotation, that is the contour numbers are the correct way round looking uphill. Both the Riemann sum simulation and the Monte Carlo simulation give us two asymptotically independent copies of a homogeneous Gaussian random field, the real and imaginary parts of some complex-valued random field, and each Gaussian random field is presented along with its "twin".

Figures 1 and 2 are contour maps on the square

$$(-3.0,3.0) \times (-3.0,3.0) \tag{7.1}$$

of Riemann sum simulations of the Gaussian random field with isotropic covariance function

$$C(x) = \exp\left[-\tfrac{1}{2}|x|^2\right] \quad , \tag{7.2}$$

The Riemann sum was taken over a 21×21 grid of squares of side 0.2 each. In the notation of Section 3 we have

$$A=2.05 \quad \text{and} \quad n=441 \quad .$$

The other figures are either contour maps of Gaussian random fields simulated by means of the Monte Carlo simulation, or contour maps of χ^2 random fields where the underlying Gaussian random fields have been simulated by the Monte Carlo simulation. In all cases the Monte Carlo simulation was based on 800 points, (M=800 in the notation of Section 4).

Figures 3 and 4 are contour maps of the same Gaussian random field as above over the square (7.1), and Figures 5 and 6 are the same random field over the square

$$(-6.0,6.0) \times (-6.0,6.0) \quad . \tag{7.3}$$

Figures 7 and 8 are contour maps on the square (7.1) of Gaussian random fields which have the anisotropic covariance function

$$C(\mathbf{x}) = \exp\{ -\tfrac{1}{2}(x_1^2+16x_2^2) \} \quad . \tag{7.4}$$

This is, of course, essentially the same field as we obtain with covariance function (7.2), but with the "x_2-axis" compressed by a factor of four. this gives rise to clearly visible ridges in the "x_1-direction".

Both the above covariance functions, (7.2) and (7.4), have Fourier transforms that can be calculated analytically, so the fast Fourier transform techniques of Section 5 are unnecessary. Consequently, all the above simulations are very quick, the slowest being the Riemann sum simulation which took 0.2 seconds of C.P.U. time on a Sun 3 computer.

Figures 9 and 10 are contour maps of simulations of the Gaussian random fields having anisotropic covariance function

$$C(\mathbf{x}) = \cos(x_1)\exp\left[-\tfrac{1}{2}|\mathbf{x}|^2\right] \quad , \tag{7.5}$$

and are plotted over the square (7.3). The fast Fourier transforms are taken over 256 points in the square

$$(-4.0,4.0) \times (-4.0,4.0) \quad .$$

In the notation of Section 5,

$$R_1 = R_2 = 4.0 \quad \text{and} \quad N_1 = N_2 = 8 \quad .$$

The integral of the estimated density function for W, $\hat{f}_W$, differed from unity by 0.0002, and the whole simulation took 0.7 seconds of C.P.U. time. It is possible to make out some periodic effect in figures 9 and 10. If we move in an "x_1"-direction across one of these fields, we tend to cross ridges and troughs at regular intervals.

The contour maps in Figures 11 and 12 are of simulations of Gaussian random fields over the square

$$(-1.8,1.8) \times (-1.8,1.8)$$

with the covariance function of Zubrzycki (1957),

$$C(\mathbf{x}) = \begin{cases} 1 - 2/\pi \left[|\mathbf{x}|(1-|\mathbf{x}|^2)^{\frac{1}{2}} + \arcsin(|\mathbf{x}|) \right] & |\mathbf{x}|<1 \\ 0 & |\mathbf{x}|\geq 1 \end{cases} \quad . \tag{7.6}$$

Again we can use fast Fourier transforms to obtain an estimated density for W, with

$$R_1 = R_2 = 1.0 \quad \text{and} \quad N_1 = N_2 = 8 \quad ,$$

and the difference of integral of $\hat{f}_W$ from unity was 0.002. The simulation took

1.3 seconds of C.P.U. time.

The remaining contour maps are of simulations of χ^2 random fields of varying degrees of freedom over the square (7.1). The underlying Gaussian random fields have isotropic covariance function given by (7.2) and so the covariance function of the χ^2 random field is given by (6.3), and the mean level of a field is its degrees of freedom. Figure 13 is a simulation of a χ^2 random field with one degree of freedom, Figure 14 has five degrees of freedom, Figure 15 has ten degrees of freedom, and Figure 16 has twenty degrees of freedom.

The $\chi^2(1)$ random field is mostly flat with values near zero with a few very steep peaks, which correspond with the maxima and minima of the single underlying Gaussian field. It illustrates the result (7.1.21) of Adler (1981), that for a $\chi^2(1)$ random field, the expected number of zeros is infinite.

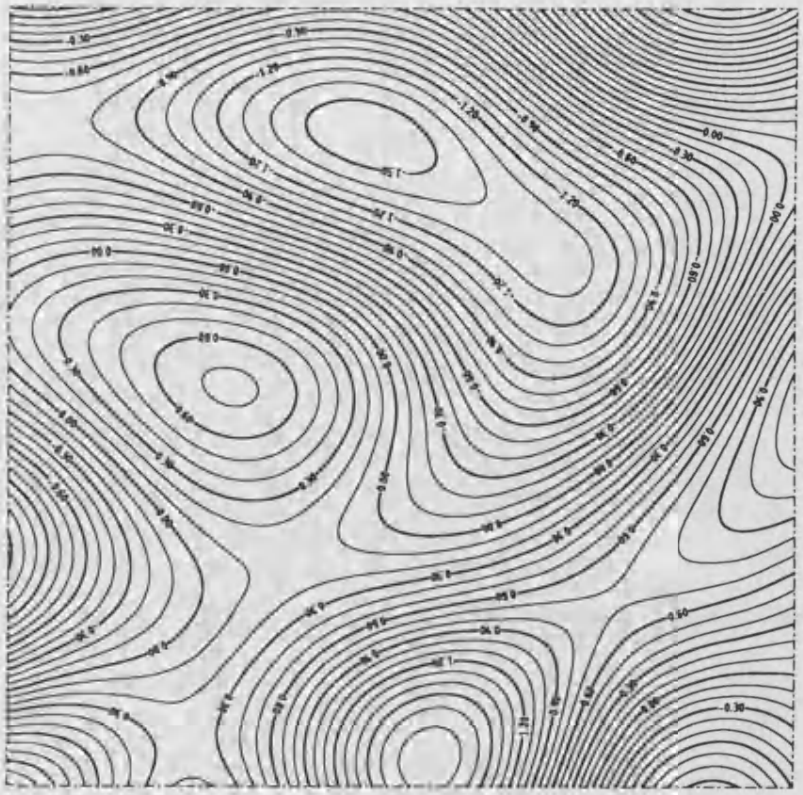

Figure 1

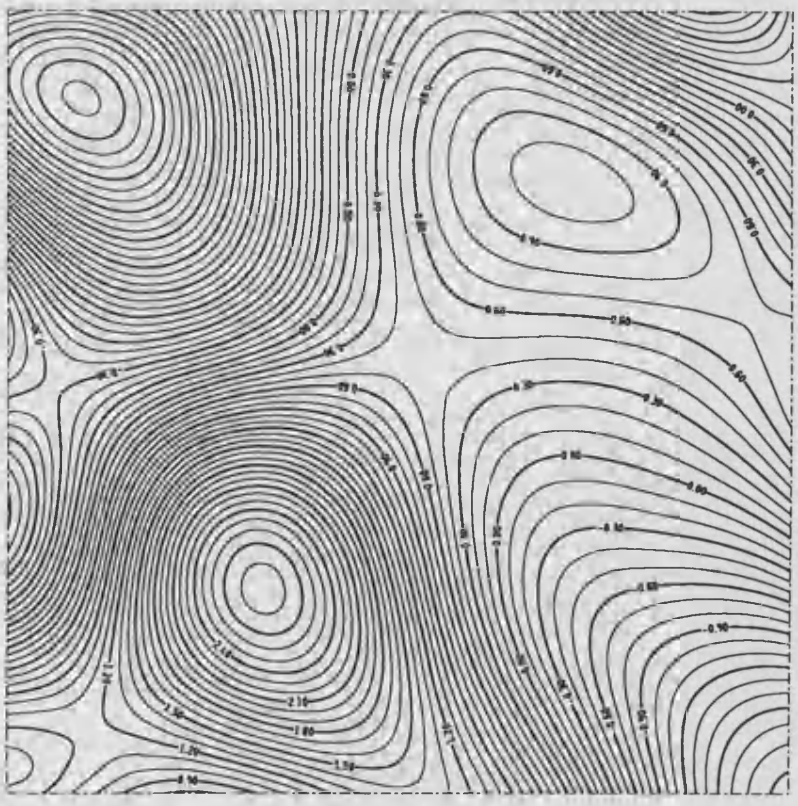

Figure 2

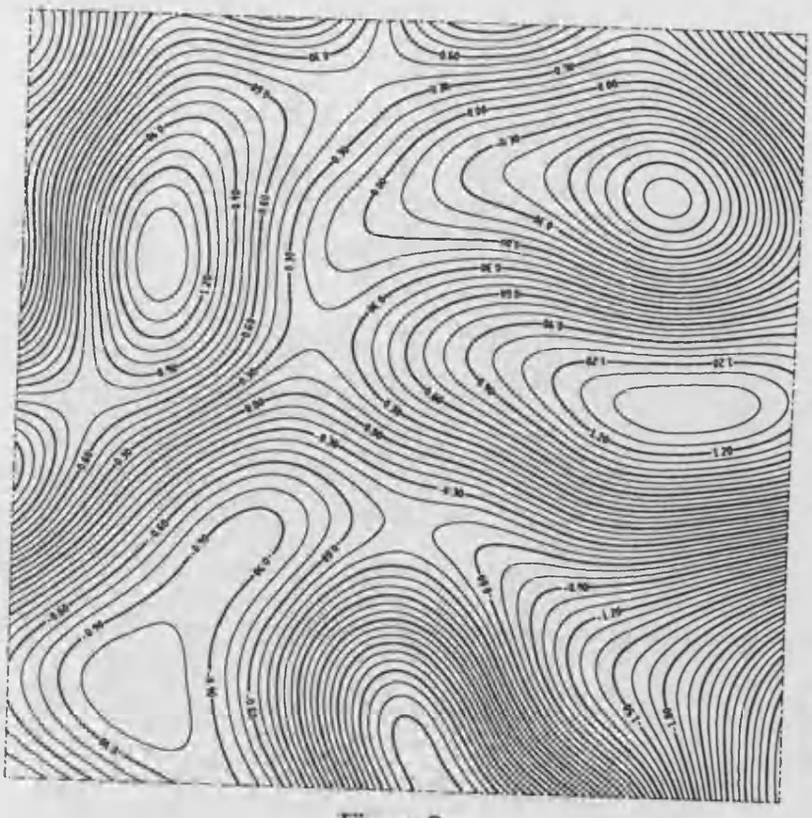

Figure 3

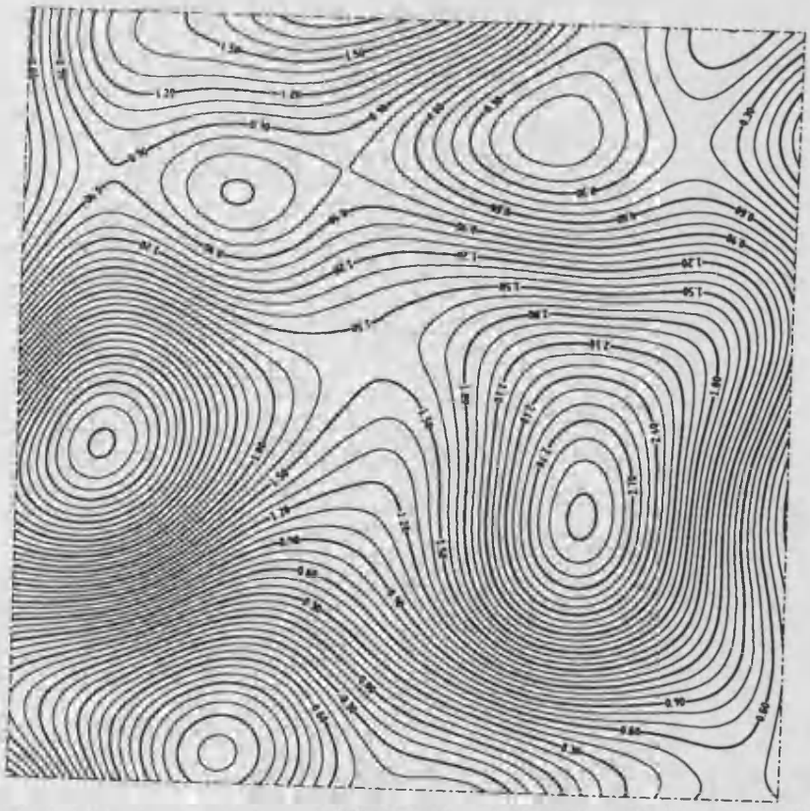

Figure 4

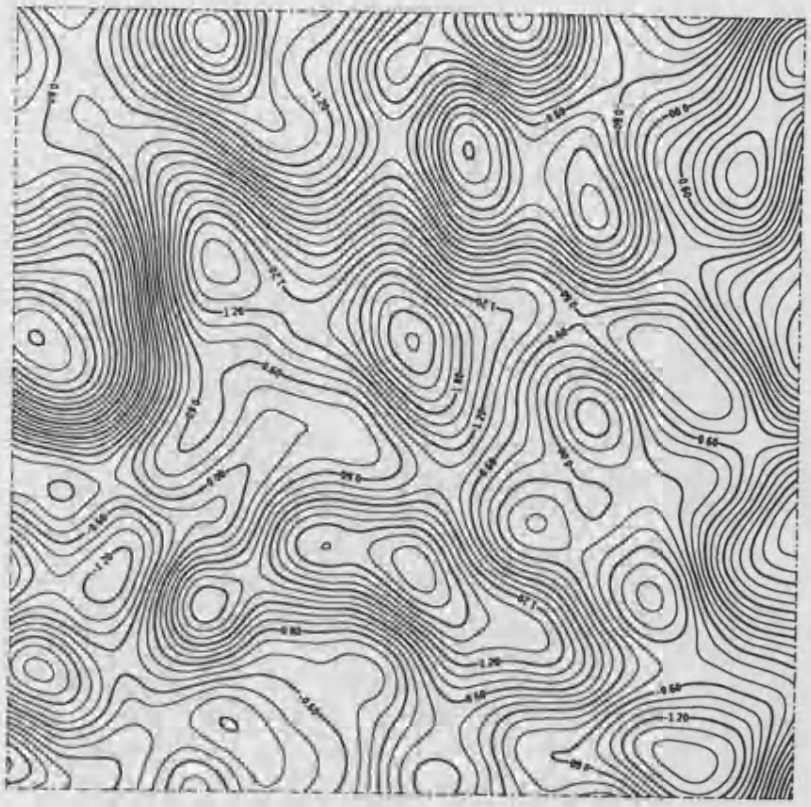

Figure 5

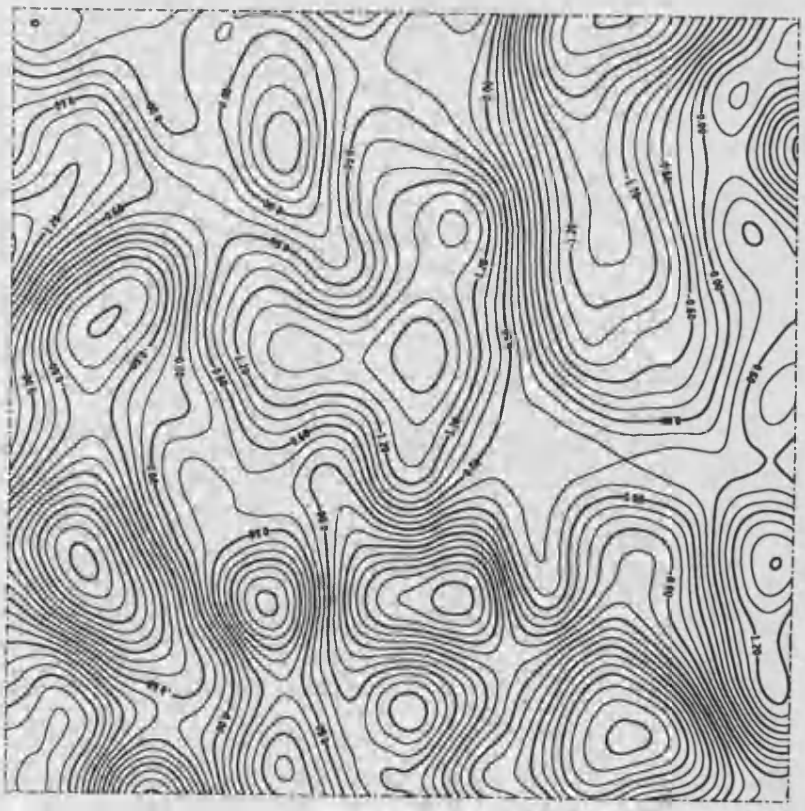

Figure 6

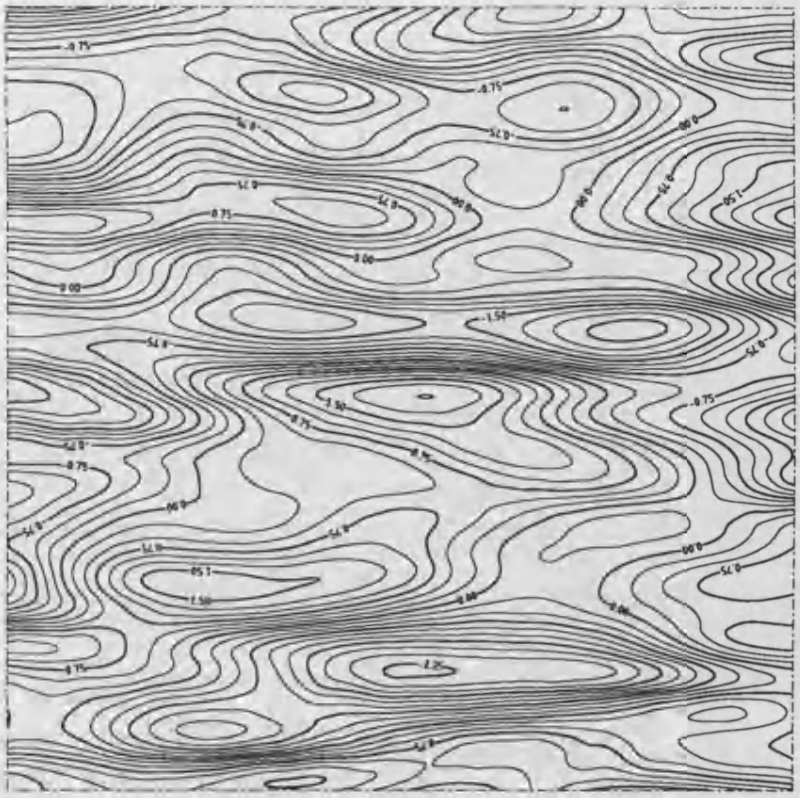

Figure 7

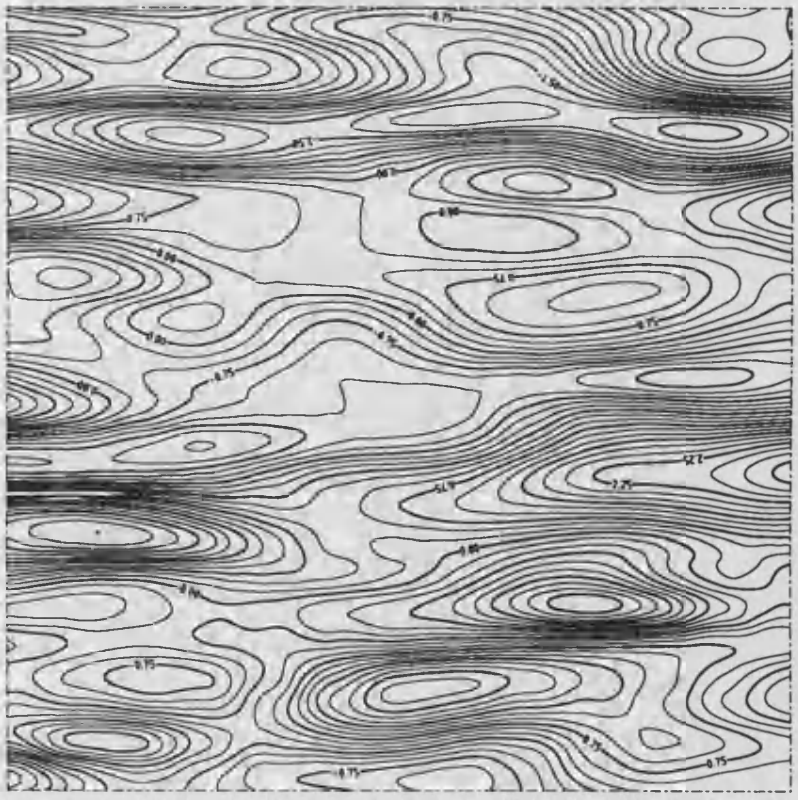

Figure 8

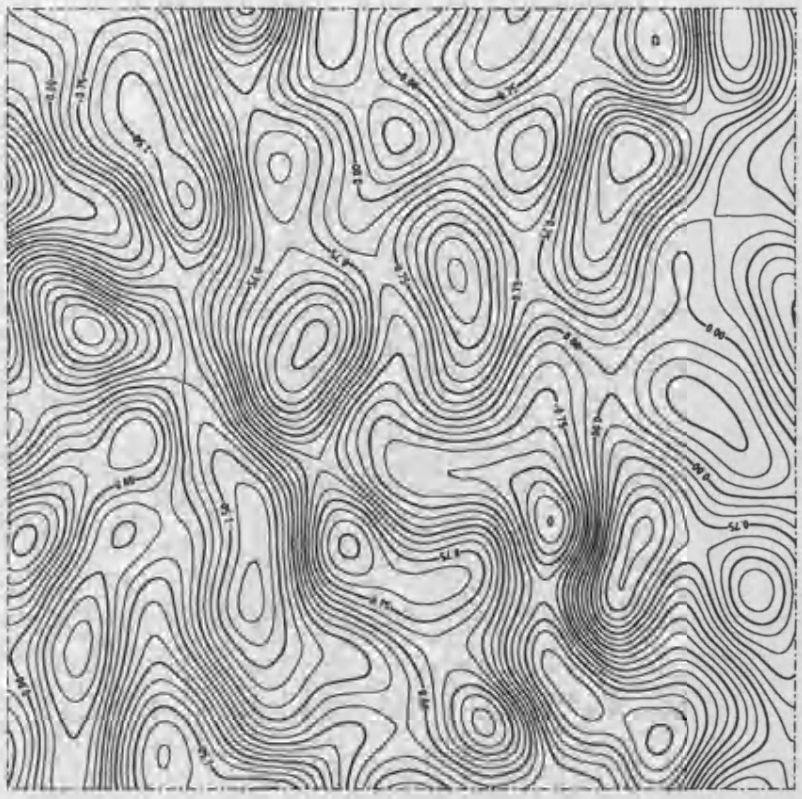

Figure 9

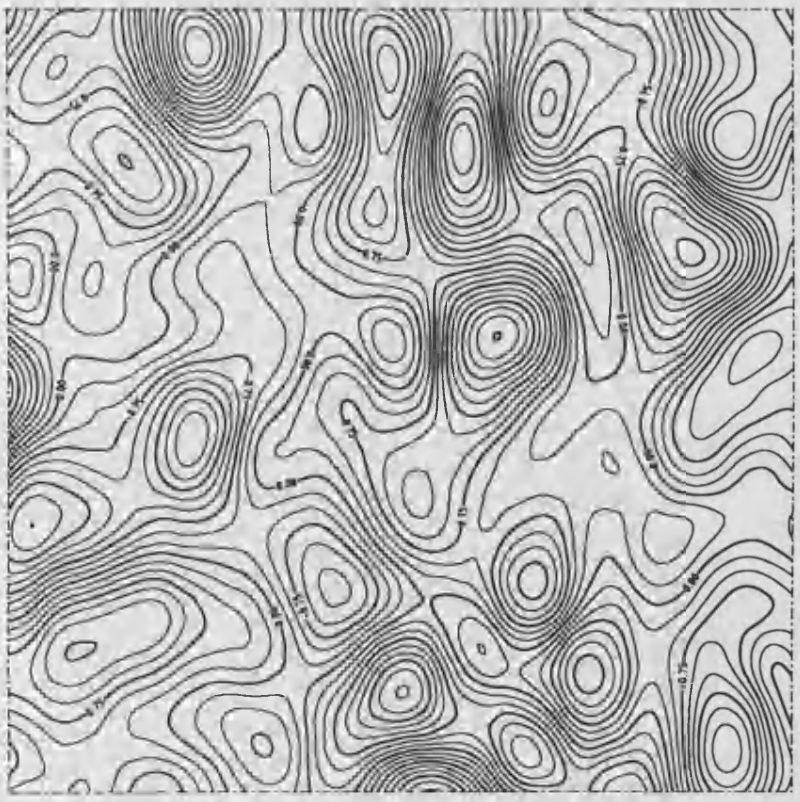

Figure 10

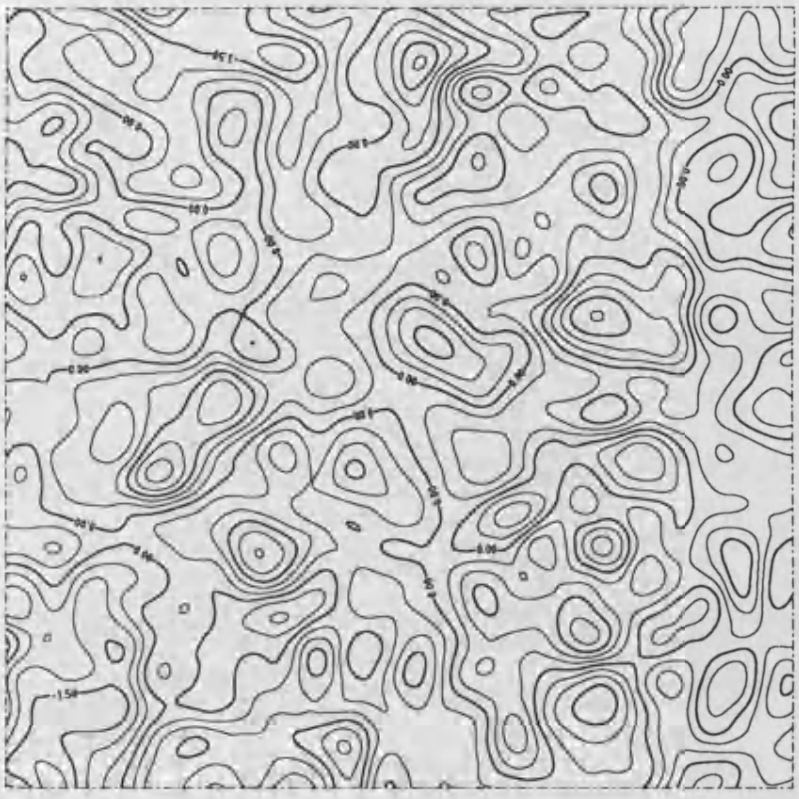

Figure 11

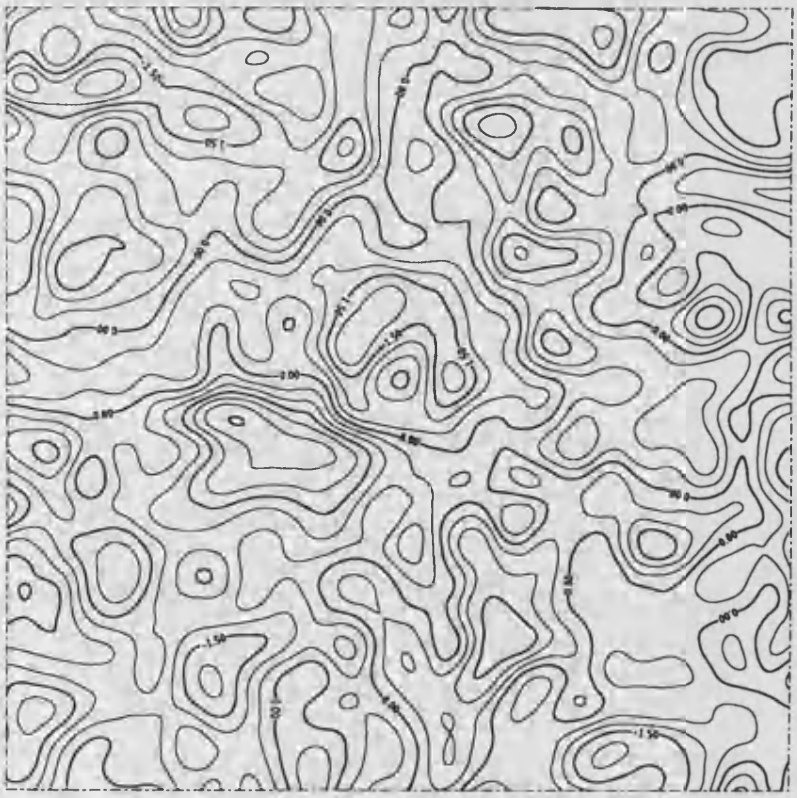

Figure 12

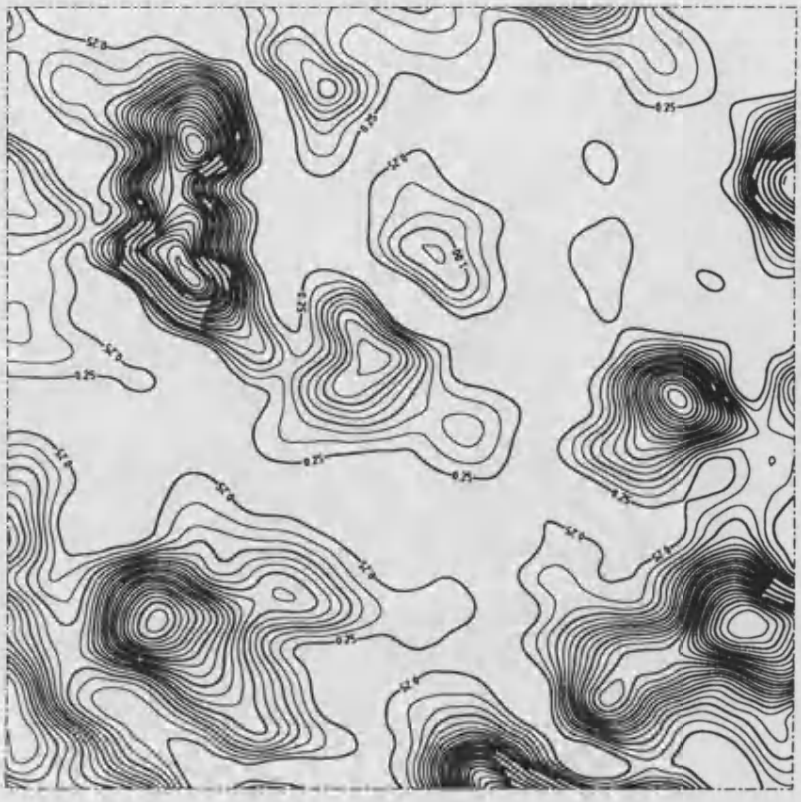

Figure 13

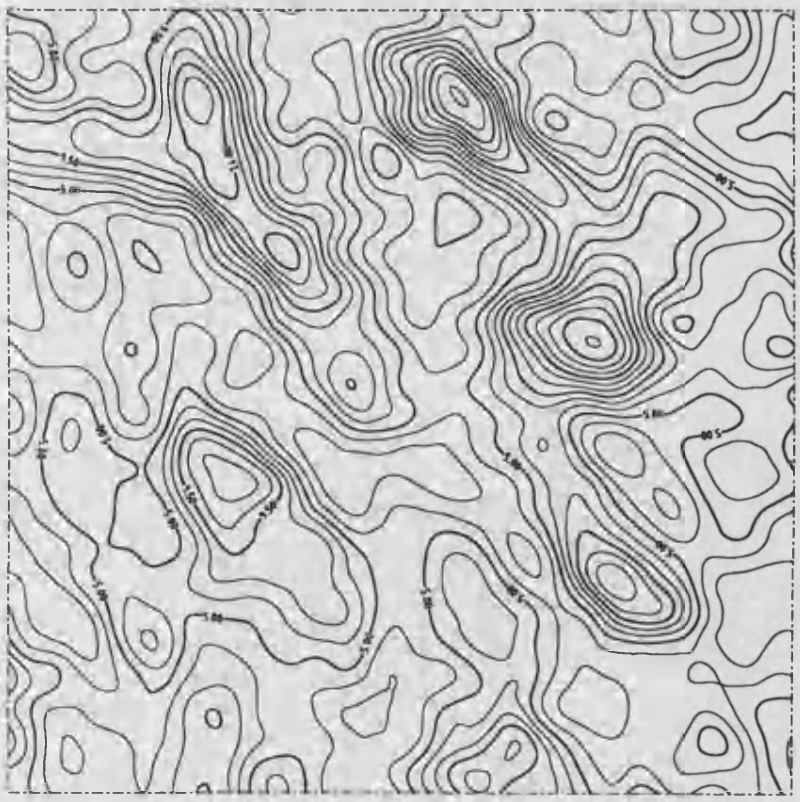

Figure 14

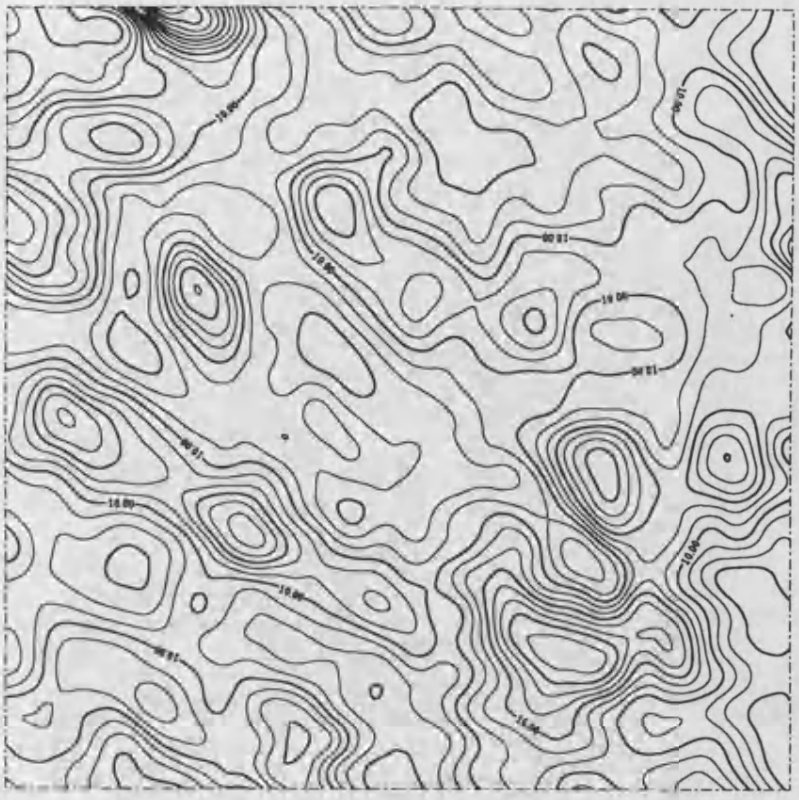

Figure 15

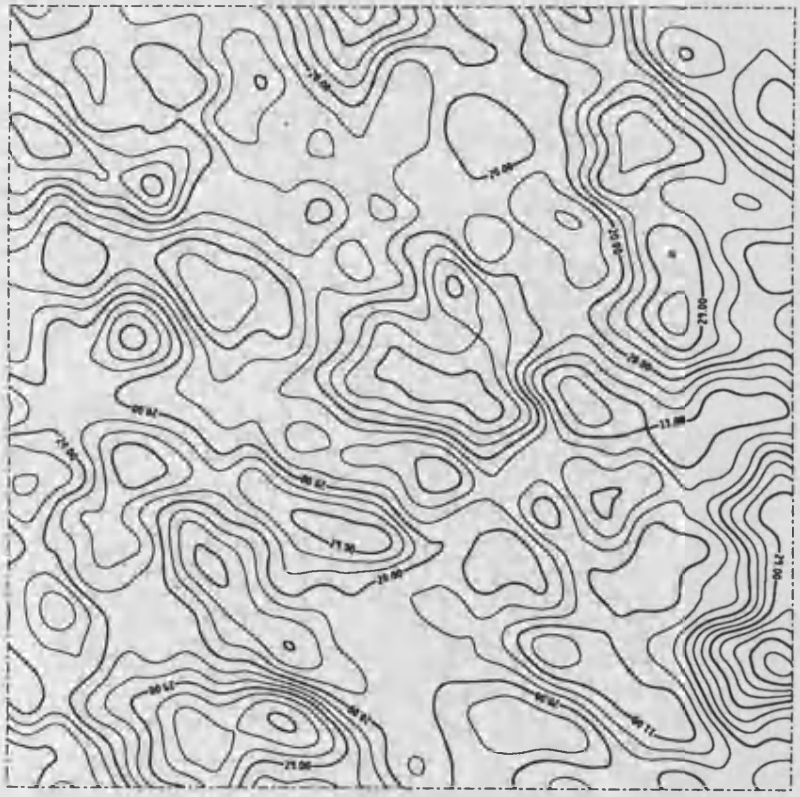

Figure 16

References

Adler, R.J., "The Geometry of Random Fields", J. Wiley, 1981.

Baddeley, A., "A Limit Theorem for Statistics of Spatial Data", *Advances in Applied Probability*, vol. 12, pp. 447-461, 1980.

Baddeley, A.J., and Silverman, B.W., "A Cautionary Example on the Use of Second-Order Methods for Analysing Point Patterns", *Biometrics*, vol. 40, pp. 1089-1093, 1980.

Bartlett, M.S., "The Spectral Analysis of Two Dimensional Point Processes", *Biometrika*, vol. 51, pp. 299-311, 1964.

Bartlett, M.S., "The Statistical Analysis of Spatial Pattern", *Advances in Applied Probability*, vol. 6, pp. 336-358, 1974.

Besag, J., and Diggle, P.J., "Simple Monte Carlo Tests for Spatial Pattern", *Applied Statistics*, vol. 26, pp. 327-333, 1977.

Billingsley, P., "Convergence of Probability Measures", J. Wiley, 1968.

Clark, P.J., and Evans, F.C., "Distance to nearest neighbour as a measure of spatial relationships in populations", *Ecology*, vol. 35, pp. 445-453, 1954.

Cliff, A.D., and Ord, J.K., "Spatial Autocorrelation", Pion, 1977.

Davis, B.M., Hagan, R., and Borgman, L.E., "A Program for the Finite Fourier Transform Simulation of Realisations from a one dimensional random function with known covariance", *Computers and Geosciences*, vol. 7, pp 199-206, 1981.

Diggle, P.J., and Cox, T.F., "Some Distance-Based Tests of Independence for Sparsely-Sampled Multivariate Spatial Point Patterns", *International Statistical Review*, vol. 51, pp. 11-23, 1983.

Donelly, K., "Simulations to determine the variance and edge-effect of total nearest-neighbour distance", in Simulation methods in Archaeology, Cambridge University Press, pp 91-95, 1978.

Gilbert, E.N., "Random Subdivisions of Space into Crystals", *Annals of Mathematical Statistics*, vol. 33, pp. 958-972, 1962.

Green, P.J., and Sibson, R., "Computing Dirichlet Tessellations in the Plane", *Computer Journal*, vol. 21, pp. 168-173, 1978.

Greenwood, J.A., and Williamson, J.B.P., "Contact of Nominally Flat Surfaces", *Proceedings of the Royal Society*, vol. A295, pp. 300-319, 1966.

Greig-Smith, P., "The Use of Random and Contiguous Quadrats in the Study of the Structure of Plant Communities", *Annals of Botany*, vol. 16, pp. 293-316, 1952.

Harkness, R.D., and Isham, V., "A Bivariate Spatial Pattern of Ants' Nests", *Applied Statistics*, vol. 32, pp. 293-303, 1983.

Kelly, F.P., and Ripley, B.D., "A Note on Strauss's Model for Clustering", *Biometrika*, vol. 63, pp. 357-360, 1976.

Kendall, D.G., "An Introduction to Stochastic Geometry", in Stochastic Geometry, J. Wiley, pp. 3-12, 1974a.

Kendall, D.G., "Foundations of a Theory of Random Sets", in Stochastic Geometry, J. Wiley, pp. 322-376, 1974b.

Kingman, J.F.C., "Markov Models for Spatial Variation", *The Statistician*, vol. 24, pp. 167-174, 1975.

Longuet-Higgins, M.S., "The Statistical Analysis of a Randomly Moving Surface" *Philosophical Transactions of the Royal Society*, vol. A249, pp. 321-387, 1957.

Lotwick, H.W., "Spatial Stochastic Point Processes", Ph.D. Thesis, University of Bath, 1981.

Lotwick, H.W., and Silverman, B.W., "Methods for Analysing Spatial Processes of Several Types of Points", *Journal of the Royal Statistical Society B*, vol. 44, pp. 406-413, 1982.

Mandelbrot, B.B., "Fractals ; Form, Chance and Dimension", Freeman, 1977.

Matern, B., "Spatial Variation", *Lecture Notes in Statistics*, vol. 36, Springer-Verlag, 1986.

Matheron, G., "The Intrinsic Random Functions and their Applications", *Advances in Applied Probability*, vol. 5, pp. 439-468, 1973.

Matheron, G., Random Sets and Integral Geometry, J. Wiley, 1975.

McCullagh, P., "Regression Models for Ordinal Data", *Journal of the Royal Statistical Society B*, vol. 42, pp. 109-142, 1980.

McCullagh, P., "On the Elimination of Nuisance Parameters in the Proportional Odds Model", *Journal of the Royal Statistical Society B*, vol. 46, pp. 250-256, 1984.

Mead, R., "A Relationship between Individual Plant-spacing and Yield", *Annals of Botany*, vol. 30, pp. 301-309, 1966.

Mead, R., "A test for spatial pattern at several scales using data from a grid of contiguous quadrats", *Biometrics*, vol. 30, pp. 295-307, 1974.

Miles, R.E., "Random Polygons determined by Random Lines in the Plane", *Proceedings of the National Academy of Sciences*, vol. 52, pp. 901-907,1157-1160, 1964.

Miles, R.E., "The Random Division of Space", *Supplement Advances in Applied Probability*, vol. 4, pp. 243-266, 1972.

Miles, R.E., "The Various Aggregates determined by Random Lines in the Plane", *Advances in Mathematics*, vol. 10, pp. 256-296, 1973.

Miles, R.E., "A Synopsis of Poisson Flats in Euclidean Space", in Stochastic Geometry, J. Wiley, pp. 202-227, 1974.

Pielou, E.C., "The Spatial Pattern of Two-Phase Patchworks of Vegetation", *Biometrics*, vol. 20, pp. 157-167 ; 891-892, 1964.

Pielou, E.C., "The Concept of Randomness in Patterns of Mosaics", *Biometrics*, vol. 21, pp. 908-920, 1965.

Pielou, E.C., "Mathematical Ecology", J. Wiley, 1977.

Ripley, B.D., "The second-order analysis of stationary point patterns", *Journal of Applied Probability*, vol. 13, pp. 255-266 1976.

Ripley, B.D., "Modelling Spatial Patterns", *Journal of the Royal Statistical Society B*, vol. 39, pp. 172-212, 1977.

Ripley, B.D., "Tests of randomness for spatial point patterns", *Journal of the Royal Statistical Society B*, vol. 41, pp. 368-374, 1979.

Ripley, B.D., "Spatial Statistics", J. Wiley, 1981.

Ripley, B.D., "Stochastic Simulation", J. Wiley, 1987.

Santalo, L.A., "Integral Geometry and Geometric Probability", Addison-Wesley, 1976.

Sharpe, K., "Some Properties of the Crossings Process generated by a Stationary χ^2 Process", *Advances in Applied Probability*, vol. 10, pp. 373-391, 1978.

Sironvalle, M.A., "The Random Coin Method : Solution of the Problem of Simulation of a Random Function in the Plane", *Mathematical Geology*, vol. 12, pp. 25-32, 1980.

Stoyan, B.D., Kendall, W.S., and Mecke, J., "Stochastic Geometry and Its Applications", J. Wiley, 1982.

Wicksell, S.D., "The Corpuscle Problem, A Mathematical Study of a Biometric Problem", *Biometrika*, vol. 17, pp. 84-99, 1925.